AALBORG UNIVERSITY

Marina Torrente Rodriguez
Felix Christian Kochendörfer

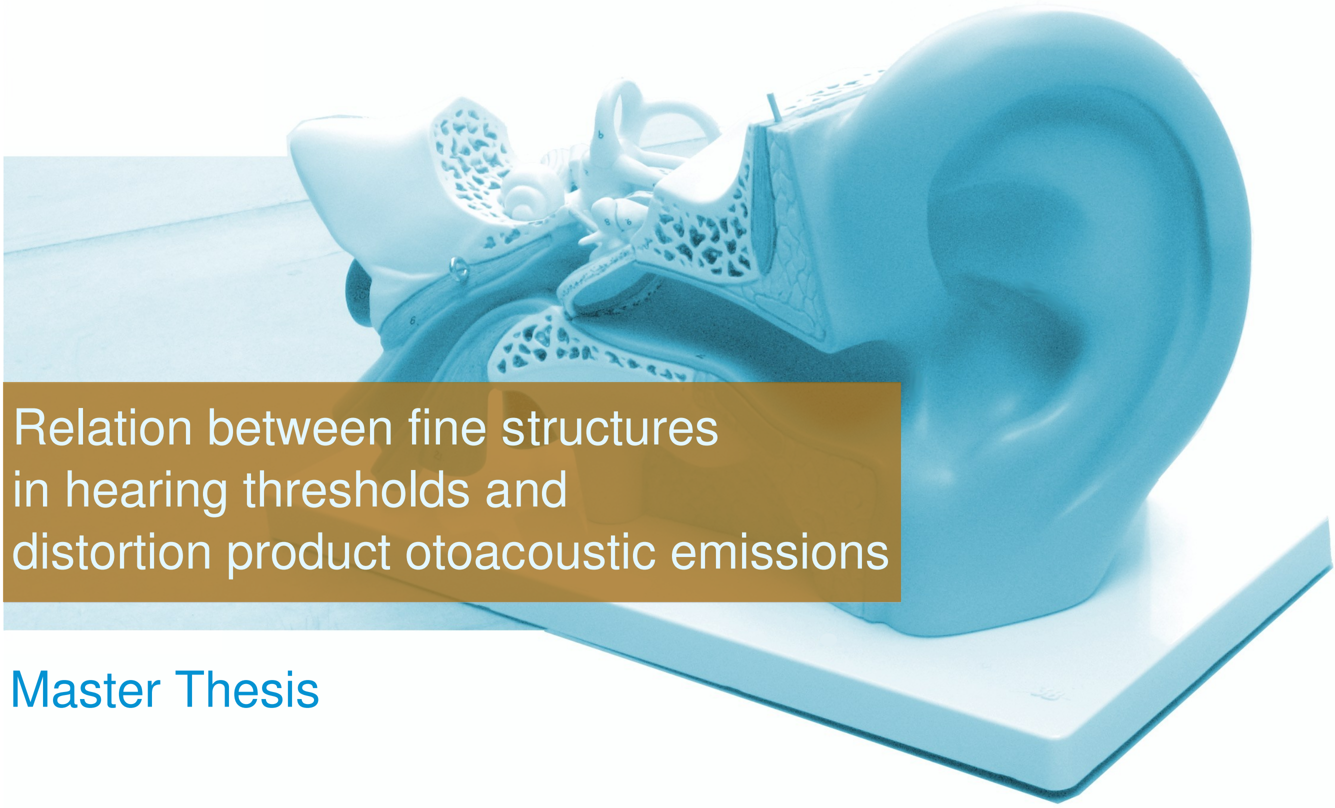

Relation between fine structures in hearing thresholds and distortion product otoacoustic emissions

Master Thesis

Section of Acoustics
Faculties of Engineering, Science and Medicine
Department of Electronic Systems

Spring 2010
Group 1061

Aalborg University
Department of Electronic Systems
Frederik Bajers Vej 7
9220 Aalborg Ø
Telephone 96 35 86 00
http://es.aau.dk/

Title: Relation between fine structures in hearing thresholds and distortion product otoacoustic emissions

Project term:
ACO10, spring 2010

Project group:
Group 1061

Members of the group:
Felix Kochendörfer
Marina Torrente

Supervisor:
Dorte Hammershøi

Number of copies: 6

Number of pages: 114

Attachments:
1 CD-ROM

Completed 02/06 2010

Synopsis:

The purpose of this project is to examine the relationship between the fine structures of DPOAE and those of the hearing threshold. An experiment was conducted with 12 subjects. Their hearing threshold was screened using an implemented audiometer with high frequency resolution and based on level presentation strategy. Measurements of the distortion product otoacoustic emissions (DPOAE) were also performed with a high frequency resolution. A developed fine structure detector was applied to extract objective parameters characterizing the threshold and DPOAE fine structure.
A direct relation between the threshold and DPOAE fine structure and level could not be found. However, similarities in the fine structure periodicity were observed.
The analysis of the results and their comparison with simplified cochlear models did not provide a universal tool for an estimation of the threshold from the DPOAE fine structure and level.

Authors

This report is written by:

Felix Kochendörfer
felik@es.aau.dk

Marina Torrente
marinatr@es.aau.dk

Preface

This report documents the Master Thesis written by group 1061 of the Section of Acoustics, Department of Electronic Systems at Aalborg University during 4th semester of the acoustics master programme of Aalborg University.

The purpose of this project is to examine the relationship between the fine structure of DPOAE and those of the hearing threshold.

The documentation presented in this report is structured as described next:

- First an introductory chapter explaining the motivation and problem statement of the present research is presented in Chapter 1.
- The necessary background theory related to the human auditory system is presented in Chapter 2 to support further explanation of the hearing threshold and OAE fine structure nature which is given in Chapters 3 and 4. Possible similarities and dissimilarities between threshold and DPOAE fine structure are described in Chapter 5 with respect to previous studies and theoretical models.
- Different threshold screening methods are analyzed and the method chosen to determine the threshold fine structure is explained respectively in Chapters 6 and 7. The characteristics and requirements of the system to measure the DPOAE fine structure are argued in Chapter 8. Chapter 9 introduces the implemented fine structure detector for an objective study of the characteristics of DPOAE and threshold fine structure.
- The experiment design and results are presented in Chapters 10 and 11. A deep analysis of the results and comparison with theoretical models is presented in Chapter 12. In Chapter 13, the experimental and analytical findings are discussed.
- Finally the conclusion achieved and the interesting points for future studies are included (Chapters 14 and 15)
- The attached CD includes the results from the experiment and the Matlab files of the implemented high resolution audiometer, the fine structure detectors and for the reconstruction of the DPOAE functions.

The members of the group would like to thank Miguel Angel Aranda de Toro, Rodrigo Ordoñez and Dorte Hammershøi for their interesting feedback and support, and to all the subjects that participated voluntarily in the experiment.

Contents

1 Introduction and problem statement

In the human auditory system, the cochlea plays a major role in the cognition of sound. The outer hair cells act as a mechanical amplifier increasing the motion of the basilar membrane. This stimulates the inner hair cells, which transform the vibrations into neural impulses. Due to the active process of the outer hair cells even very low signals will be amplified which highly influences the absolute hearing threshold. However, the outer hair cells are the most sensitive to damage caused by high noise levels.

The active process of the outer hair cells also causes emissions of sound from the cochlea, known as otoacoustic emissions. Otoacoustic emissions are often observed as a result of a distortion product when the cochlea is excited with two sinusoidal sounds. When recording those distortion product otoacoustic emissions (DPOAE), quasi-periodic level variations with minima and maxima can be observed, known as DPOAE fine structure. The presence or absence of this fine structure is considered to be an indication of the status of the outer hair cells.

A similar fine structure can also be found when determining the hearing threshold with a very high frequency resolution. This might be a result of similar mechanisms which are responsible for the fine structure of the DPOAE. Hence, this small variations in the hearing threshold curve, which can be up to 15 dB, are not an indication of hearing disorder.

The purpose of this project is to examine the relationship between the fine structures of DPOAE and those of the hearing threshold.

For this purpose the hearing threshold and the DPOAE of the same subjects have to be determined with a high frequency resolution.

With a "classical" audiometry this fine structure cannot be observed due to the low frequency resolution. The audiometric test is always dependent on the subject's response and requires a high concentration. An increase of the frequency resolution leads to a longer duration of the experiment which influences the subject's concentration.

An audiometric algorithm to detect fine structure in the hearing threshold has to be developed. It has been chosen to use the FINESS (FINE Structure Screening) algorithm developed by Heise et al. [Heis 08], which detects threshold changes using a fixed-frequency tracking procedure based on the variation of the presented levels.

The DPOAE measurement will be performed with the commercial ILO96 research system using a high frequency resolution. In order to analyze the different components involved in the DPOAE generation, a wider frequency range will be measured compared to the high resolution audiometry.

The results of both methods, the high resolution audiometry and the DPOAE measurement, will be analyzed in the same frequency range in order to find similarities and differences. The analysis is extended by the use of cochlear models to study a relationship between the fine structure of the hearing threshold and that of the DPOAE.

2
The human auditory system

A basic description of the anatomy and functionality of the human auditory system is given in this chapter to support further explanation of the nature of hearing threshold and OAE fine structure.

The human auditory system can be divided into three parts: the outer ear, the middle ear and the inner ear. The different elements that constitute the human auditory system are represented in Figure 2.1.

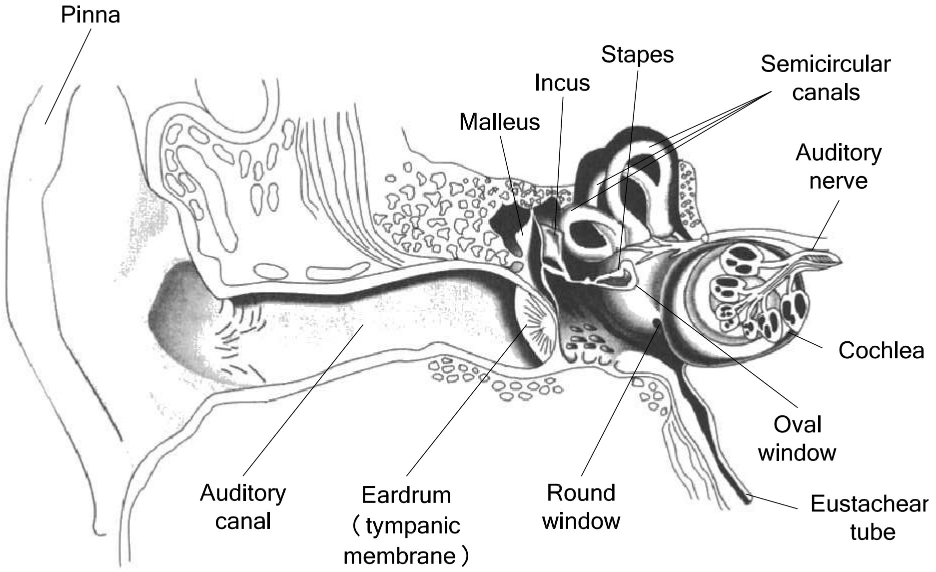

Figure 2.1: The human auditory system. Source: `http://www.skidmore.edu/~hfoley/images/AuditorySystem.jpg`.

The outer and middle ear are separated by the eardrum or tympanic membrane, while the oval window constitutes the boundary between the middle and inner ear. The acoustic waves are conducted through the outer ear.

The sound pressure variations produce mechanical vibration of the eardrum. This vibration is transmitted by three small bones in the middle ear, the ossicles. The forces applied to the oval window by the ossicles set the fluids inside the cochlea in motion. The cochlea is a snail shell shaped organ present in the inner ear. In the cochlea the mechanical energy is transformed into neural impulses that carry the acoustical information to the brain via the auditory nerves [Soun 07].

The characteristics and influence of each part of the human auditory system in the hearing process are described in the following.

2.1 Outer ear

The outer ear includes the pinna and the ear canal (see Figure 2.1). The pinna is the external part of the ear. The complex shape of the pinna causes peaks and dips in the sound spectral information. The ear canal acts as an open pipe with a resonant frequency of about 4 kHz, due to its length of 25 mm to 35 mm. The human hearing is thus very sensitive around this frequency and therefore the risk of hearing damage around 4 kHz is higher [Fast 07].

2.2 Middle ear

The malleus, incus and stapes are the three small bones present in middle ear, known as ossicles (see Figure 2.1). The malleus is fixed to the eardrum and the stapes footplate is attached to the oval window. The middle ear acts as an impedance matching, enabling to transform the acoustics pressure variations, with weak forces and large displacements, to motion of the liquids in the cochlea, with large forces and small displacement [Fast 07].

The impedance matching is achieved mainly by the area of the eardrum and the stapes footplate ratio, but in a small scale also by the lever ratio, produced by the difference in length between the malleus and the incus [Howa 96], [Fast 07], [Moor 07].

2.3 Inner ear

In some literature the inner ear is presented as the cochlea, which is the auditory organ itself. However, the inner ear comprises also the balance organ. It is of interest for this project to focus here only on the anatomy and functionality of the cochlea, where the mechanical energy transferred to the oval window is transformed into neural impulses that are sent to the brain.

A cross section of the cochlea is shown in Figure 2.2. The cochlea is subdivided into three cavities (scala vestibuli, scala tympani and scala media). The cavities are separated by two membranes, the Reissner's and basilar membranes (BM), and they extend all along the cochlea. The part of the cochlea closer to the middle ear is known as the base and the tip of the cochlea is known as the apex.

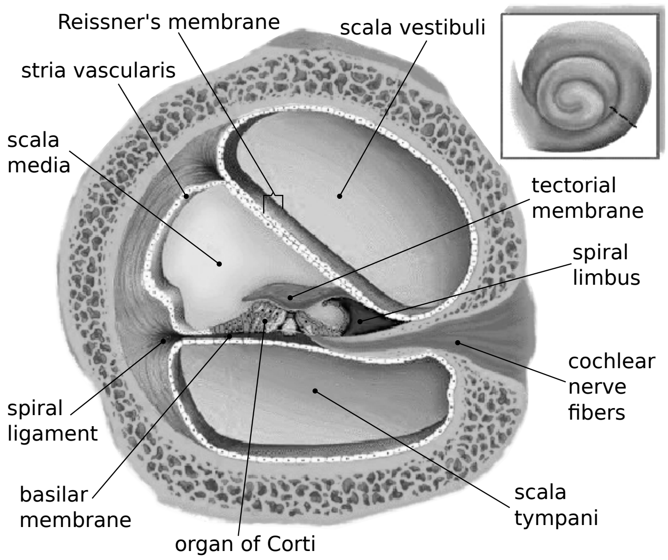

Figure 2.2: Cross section of the cochlea, divided into the three fluid-filled cavities: scala vestibuli, scala media and scala tympani. Redrawn from source: `http://media-2.web.britannica.com/eb-media/01/14301-004-4B6F34DA.gif`.

The scala vestibuli terminates in the oval window and the scala tympani in the round window. They are filled with a fluid called perilymph. The perilymph can flow thanks to an opening in the apex of the cochlea, the helicotrema. Piston like movements of the oval window set the perilymph in motion producing traveling waves along the Reissner's and basilar membranes [Howa 96].

The hair cells present in the organ of Corti (see Figure 2.3) are responsible for the generation of neural impulse responses that are conducted via the auditory nerves to the central auditory nervous system.

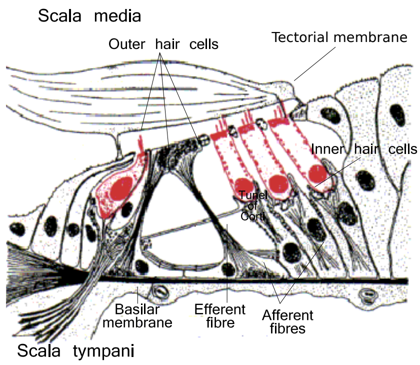

Figure 2.3: Organ of Corti in a cross section of the cochlea. Redrawn from source: `http://download.videohelp.com/vitualis/med/organ_of_corti.gif`.

2.3.1 Traveling waves

Traveling waves produce a maximum vertical displacement at an specific place of the BM, known as the tonotopic location, showing a resonant behavior. After reaching its maximum, the wave amplitude decreases rapidly and dies near the apex [Moor 07].

The BM acts as a frequency analyzer. At the base of the cochlea it is thin and narrow, and it becomes thicker and wider as it approaches to the apex. Hence, high frequency tones will excite points of the BM close to the base, whereas low frequency tones will excite points closer to the apex. The tonotopic location is logarithmically dependent on frequency. [Howa 96] [Fast 07].

Figure 2.4 shows the excitation pattern of the BM when it excited with a three tonal frequency signal. Each tone produces a maximum of excitation in the BM corresponding to their characteristic tonotopic place.

This linear and passive mechanism, which relies on the mechanical properties of the BM, is not the only process involved in the generation of traveling waves. A non-linear active mechanism dependent on the operation of the outer hair cells also influences the BM traveling waves pattern in response to sound.

2.3.2 The outer and inner hair cells function

The outer hair cells (OHCs) contain muscle components. This enables them to change their shape, length and stiffness. The OHCs actively influence the response of the BM to sound. When a point in the BM is excited by

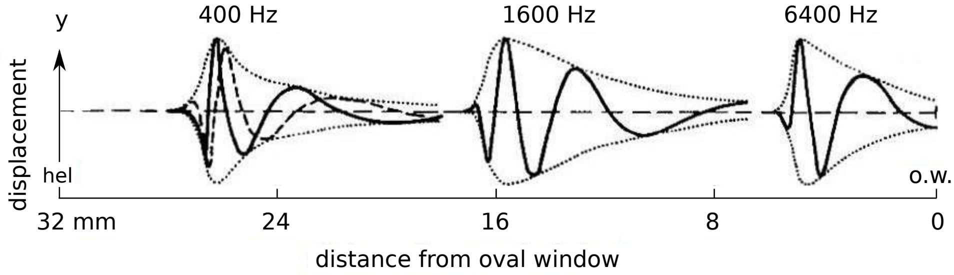

Figure 2.4: Schematic excitation pattern of the BM places using an exciting signal composed by three separated tonal frequencies (400, 1600 and 6400 Hz). For the 400 Hz tone the instantaneous traveling waves are also represented. The dashed lines represent the envelope which maximum is produced at the tonotopic place in the BM. Redrawn from [Fast 07, Page 29].

a traveling wave maximum the movements of the OHCs increase. At low levels the OHCs act as an amplifier increasing the displacement of the BM, hence the inner hair cells (IHCs) are stimulated [Moor 07].

The IHCs positioned at the BM places that are in motion produce neural impulses. Those impulses are carried to the brain by the afferent fibers. From the brain, the neural impulses travel back to the ear being carried by a different fibers known as the efferent fibers. Most efferent fibers are connected to the OHCs. It is believed that the active mechanism of the OHCs might be controlled by the efferent fibers [Moor 07].

3 The audible range and hearing thresholds

The absolute hearing threshold is the lower limit of audible sound pressures and an important element to describe the status of the individual hearing. In which way the threshold is defined and how it is used for clinical hearing assessment is explained in this chapter. Furthermore, the origin of threshold fine structure and its characteristics are described.

The determination of the absolute hearing threshold is one of the most common psychoacoustic measurements. It is performed by presenting sinusoidal sounds of different levels to the test subject under the condition that no other external sounds disturb the experiment.

The absolute hearing threshold is defined as the level at which a sound at a specific frequency is just audible in the absence of any other sounds [Moor 03]. It is determined experimentally as the level at which the stimulus is detected in 50 % of repeated trials [Lydo 99].

The absolute threshold is different from subject to subject, but a strong deviation from the average of normal listeners is often an indicator of auditory system damage.

3.1 Audible range

The human hearing is limited in frequency and sound pressure. The area enclosed by those limits is described as the audible range, which is illustrated in Figure 3.1. In the cochlea, sound with an appropriate pressure normally produces sensations in a range between 20 Hz and 20 kHz [Zwic 90]. The absolute hearing threshold defines the lower limit of the sound pressure in the audible range, whereas the higher limit is described as the threshold of pain.

All important spectral components of speech and music are within the audible range. The area between 100 Hz and 7 kHz contains all frequencies guaranteeing a full speech intelligibility. For this reason an audiometry is typically performed within this range [Cran 08].

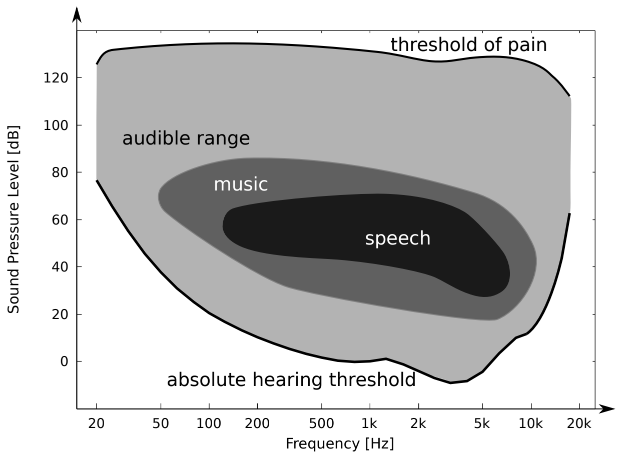

Figure 3.1: The audible range of normal hearing humans between the absolute hearing threshold and the threshold of pain. Redrawn from [Zwic 90] and [Soun 07].

The absolute hearing threshold is the most examined limit of the audible range. It is different for each person, but shows a somewhat common shape for healthy ears. As shown in Figure 3.1, normal hearing subjects are most sensitive in the range between 2 and 5 kHz, whereas the threshold increases towards the boundaries of the hearing range. Hence, a relatively high sound pressure level is required in order to make sounds of low or high frequencies audible.

Since the threshold is strongly dependent on the frequency, a reference has been developed according to numerous measurements on young adults free of all signs of hearing disease. This reference is used to evaluate individual hearing loss compared to the human average [Cran 08].

There are different threshold references regarding the way of presenting the signal. A number of psychoacoustic researches refer to a binaural listening in free-field. In this case a different reference has to be considered than e.g. for a standard audiometry where the sound is presented just at one ear each time with headphones. For monaural headphone playback the resulting threshold curve shows a higher sound pressure level and a slightly different shape compared to the binaural free-field threshold [Moor 07]. A reference resulting from such experiments, especially for audiometric equipment, is given in ISO 389.

3.2 The audiogram

Audiometric measurements are developed to detect individual differences from an average human hearing threshold. In order to present those differences a so called *audiogram* is typically used. The individual hearing threshold is normalized to an average reference as proposed in ISO 389. A specific logarithmic scale called hearing level (HL) is accepted for thresholds specified with this method. Hence, if a subject shows exactly the same hearing threshold as the average of healthy humans, its audiogram will be 0 dB HL for all frequencies.

However, an increased hearing threshold is typically plotted downwards to illustrate a loss of hearing [Moor 07]. Figure 3.2 shows a typical hearing loss compared to the reference, expressed in sound pressure level and hearing level. The threshold in this example is 40 dB higher than 'normal' at 1 kHz.

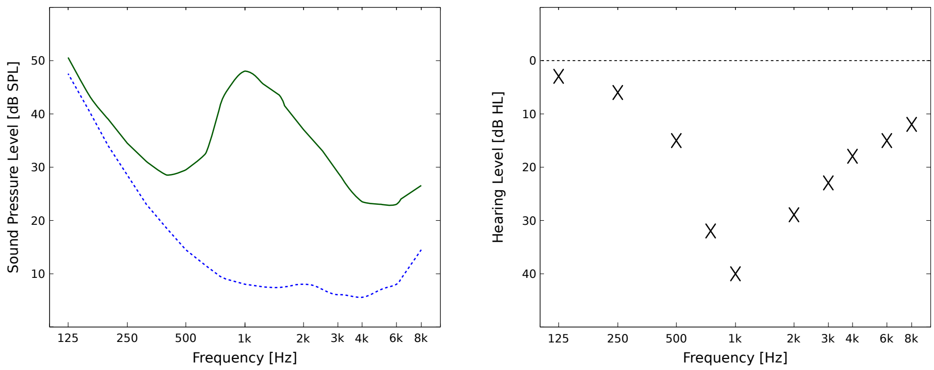

Figure 3.2: Changes of the absolute hearing threshold up to 40 dB presented as physical sound pressure level (left) and in a clinical audiogram (right). The dashed line represents the reference according to ISO 389.

Especially young people might present a negative absolute threshold in dB HL. This simply indicates that their hearing is more sensitive than the average [Cran 08].

3.3 Audiometric fine structure

When determining the absolute hearing threshold with a very high frequency resolution, quasi-periodic level variations can be observed in the audiogram. The differences between adjacent peaks and dips can thereby be up to 15 dB [Heis 08]. These ripple effects have been discovered first by Elliott in 1958 [Elli 58] who already assumed this as a universal phenomenon. He demonstrated that *fine structure*, as it is specified nowadays, is stable over a long period of time, but differs from ear to ear. Apparently, fine structure can only be found in frequency ranges where the subject does not show signs of a hearing impairment. On the other hand, listeners without a detected fine structure do not necessarily show a hearing loss [Heis 08].

Although the origin of the threshold fine structure is not completely understood, it is assumed to be a result of reflections of the traveling waves inside the cochlea. Following this hypothesis, the incoming wave traveling from the base towards the apex is reflected in a certain frequency dependent region along the basilar membrane [Kemp 79]. This is commonly referred to as the apical reflection. Zweig and Shera [Zwei 95] considered that this reflection is due to random inhomogeneities or "roughness" near the tonotopic location (see Section 2.3.1). This roughness is assumed to be the reason why the phase of the reflectance is strongly dependent on frequency.

Due to an imperfect impedance matching at the stapes, the retrograde traveling wave will be reflected again, resulting in an overlay of the reflected and incoming wave. Their phase difference, which is mainly caused by the apical reflectance at the tonotopic location, will cause a constructive and destructive interference of the waves and thus either enhance or reduce the amplitude of the traveling wave. Hence, the rapidly changing phase of the apical reflectance causes an uneven distribution of the energy with minima and maxima for different frequencies [Talm 98] [Heis 08].

Comparisons between analogue model computations and fine structure measurements predict in some cases that the apical reflectance is very high and even exceeds 1 [Kemp 79]. The active process of the outer hair cells (see Section 2.3.2) is therefore assumed to be involved in the reflection.

With increasing stimulus intensity, the active mechanism and hence the reflectivity would decrease, avoiding an excessive growth of the standing wave oscillations. This explains why equal loudness contours show a reduced fine structure at higher sound pressure levels [Maue 04a] [Kemp 79].

The presence of minima and maxima at specific frequencies highly depends on each individual ear. Hence, a specific apical reflectance can not be determined for each frequency or level, it rather appears that it changes individually in a random way [Kemp 79].

4

Otoacoustic emissions

In this chapter the origin of otoacoustic emissions (OAE) is explained. A classification of the OAE depending on the measurement conditions is also presented. The arguments for choosing the DPOAE for a comparison with the hearing threshold is given. Finally, the main theories regarding the generation of the DPOAE fine structure are analyzed.

The OAE measurements are employed as a physiological test for hearing assessment. Since they do not require of the active participation of the subject, they can be useful when the subject is not capable to perform psychoacoustical tests such as the audiometry method (see Chapter 3), i.e. neonates or young children.

OAE can be defined as "sound generated by the ear" [Kemp 07]. The basic concepts regarding the generation of OAE are presented in the following.

4.1 Physiology behind the generation of OAE

OAE are sound pressure variations in the ear canal generated by the vibration of the eardrum driven by the cochlea [Kemp 07]. Although this phenomenon is still not completely understood, experiments have demonstrated that OAE are directly related to the active mechanism of the cochlea (see Section 2.3.2).

The fact that the cochlea induces the vibration of the eardrum suggests that an imbalance of fluid pressure between the oval and round window must exist. This imbalance is only possible if an additional energy of vibration, different from the primary hearing process, exists and is transmitted backwards to the base of the cochlea causing the middle ear motion. The middle ear impedance matching will cause the vibration of the eardrum.

It is believed that the additional energy of vibration is generated by the action of the OHCs as a "cochlea amplifier" (see Section 2.3.2). The backwards transmission of this energy can be explained by the reverse traveling waves theory. However, according to Kemp [Kemp 07], it has not been experimentally demonstrated directly yet that the reverse traveling waves are involved in the generation of OAE.

4.2 OAE measurement techniques

The sound pressure generated by the eardrum back to the ear canal is very small. It is only enhanced at high frequencies by the action of the ear canal as a horn. Therefore, to record OAE the ear canal has to be sealed, thus providing a confined air volume that can be moved by the small vibration of the eardrum.

A classification of the OAE can be made, depending on the measurement technique and on the type of stimulus applied. This classification is described in the following together with the method of analysis used in each case to separate the emissions from the excitation signals [Kemp 07]:

- *Spontaneous otoacoustic emissions* (SOAE). No stimulus signal is applied. In some healthy ears oscillations are produced in the cochlea that feed back itself, producing OAE that can be recorded without using any external stimulus [Kemp 07]. The observation of SOAE is denoted by peaks that stand out from the background noise spectrum. The noise spectrum is obtained as the average of the power spectrum of the signal recorded [Maue 04b].

- *Stimulus frequency otoacoustic emissions* (SFOAE) are measured by applying a single tone. The OAE generated are of the same frequency and they are produced at the same time as the stimulus. The non-linear characteristics of the SFOAE are used to separate the emission from the stimulus. An alternative to observe the SFOAE is to apply a suppressor tone of a different frequency [Kemp 07].

- *Transient evoked otoacoustic emissions* (TEOAE) can be measured by playing a narrow band tone burst stimulus, or by broad band short duration stimuli (< 3ms) applied repetitively [Kemp 07]. A delayed low-level signal which contains the TEOAE is recorded in the ear canal. The TEOAE can be separated from the stimulus signal by signal processing based on the time delay and non-linearity of the OAE [Knig 98].

- *Distortion product otoacoustic emissions* (DPOAE) are the response of the ear canal to a stimulation consisting on two different frequency tones (f_1 and f_2) with a frequency ratio f_2/f_1. The non-linear behavior of the cochlea generates intermodulation products of the two tones, where $2f_1 - f_2$ the most prominent of them. Measurements of DPOAE over a specific frequency range are carried out by keeping f_2/f_1 constant while varying f_1 and f_2 simultaneously [Reut 06]. At the ear canal a signal containing the stimulus frequencies f_1 and f_2 together with intermodulation frequencies components can be recorded [Knig 98].

The techniques most commonly used for clinical applications are the TEOAE and DPOAE [Knig 98].

With a hearing loss of more than 30 dB, the presence of TEOAE is in general not detectable. Therefore, if such emissions are measured, it is an indicator of a healthy ear [Maue 04b]. The high sensitivity of TEOAE make them an appropriate measurement to test young ears. It is more successful at low frequencies (< 1 kHz). However, it is not possible to record any emissions above 5 kHz [Fitz 04]. To test older ears, hearing assessment using TEOAE has to be supported by the study of DPOAE [ILO 97].

In DPOAE measurements more energy is induced since continuous tones are used as stimuli, instead of brief clicks. Emissions can still be recorded with a hearing loss up to 50 dB [ILO 97] [Maue 04b]. Moreover, with the DPOAE it is possible to perform hearing assessment at specific frequencies.

The frequency specificity of the DPOAE measurements makes them suitable when investigating a possible relationship between OAE and hearing threshold fine structure.

4.3 DPOAE fine structure

Experimental researches and cochlear models by Talmadge et al. [Talm 98] [Talm 99] claim that DPOAE are produced by two sources caused by two different mechanisms.

One of the sources is placed in the BM at the tonotopic region of primaries overlap near f_2, and the other at the quadratic distortion product $f_{dp} = 2f_1 - f_2$ [Reut 06] [Shaf 03]. The first one will be referred to as the distortion component and the second as the reflection component. The energy of the distortion component travels both towards the base and the apex. When this energy reaches the activity peak of the reflection component in the BM the apical energy is reflected backwards to the ear canal. The DPOAE fine structure results from the constructive and destructive interference of the two DPOAE sources in the BM [Shaf 03]. The traveling waves behavior is illustrated in Figure 4.1.

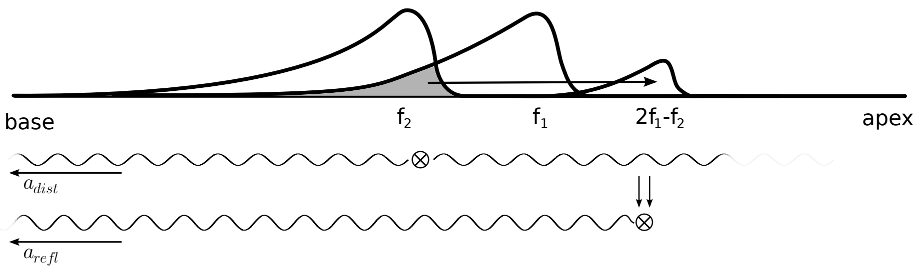

Figure 4.1: Sketch of the non-linear distortion at the region traveling waves of frequencies f_1 and f_2 overlap. The energy of $2f_1 - f_2$ is transmitted to its characteristic tonotopic place in the BM where is reflected backwards to the base.

As stated in 3.3, theoretical models [Zwei 95] [Talm 98] [Talm 99] assume that the roughness of the BM is responsible for the apical reflectance that produces the threshold and DPOAE fine structure. According to Talmadge et al. [Talm 98] [Talm 99], for a constant f_2/f_1 ratio the distortion component will present a short latency and small phase variation with frequency, whereas the reflection component will present long latency and its phase will vary rapidly as a function of frequency. The generation of the DPOAE fine structure will be due to this phase difference between the two components.

The variations in the phase of the reflection component are assumed to depend on the phase of the apical reflectance which varies with $\omega_{dp} = 2\pi f_{dp}$ (or the tonotopic place equivalently). Hence, if the phase of the distortion component is assumed to be constant, the ideally periodic DPOAE fine structure will be generated as illustrated in Figure 4.2, due to the interference of the two components.

It has been suggested among the literature that the presence of fine structure is an indicator of a healthy ear [Reut 06]. The experiments and simulations described in [Maue 99] were conducted to analyze the DPOAE fine structure in subjects with different kinds of known hearing impairment. It was observed that when the reflection component f_{dp} was in the frequency region of damage, the fine structure disappeared, the amplitude of the DPOAE recorded was flattened. However, if the frequency region of impairment corresponded to the distortion component f_2, the DPOAE level was reduced but the fine structure could still be observed. Therefore, not only the level of DPOAE can be used in hearing diagnosis. If no fine structure is present, a cochlear damage at the reflection component f_{dp} can be expected.

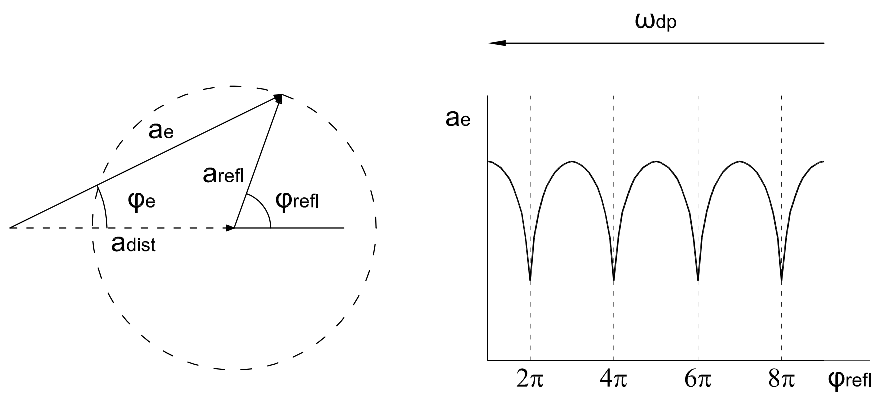

Figure 4.2: Two-generation source components phasor diagram (left) and DPOAE fine structure pattern (right), where a_{refl} is the amplitude of the reflection component and φ_{refl} is its varying phase, responsible for the constructive and destructive sources interference and dependent on the distortion product frequency ω_{dp}. The amplitude and phase of the DPOAE signal are a_e and φ_e respectively. The amplitude of the distortion component is a_{dist}.

5

Models of DPOAE and hearing threshold fine structure

The previous chapters revealed that the active nonlinear process in the cochlea is responsible for the generation of otoacoustic emissions and it is involved in the appearance of fine structure in the human hearing threshold. Hence a direct relation between both phenomena is presumed. In this chapter, possible similarities and dissimilarities regarding previous studies and cochlear models are presented, focusing especially on the otoacoustic emissions and hearing threshold fine structure.

As already mentioned in Section 3.3, reflections along the basilar membrane are involved in the hearing threshold fine structure. When the reflectance exceeds 1 those reflections cannot longer be considered as passive. This suggests that the cochlea produces an active mechanical response to an acoustic stimulation [Kemp 79]. Further observations revealed that the time delay between the initiation of a wave and its returning reflection at the base is much higher than expected regarding propagation time. Hence, the reflections do not occur before a certain reaction time passes [Kemp 79].

Similar time delays can also be observed when measuring otoacoustic emissions, e.g. TEOAE (see Section 4.2). In fact, TEOAE and threshold curves show the same degree of frequency selectivity, resulting in coincident minima and maxima [Kemp 79]. Furthermore, spectral peaks of spontaneous otoacoustic emissions are observed at frequencies of TEOAE and threshold maxima [Zwei 95] [Talm 98].

Talmadge et al. [Talm 98] developed cochlear models to evaluate fine structures of threshold and otoacoustic emissions based on the research by Zweig and Shera [Zwei 95]. The variations of the apical reflectance with frequency appear to be the main reason for fine structure (see Sections 3.3 and 4.3). Other involved parameters, such as the transformation through the middle ear or the basal reflectance show just little variations with frequency.

During an audiometry, the ear canal is excited by an external stimulus with the driving pressure P_{dr} resulting in a traveling pressure wave in the cochlea. A simple illustration of the cochlear response to an initial pressure wave $b(\omega)$ is shown in Figure 5.1.

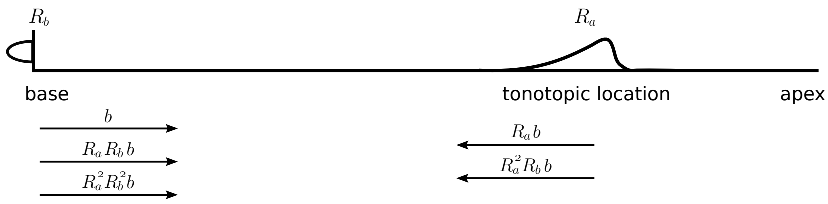

Figure 5.1: Schematic illustration of the reflections due to excitation of the pressure wave b at the stapes. Redrawn from [Talm 98].

The threshold microstructure model suggests a direct relation between the ear canal driving pressure $P_{dr}(\omega)$ and the BM displacement amplitude $\xi(\omega)$ at the tonotopic location. Under the assumption that the transformation of P_{dr} through the middle ear is constant over a small frequency range, it can be stated that:

$$\frac{\xi(\omega)}{P_{dr}(\omega)} \propto \frac{P_a(\omega)}{b(\omega)} \tag{5.1}$$

where $P_a(\omega)$ is the resulting apically traveling pressure wave including all apical and basal reflections (R_a, R_b) of $b(\omega)$ [Talm 98]:

$$\frac{P_a(\omega)}{b(\omega)} = \frac{1}{1 - R_a R_b} \approx 1 + R_a R_b + (R_a R_b)^2 + ... \tag{5.2}$$

Considering that ξ_{th} is the minimum detectable BM amplitude and the phase of R_a varies logarithmically with frequency, the threshold level $P_{th}(\omega) = P_{dr}(\omega, \xi_{th})$ shows a periodic pattern as illustrated in Figure 5.2.

A similar interpretation can be made for the DPOAE fine structure (see Section 4.3). In this case, the complex amplitude of the reflection component P_{refl} can be evaluated as a function of the distortion component P_{dist} with

$$P_{refl} = \mathscr{R}_d(\omega_{dp}) R_a(\omega_{dp}) P_{dist} \tag{5.3}$$

where $\mathscr{R}_d(\omega_{dp})$ is the (complex) relation between the apical and basal traveling wave amplitude of the distortion component. The summation of the two sources predicts a DPOAE wave amplitude $P_e \approx (1+\mathscr{R}_d(\omega_{dp}) R_a(\omega_{dp})) \cdot P_{dist}$. The waves generated by the two sources will also be reflected at the

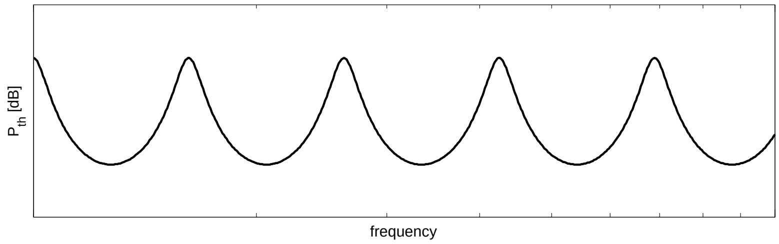

Figure 5.2: Threshold fine structure pattern as a result of $1/(1 - R_a R_b)$ with $R_a = |R_a| e^{\varphi_a}$, ($\varphi_a \propto -\log(f)$). $|R_a|$, R_b and ξ_{th} are set to be constant for this illustration and $|R_a R_b| < 1$.

base. Consequently, a more precise description for P_e is given by [Talm 98] [Talm 99]:

$$\frac{P_e(\omega_{dp})}{P_{dist}(\omega_{dp})} = \frac{1 + R_a(\omega_{dp})\mathscr{R}_d(\omega_{dp})}{1 - R_a(\omega_{dp})R_b(\omega_{dp})} \approx 1 + R_a\mathscr{R}_d + R_a R_b + ... \qquad (5.4)$$

Similar to R_b, the variation of $\mathscr{R}_d$ with frequency is expected to be much lower than the phase variation of R_a. Hence, the variations of $\varphi_{refl}(\omega_{dp}) = \varphi_d + \varphi_a(\omega_{dp})$ appear to be dominated by the phase variations of R_a.

Comparing Equations 5.2 and 5.4, the periodicity in both the threshold the DPOAE fine structure seems to be mainly the result of $\varphi_a = \arg(R_a)$. Hence, the frequency spacing between adjacent fine structure minima is expected to be similar in both cases, according to these simplified models [Talm 98].

In contrast, the shape of the different fine structures is also influenced by the absolute values of each reflectance and their (slow varying) phase. Hence, a direct relation between levels or ripple heights of DPOAE and threshold fine structure is hard to predict, since parameters like e.g. $\mathscr{R}_d$ vary from subject to subject.

6
Threshold fine structure screening methods

A screening method is necessary to be able to determine the threshold fine structure. Two different strategies are analyzed: level presentation and frequency sweeping. Finally, the choice of method for the implementation of the high resolution audiometer is argued.

A screening method for detecting threshold fine structure requires a higher frequency resolution than the classical pure-tone audiometry. Therefore, the method should be not only precise regarding the threshold's shape, but also fast, since high resolution audiometry tests are long and require of a high concentration of the subjects. Tracking methods are hence well suited for high resolution audiograms because of their speed [Heis 08].

In audiometric tracking methods the stimulus presented to the subject varies on time. These variations are usually either in level or in frequency, whereas in some cases both frequency and level are varied simultaneously. The subject is normally asked to press a button for as long as a stimulus is heard. The speed of the tracking will influence the method's precision. Moreover, the tracking strategy, i.e. the choice of constant or varying level and frequency, will affect the results.

Both tracking strategies, level presentation and frequency sweeping, are analyzed in the following, supported by an example. A discussion of their advantages and disadvantages is also presented at the end of this chapter.

6.1 Level presentation strategy

To determine the absolute hearing threshold an auditory stimulus is presented to the test subject. The intensity of the stimulus is varied in order to find the limit level between an audible and an inaudible stimulus. This is known as the *level presentation strategy*, according to Lydolf

[Lydo 99], where the influence of different level presentation strategies in hearing threshold measurements is examined. It was concluded from this study that the Bèkèsy is the most efficient of the methods analyzed. The Bèkèsy method has also the advantage that it is standardized for clinical applications. Hence, this method is further described as an example for the level presentation strategy.

6.1.1 The Békésy method

Originally the Békésy audiometry was performed with continuous sweep-frequency tone from 100 Hz to 10 kHz. During the sweep, the level of the stimulus presented is varied according to the subject's response with an attenuation rate of 2.3 dB/s [Lydo 99]. The subjects are instructed to press a button while the stimulus is heard and to release it otherwise. While the button is pressed the level of the stimulus decreases and it increases while the button is released.

Nowadays, a modified version with fixed discrete frequencies is often implemented. The level increases or decreases according to the subject's response, while the frequency is kept constant. After certain number of reversals the methods stops. The hearing threshold is estimated by averaging the mid-point between the tracked peaks and valleys [Lydo 99].

Parameters as the attenuation rate, the minimum number of reversals and the maximum deviation between peaks and valleys influence the efficiency of this audiometric method. This way, a more accurate threshold level can be obtained at specific frequencies compared to the original Békésy audiometer.

6.2 Frequency sweeping strategy

An alternative to the level presentation strategy is the frequency sweeping. While the level of the stimulus is kept constant, the frequency varies on time. In the following this strategy is explained using the *Audioscan* developed by Meyer-Bisch (reviewed in [Zhao 02]) as an example. The Audioscan is based on iso-hearing level frequency sweeps. Its efficiency was tested using the Békésy method as reference [Laro 97]. The high correlation between both methods confirmed the validity of Audioscan.

6.2.1 The Audioscan method

The Audioscan method is based on constant level frequency sweeping. A constant level stimulus is presented in octave intervals. The subjects are instructed to press a button for as long as the stimulus is heard and to release it whenever the stimulus becomes inaudible. At first, the frequency is swept at a constant level. If no response is obtained, the level of the stimulus increases for the next sweep. When a subject's response is detected throughout a defined frequency range a new stimulus of higher intensity is presented only over the frequency range where no response was recorded.

The method's procedure is graphically explained in Figure 6.1. The first sweep is presented at 0 dB HL, starting at 1 kHz to the maximum frequency and then from 1 kHz again to the minimum frequency. The limits of the frequency range where the stimulus is not heard are represented by F_{a1} and F_{b1}. A new sweep at 5 dB HL is therefore presented from F_m towards F_{b1} first and F_{a1} later. The central frequency F_m is calculated as $F_m = \sqrt{F_{a1} \cdot F_{b1}}$. As a result, two new frequency limits F_{a2} and F_{b2} are found. Hence, a new sweep at a higher level than the previous is presented over the new frequency range.

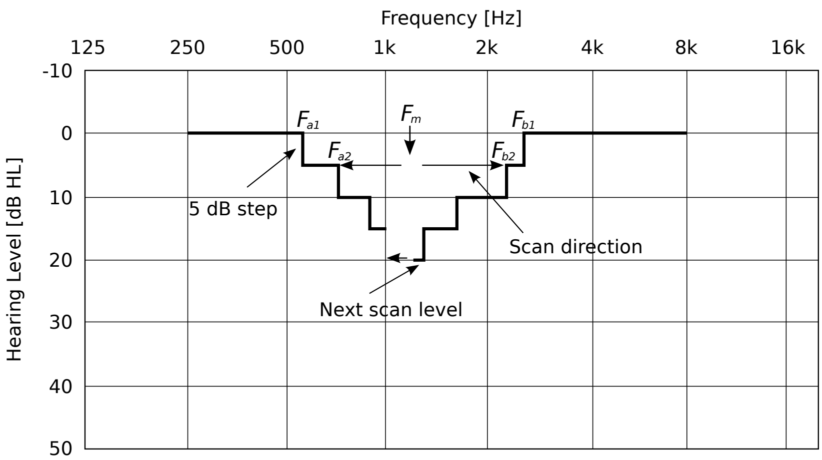

Figure 6.1: The Audioscan sweeping procedure [Zhao 02].

With this method, notches in the absolute threshold can be screened. On the other hand, the speed of the sweepings will influence the reliability of the experiment [Laro 97].

6.3 Level tracking vs. frequency sweeping

Since an audiometry is a psychoacoustic test, it depends on the responses of the subjects. Hence, a lack of precision is always produced due to the reaction time that takes the subjects to realize that a stimulus is being heard, until the button is pressed. These uncertainties will appear on the frequency axis with the frequency sweeping strategy, and on the level axis if the level presentation strategy is used.

For the same measurement time, frequency sweeping methods generally provide a higher frequency resolution than level tracking methods. However, the duration of the Audioscan increases with the number of level variations or ripples to be detected and is therefore heavily dependent on the threshold's shape. The level resolution of 5 dB used in the Audioscan is not sufficient to detect threshold ripple which can have heights from 2 dB [Heis 08].

For a comparison with OAE measurements, it is of interest that threshold fine structure screening methods are precise in frequency. Therefore, a fixed-frequency level tracking procedure seems more suitable. It has to provide a frequency resolution of at least 50 points per octave, since periodicities of 1/21 octaves have been observed in previous studies [Heis 08].

The method named FINESS (FINE Structure Screening) developed by Heise et al. [Heis 08] is chosen for implementation. It is a fixed-frequency tracking procedure based on the level presentation strategy. The method presents high frequency resolution and, at the same time, the precision of the screening is ensured by performing several repetitions and consistency checks. However, the method is very fast since only one reversal per frequency is performed, relying on the fact that using small frequency steps the threshold does not vary abruptly from one point to the next.

The algorithm of the threshold fine structure screening method implemented is described in Chapter 7.

7
The FINESS algorithm

The high resolution audiometer is implemented using the FINE Structure Screening algorithm, which has been developed by Heise et al. [Heis 08]. The procedure and the characteristics of this method are described in this chapter.

As stated in Section 6.3, the FINE Structure Screening (FINESS) algorithm [Heis 08] is a fixed-frequency tracking method for threshold fine structure screening based on the level presentation strategy. The algorithm has been implemented in Matlab[1]. The system setup and calibration are described in Appendixes B and E.

Heise et al. [Heis 08] checked the reliability of the FINESS algorithm with a test/retest experiment. The results showed a high agreement when subjects performed the audiometric test twice. The accuracy of the shape of the threshold determined with the FINESS algorithm was also tested by comparison with an adaptive three-alternative force choice (3-AFC). The high correlation between the shape of the thresholds obtained by the two methods proved the validity of the FINESS algorithm. However, this comparison with the 3-AFC method revealed the limitation of the algorithm regarding accuracy on the absolute threshold level.

7.1 FINESS procedure

The subjects are instructed to press a button for as long as they can hear a tone. The level of the stimulus decreases while the button is pressed and it increases when it is released.

[1]The Matlab files necessary to run the audiometer are included in the enclosed CD. The main function *Audiometry_Gui.m* constitutes the interface for the experimenter to proceed to the threshold measurements.

The stimuli consist of 250 ms tones with a stable interval of 200 ms and a raised-cosine raise and fall of 25 ms to make the detection easier. There are no silence intervals between the tones presented. The level of presentation is adjusted to a dB HL scale according to ISO 389 and the calibration of the system (see Appendix E).

The level of the tones varies with an attenuation rate of ±3 dB/s and the level is changed by 0.75 dB steps. The frequency resolution is of 100 points/octave. The frequency points are screened in ascending order. The small frequency steps size allows the possibility to have just one reversal per frequency.

The frequency steps are half the size of the minimum expected spacing between fine structure minima and maxima. Hence, it is expected that no abrupt changes will occur due to fine structure in the threshold from one point to the next. The algorithm focuses on the shape of the threshold fine structure rather than on the absolute threshold level accuracy.

Since only one reversal per frequency is presented, the determined threshold is expected to be higher than the true threshold when the level of the stimuli presented increases. On the other hand, the determined threshold will be lower when the level of the stimuli presented decreases. This is due to the reaction time of the subjects. Therefore, the threshold is described by the average between those peaks and valleys. The best result to calculate the threshold estimate is obtained by applying locally weighted quadratic regression[2] with a span of 9 data points [Heis 08]. Figure 7.1 shows an example of a screened threshold using the FINESS algorithm.

A familiarization period is presented at the beginning of the screening to help the subjects to get accustomed to the method. The first frequency of the screened range is kept constant and several reversals are presented before a stable level is reached. Therefore, the familiarization is implemented to avoid a bias in the threshold screening produced by the period that the subjects need to get accustomed to the method. Once the difference between consecutive detections is less than 1.3 dB, it is considered that the value of the determined threshold is stable. A maximum of 16 reversals is presented. This number is enough to ensure that the threshold of the subjects is determined within ±2 dB of their "asymptotic" threshold [Heis 08].

The frequency range for the threshold fine structure screening is limited due to time considerations. A range of one octave centered at 2 kHz is chosen. The high prevalence of DPOAE fine structure in the mid frequency range influences the choice of the range for the threshold screening (see Section 8.1.3 for further information with this regard). Thus, the threshold fine

[2] The smoothing by locally weighted quadratic regression is performed by using the "LOESS" method of the *smooth.m* Matlab function. For further information see [Clev 79].

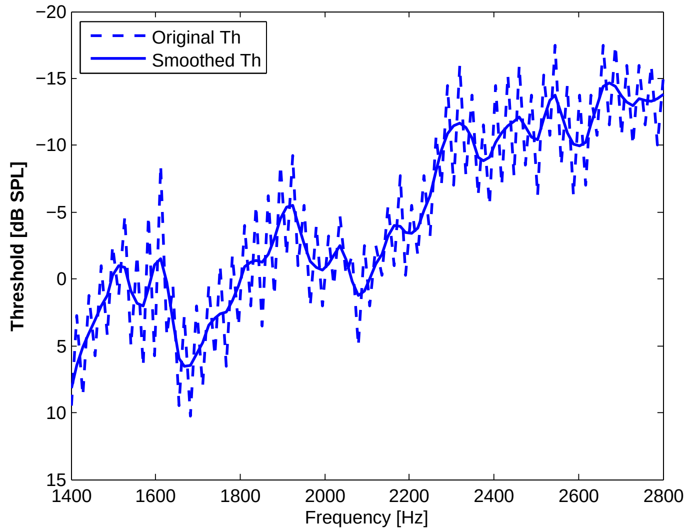

Figure 7.1: The threshold obtained by the FINESS algorithm (dashed line) is smoothed by applying locally weighted quadratic regression to calculate the threshold estimate (solid line) with a span of 9 data points.

structure will be tracked in one octave in the range from 1.4 kHz to 2.8 kHz[3].

7.2 Repetitions and consistency checks

The screening is performed at least twice to ensure the reliability of the experiment. To avoid rhythmic responses, in the first run the level of the tone starts decreasing from the highest level allowed (50 dB HL), while in the second run the level tracking begins at -20 dB HL and increases until the button is pressed.

The consistency between the two determined thresholds is checked. An offset difference is permitted since this method focuses on the threshold's shape rather than on the level, as stated before.

The consistency between the two curves is checked at each single frequency, taking into account the neighboring values. The thresholds are multiplied by a window w of 11 samples centered at the frequency of study[4]. The

[3]The screening of the threshold as described in this section is performed by means of the Matlab function *Heise_algorithm_up_down*, included in the enclosed CD.

[4]The 11 samples window w is generated by the Matlab function *weighting_window.m*, included in the enclosed CD.

windows consist of 2 samples of raised-cosine raise, 7 flat samples, followed by 2 raised-cosine fall samples. The standard deviation of the normalized difference between the two thresholds windowed data is calculated in each 11 samples segment, as follows:

$$\Sigma_s = \sum_{i=1}^{n} \frac{\left(\Delta_i - \frac{1}{n}\sum_{k=1}^{n} \Delta_k\right)^2}{n-1} \tag{7.1}$$

where

$$T_{1norm}(f_i) = w_i T_1(f_i) - \frac{1}{n}\sum_{k=1}^{n} w_k T_1(f_k) \tag{7.2}$$

$$T_{2norm}(f_i) = w_i T_2(f_i) - \frac{1}{n}\sum_{k=1}^{n} w_k T_2(f_k) \tag{7.3}$$

$$\Delta_i = T_{1norm}(f_i) - T_{2norm}(f_i) \tag{7.4}$$

$T_1(f_i)$ and $T_2(f_i)$ represent the two threshold values at each frequency f_i, and $n = 11$ is the number of frequency samples in each segment s.

If Σ_s exceeds the value of 2.5 dB, the consistency of the screening at that specific frequency is not valid[5].

In the frequency regions where the two determined thresholds are not consistent a third repetition is performed. The minimum number of frequency points within a frequency range to be repeated is 11. If the consistency check fails for a frequency range smaller than 11 frequency steps, it is extended to the neighboring frequencies. If the number of frequency point between two non-consistent ranges is less than 11, the ranges are unified.

In the remeasured frequency range the two more consistent thresholds are determined by finding the minimum Σ_s. If the threshold obtained in the third run is more consistent than one of the other two, the third curve replaces the other. In the limit frequencies of the repeated range the transition is smoothed by cross-fading between the replaced and the third threshold.

An example of a cross-fade between two thresholds is illustrated in Figure 7.2. The transition points between thresholds are calculated as follows:

$$T_{cr\text{-}fd} = (1-\alpha)T_x + \alpha T_y \tag{7.5}$$

where α varies in steps of 0.125 from 0 to 1 or from 1 to 0, depending on the remeasured frequency limit. T_x corresponds to the threshold from

[5] The consistency check between the two thresholds measured is performed by the use of the Matlab function *consistency_check.m*, included in the enclosed CD.

the third repetition of the test in a specific frequency range. T_y is the less consistent within the thresholds from the two first repetitions. The cross-fade is applied to the four previous and subsequent frequency points regarding the remeasured frequency range limit. Since the third repetition is not performed outside the specific range, the limit value is used in the calculations.

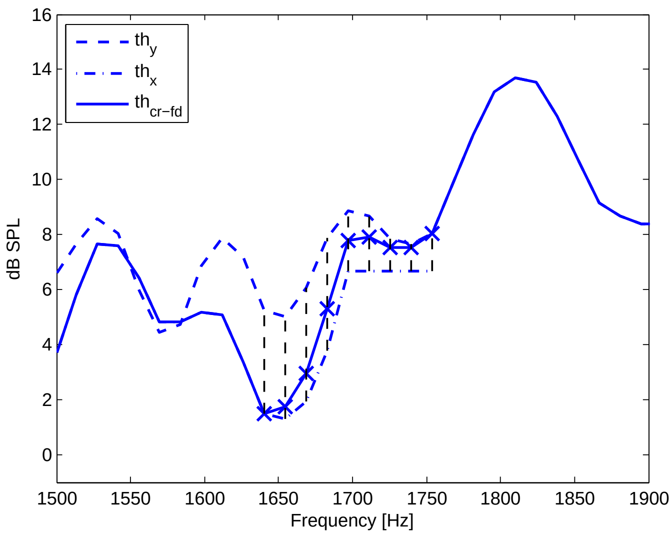

Figure 7.2: Example of a cross-fade between thresholds in the limit of the frequency range of the third repetition.

The final threshold is calculated as the average between the two resulting curves[6]. Figure 7.3 shows an example of the whole procedure. In upper figure, the standard deviation of the normalized difference between the two thresholds Σ_s is compared with the limit value of 2.5 dB. In the frequency ranges where Σ_s exceeds the limit the threshold is remeasured. In the middle figure the three measurements are represented. Finally, the figure in the bottom shows the two most consistent thresholds with a smoothed transition in the overlapping regions, and the final threshold as the average of the former.

[6]The Matlab function *two_closest_thresholds.m* included in the enclosed CD provides the two more consistent cross-faded thresholds.

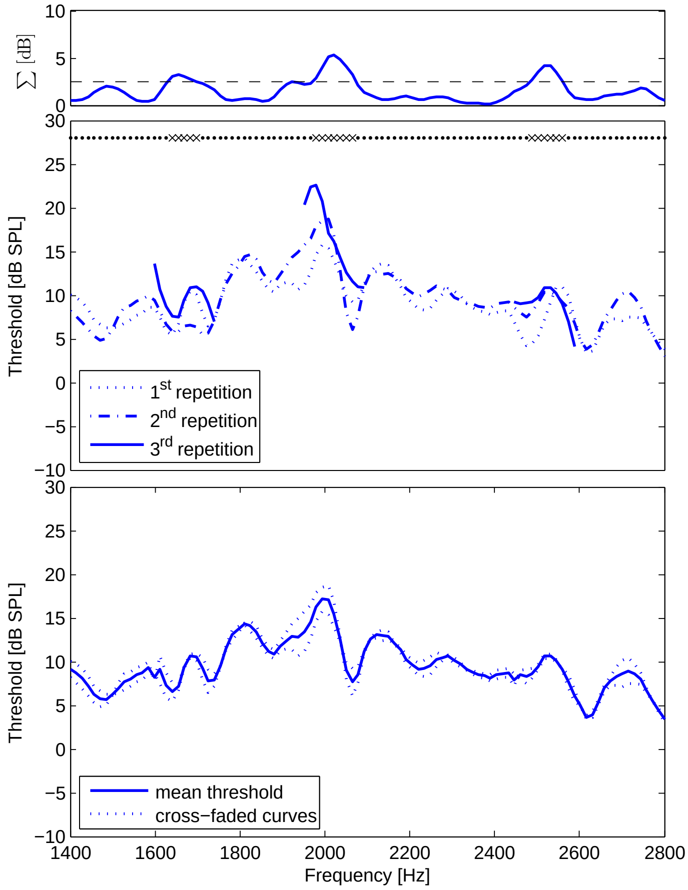

Figure 7.3: Hearing threshold of a subject determined using the implemented FINESS algorithm. The consistency of the two first repetitions is calculated as the normalized difference between the two thresholds Σ_s, which is compared with the criteria value of 2.5 dB (up). A third repetition is carried out in the inconsistent frequency ranges, marked by an "x". The ranges for third screening are extended to a minimum of 11 sample frequencies. The thresholds obtained from the three repetitions are shown (middle). The two cross-faded more consistent threshold are averaged obtaining the final threshold values (down).

8

DPOAE measurements

A description of the system used to measure the DPOAE fine structure and its specific requirements is presented in this chapter.

The DPOAE fine structure is measured by using the commercial ILO96 system from Otodynamics. The parameters of the system should be setup in order to fulfill the system requirements.

8.1 System requirements

The amplitude and presence of fine structure on the measured DPOAE depends in the measurement parameters. Thus, the choice for the ratio of primary frequencies f_2/f_1as well as of the level of the primaries L_1 and L_2 needs to be discussed.

The prevalence of the DPOAE fine structure might vary depending on the measured frequency range. Hence, and also due to practical limitation, the frequency range for measuring DPOAE fine structure needs to be defined.

8.1.1 Primaries frequency ratio

Harris et al. [Harr 89] studied the influence of primaries frequency ratio f_2/f_1 on the DPOAE amplitude. It was concluded that a ratio of $f_2/f_1 = 1.22$ provides the largest DPOAE amplitude regardless frequency and level. Therefore, this is the value of the primaries ratio chosen for the DPOAE fine structure measurements.

8.1.2 Primaries level choice

Decreasing L_2 below L_1 when $L_1 < 75$ dB increases the DPOAE amplitude. This effect depends on the value of L_1 and on the frequency [Whit 95a].

The choice of primary levels $L_1/L_2 = 65/45$ dB is made according to the discussion presented by Reuter and Hammershøi [Reut 06]. It was based on the experimental results presented by Whitehead [Whit 95b], where different level combinations L_1/L_2 where tested at three geometric-mean frequencies (1.39, 2.79 and 5.57 kHz), with $f_2/f_1 = 1.21$. This study revealed that the combination of primary levels $L_1/L_2 = 65/45$ dB provided relatively high DPOAE amplitude, and it appeared to be a good compromise for measuring presence of fine structure.

8.1.3 Frequency range

As stated by Reuter and Hammershøi [Reut 07], the prevalence of the fine structure is stronger in the mid frequency range from 1 kHz to 3 kHz. It was claimed that the DPOAE fine structure presents higher ripple prevalence at 2.5 kHz.

Therefore, it is chosen to perform the measurements of the DPOAE fine structure within a frequency range so that both f_2 and the distortion product frequency f_{dp} cover one octave band centered at 2 kHz (from 1.4 to 2.8 kHz). Thus, 17 pairs of primary tones are presented within a range of 200 Hz for $f_2 < 3000$ Hz, and within a range of 400 Hz for $f_2 > 3000$ Hz (with f_2 from 1300 Hz to 4700 Hz).

8.2 ILO96

The DPOAE measurements function of the ILO96 system is used for screening the DPOAE fine structure by means of the DP-gram test. A DP-gram test consists of measuring the distortion product $2f_1 - f_2$ amplitude with fixed stimulus intensities L_1 and L_2 and primaries ratio f_2/f_1 at several discrete frequencies f_2.

The DP-gram test allows to setup the following parameters that remain constant during the measurements:

- level of the primary frequencies: L_1 and L_2
- primaries ratio f_2/f_1
- frequency resolution

- f_2 central value of the sweeping

In order to measure the DPOAE fine structure a high resolution is needed. Therefore, to screen the frequency range specified in Section 8.1.3 several DP-gram test should be carry out, due to the resolution limitation of the ILO system. The DPOAE measurements procedure is detailed in Appendix C.

9
Fine structure detection algorithm

This chapter introduces an algorithm to classify fine structure in DPOAE and high resolution threshold measurements. The procedure for the detection of separate ripples is outlined as well as the choice of the parameters for the classification.

The existence of fine structure in hearing threshold or otoacoustic emissions is often determined just by visual inspection. In order to analyze the obtained data, an objective classification of the fine structure is required. Hence, an algorithm has to be developed to detect fine structure in threshold or otoacoustic emissions and to extract the main characteristics of a ripple. These characteristics allow an overall statistical analysis of the experiment results, even though the fine structure varies from subject to subject.

The implemented fine structure detector is based on two different algorithms: Heise et al. [Heis 08] introduced a method for the detection of significant extreme values in threshold fine structure, whereas Reuter and Hammershøi [Reut 05] developed an algorithm for the classification of DPOAE fine structure.

The determined fine structure is separated into single ripples, which are analyzed individually. A ripple is characterized by a maximum and two neighboring minima. As stated before, a more detailed description of the ripples is needed. Hence, the main characteristics are defined by the following parameters:

- **ripple spacing**, which describes the frequency spacing between the two minima
- **ripple height**, which is the level difference between the maximum and the average of the two minima

In order to be accepted as fine structure, adjacent extreme values have to fulfill specific requirements: the level difference between adjacent minima and maxima should be higher than a minimum level ΔL_{min} and the ripple spacing should be in a range between Δf_{min} and Δf_{max}.

Reuter and Hammershøi [Reut 06] reported a ripple spacing between 1/21 and 1/6 octaves for DPOAE fine structure, whereas Heise et al. [Heis 08] proposed a criterion for the spacing of two adjacent extreme values (minimum - maximum) between 1/50 and 1/10 octaves. The chosen parameters $\Delta f_{min} = 1/25$ octaves and $\Delta f_{max} = 1/5$ octaves are based on Heise's proposal and agree with the observations of Reuter and Hammershøi.

For DPOAE measurements, $\Delta L_{min} = 3$ dB was chosen according to Reuter and Hammershøi [Reut 06], since a high number of low-level variations appears in the measurements. However, thresholds show in general a lower ripple height, but also less fluctuations which are not considered as fine structure. Hence, the minimum level criterion applied for the detection of threshold fine structure is set to $\Delta L_{min} = 2$ dB.

9.1 Detection procedure

The detection of relevant extreme values which characterize a ripple follows an iterative process. Each detection starts at a maximum with the frequency f_{max}. All minima within the range $[f_{max} - \Delta f_{max}, f_{max} + \Delta f_{max}]$ which fulfill the criterion of ΔL_{min} are used for further analysis. In the following, minima at frequencies lower than f_{max} will be referred to as 'left' minima (according to their position in the graph regarding the maximum) and minima at frequencies higher than f_{max} as 'right' minima. For the selection of those minima which can be considered to represent a ripple, the left and the right minima are analyzed individually.

Figure 9.1 presents two examples for the detection of minima and maxima as fine structure elements. The 'X' denotes the maximum under current analysis. Minima in the range $[f_{max} - \Delta f_{max}, f_{max} + \Delta f_{max}]$ are marked with a circle. Whether an extreme value is accepted or not is explained in the following.

Minima that are more separated in frequency from f_{max} than closer minima presenting a lower level are neglected, since they do not represent an absolute minimum in the range of a ripple. Furthermore, if two minima are separated by a maximum which fulfills the ΔL_{min}-criterion, the minimum with a higher distance in frequency regarding f_{max} is neglected in the current analysis as well, since it is considered to belong to a new ripple.

This is illustrated in the threshold curve of Subject 12 in Figure 9.1. Minima 1 and 2 are considered to be left, and 3 and 4 right minima. Minimum 1 is not considered as a possible minimum representing a ripple around f_{max}, because minimum 2 appears at lower level, whereas minimum 4 is neglected because of the maximum between 3 and 4 which may represent separate ripple.

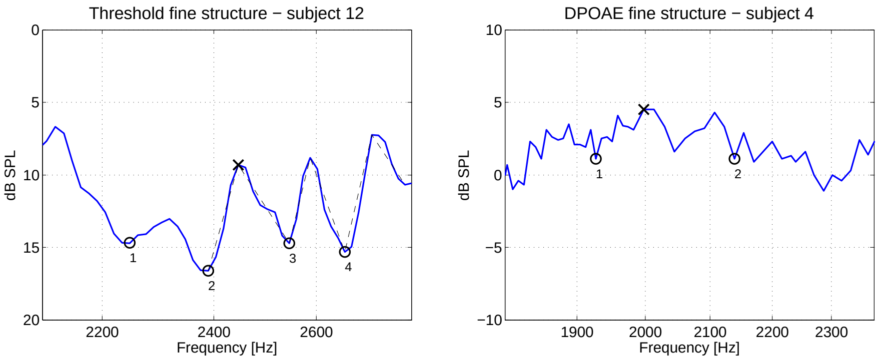

Figure 9.1: Segments of the threshold curve from subject 12 (left) and DPOAE curve from subject 4 (right). Minima which fulfill the criteria with respect to the maximum (marked with 'X') are indicated by circles. The dashed line shows the finally accepted extreme values which characterize the fine structure.

The maximum under analysis is considered as subsidiary and will therefore be neglected if one of the following cases occur:

- No left or no right minimum is detected.
- No pair of left and right minima are separated by frequency spacing between Δf_{min} and Δf_{max}.
- A higher maximum appears between the closest left and right minima, meaning that the current maximum does not represent an absolute maximum in the analyzed range.
- The relation of the frequency spacing of the closest detected minima to the ripple height is higher than $\frac{\Delta f_{max}}{(2\,\Delta L_{min})}$, meaning that the lower the height of the ripple the narrower it has to be.

The latter restriction is due to detections in curves as a result of low fluctuations and not of real existing fine structure. This can be observed in the DPOAE measurement of subject 4 in Figure 9.1, where the minima 1 and 2 would fulfill the initial requirement regarding the maximum marked with an 'X', but obviously those extreme values do not represent a ripple.

Once a maximum is neglected the whole procedure continues at the next maximum at a higher frequency.

If the maximum fulfills all requirements, the remaining left and right minima are analyzed further in pairs of all possible combinations. An ideal ripple is considered to have following characteristics:

- the frequency of the maximum is centered between the frequencies of the two adjacent minima
- both adjacent minima have the same level
- the height of the ripple is as high as possible

Hence, the pairs are analyzed regarding those three criteria. The two minima, which are closest to this ideal ripple are accepted and characterize a ripple together with the current maximum.

9.2 Modifications for DPOAE fine structure detection

For the detection of fine structure in DPOAE measurements, the algorithm is slightly modified compared to the threshold fine structure detector. The ILO system analyzes additionally the noise around the distortion product. It is represented by two curves. The lower curve indicates one standard deviation and the higher two standard deviations from the background noise, thus specifying the limit of the 95 % confidence region. According to the algorithm proposed by Reuter and Hammershøi [Reut 06], ripples shall be rejected whenever a maximum is less than 3 dB above the limit of 95 % confidence region. However, minima below this curve are still regarded for the analysis.

Furthermore ripples in the DPOAE fine structure often appear higher than threshold ripples and show typically very narrow notches characterizing a minimum. Absolute maxima of ripples are not necessarily centered between the two minima, hence the detection of the optimal pairs of minima is weighted more to ripple height than to an equally frequency spacing.

10
Experiment design

In this chapter the motivation for conducting an experiment to screen threshold and DPOAE fine structure is presented. The experiment procedure is also described. Finally, the strategy followed for the analysis of the results is outlined.

10.1 Motivation

Otoacoustic emissions measurements are nowadays mainly employed for screening hearing loss, providing an objective tool for hearing assessment. However, knowledge of the relationship between OAE and threshold curves is required in order to use OAE in clinical diagnosis.

As already stated, fine structure can be observed in both threshold and DPOAE measurements. Investigating the nature of the relationship between threshold and DPOAE fine structure is the focus of this project. Both measurements provide information about the active cochlear processes. Moreover, similar periodicity in the OAE and threshold fine structure has been reported in the literature, suggesting a common origin in their mechanism of generation.

Hence, an experiment was conducted where the threshold and DPOAE fine structure of different subjects were measured and the results were analyzed in order to find a relationship between them.

The DPOAE measurements were carried out using a calibrated commercial system (see Chapter 7), and the threshold fine structure was tracked with the implemented high resolution audiometer (see Chapter 8). To be able to rely on the determined threshold curves, correspondent validation tests were necessary. A comparison with a standard audiometry results and a test/retest were conducted for this purpose.

Direct comparison of the threshold and DPOAE curves is complex and not always possible. A thorough analysis of individual and averaged results should be regarded instead. Thus, the fine structure detector implemented (see Chapter 9) was applied to objectively study the relationship between the presence, periodicity and level of the threshold and DPOAE ripples.

Theoretical models of the cochlea have tried to explain the mechanisms of generation of fine structure in the threshold and DPOAE. Comparison of these models with the experimental results can be useful to find out a possible relationship between both generation mechanisms.

10.2 Procedure

The experiment was carried out in the Acoustics Laboratory in Aalborg University, Fredrik Bajers Vej 7, 9220 Aalborg E.

A total number of 12 subjects (7 males and 5 females), between 20 and 31 years of age, participated in the experiment. Two of the subjects suffered of undiagnosed occasional tinnitus. One subject had surgery at the age of 3 and another subject suffered from otitis during childhood. All the subjects showed neither a severe hearing impairment nor an exceptional hearing sensitivity.

The experiment consisted of three tests:

1. Standard audiometry
2. High resolution audiometry
3. DPOAE fine structure measurements

Before starting the experiment the subjects were asked not to come directly from a noisy environment. Thus, at least during half an hour prior to the experiment they should stay in a relaxed and advisable quiet atmosphere.

The subject were suitably instructed before starting the tests (see Appendix F). They were also asked to fill in a questionnaire (see Appendix G), to obtain general information about the subjects and their hearing status. Breaks of 5 minutes were included between the tests in order to ensure the comfort of the subjects. This way they could stay concentrated during the performance of the tests when required.

The first test carried out in the experiment was the standard audiometry. The standard audiometry was conducted to obtain an estimate of the absolute threshold level at a discrete number of frequencies. In Appendix

A the equipment, test setup and procedure used to perform the standard audiometry are described. The test lasted approx. 10 minutes.

The second test was the high resolution audiometry. Its aim was to screen the subject's threshold fine structure. The procedure and setup of the test, which lasted approx. 20 to 25 minutes, is described in detail in Appendix B.

The third test was the DPOAE fine structure measurements. This test did not imply the active participation of the subjects. The subject's DPOAE fine structure was measured with the ILO96 system as described in Appendix C. The test had a duration of approx. 20-30 minutes.

In order to test the reliability of the implemented high resolution audiometer a subset of 4 subjects (2 males and 2 females) performed the high resolution audiometry test twice. The first test was conducted at least one week before the retest, which was performed together with the standard audiometry and the DPOAE measurements. The reasons for conducting the test/retest threshold screening experiment in different days was entirely practical, maintaining the duration of the main experiment to less than one and a half hours.

10.3 Analysis strategy

The analysis of the results is divided in three parts:

- Comparison of Standard and High resolution audiometry results
- High resolution audiometer reliability
- Relationship between DPOAE and threshold fine structure

The strategy used in each part of the analysis is described in the following sections.

10.3.1 Comparison of standard and high resolution audiometry results

The main purpose for conducting the standard audiometry test is to obtain an estimate of the absolute threshold level at a discrete number of frequencies. Since threshold tracking methods are not expected to be precise absolute threshold level estimates [Heis 08], the standard audiometry performed in a wider range is conducted to provide information regarding the hearing status of the subjects.

However, the results from the standard and high resolution audiometry tests can be compared to check whether the thresholds present similar distribution. The common frequency points within the two audiometries can be analyzed for this purpose. At each analyzed frequency, the results across the subjects from the two audiometries represent two groups of data. To check whether the two groups of data are significantly different or not (or equivalently, how much the mean of the thresholds differs), a Two-sample t-Test can be conducted thus considering the null hypothesis [Ross 04]:

- H_0: $\mu_x = \mu_y$, the threshold distributions do not present significant differences.

The average across the subjects at the common frequencies of both tests is compared with the ISO 389 reference curve of the hearing threshold.

10.3.2 High resolution audiometer reliability

The reliability of the implemented high resolution audiometer is analyzed as the repeatability of the test/retest experiment. The aim of this analysis is to check how reproducible the screening of the threshold fine structure is when the test is performed twice by the same subject.

Thus, the similarity between the shape of the thresholds is rated by calculating the correlation coefficient r as follows [Heis 08]:

$$r(T_1, T_2) = \frac{(T_1 - \bar{T_1}) \bullet (T_2 - \bar{T_2})}{\left|T_1 - \bar{T_1}\right| \left|T_2 - \bar{T_2}\right|} \tag{10.1}$$

where T_1 and T_2 are the vectors containing the two determined thresholds, $\bar{T_1}$ and $\bar{T_2}$ are the mean values of the threshold curves and $\bullet$ denotes the dot product of two vectors.

Since the implemented high resolution audiometer is designed to track threshold fine structure, the reproducibility of ripples is also analyzed. The difference in the ripple prevalence[1] among the analyzed frequency range is studied. The reliability of position and height of the ripples should be checked by reporting frequency shifting of the extreme values and deviation in ripple height and ripple spacing.

[1]The ripple prevalence is the percentage of DPOAE or threshold curves classified as fine structure within a specific frequency range.

10.3.3 Relationship between DPOAE and threshold fine structure

By simple visual inspection of the shape of threshold and DPOAE curves it is very complicated to try to establish a relationship between them. Hence, the implemented fine structure detector algorithm described in Chapter 9 is used to extract the characteristic features of the fine structure. Thus, an objective criterion is obtained, providing a suitable tool for comparing threshold and DPOAE fine structure.

From the detected ripples objective parameters such as the ripple prevalence, spacing and height can be analyzed.

Since the generation of both fine structures is a complex phenomenon and they vary from subject to subject, not only average result have to be considered, but also an individual analysis should be included.

The frequency range in the DPOAE measurements is chosen allowing direct comparison of the threshold curve with the DP-gram as a function of $2f_1 - f_2$ and f_2 for the same subject. The tonotopic locations of $2f_1 - f_2$ and f_2 are regarded as the DPOAE generation sites. An individual analysis of the results is made in order to investigate the influence of cochlear mechanisms on the generation of threshold and DPOAE fine structure. The comparison of both curves as a function of $2f_1 - f_2$ and f_2 may reveal the influence of the generation sources on the DPOAE fine structure and level. The influence of the generation sources is assumed to be dependent on the information given by the threshold regarding the cochlea status.

Different authors have developed analytical models of the cochlear behavior. This models try to explain the complicated generation processes of threshold and OAE fine structure, which are still not fully understood. Nevertheless, the implementation of cochlear models can be beneficial to analyze the experimental results.

11 Results

The results obtained from the three tests carried out in the experiment are shown in the Appendices A, B and C respectively. In this chapter a detailed analysis of the results is presented.

The analysis of the results is divided in three parts, following the strategy presented in Section 10.3. The first part consists of comparison of the results obtained from the standard and high resolution audiometries. The next part examines the reliability of the implemented high resolution audiometer regarding the shape of the threshold and fine structure detected. Finally, the last part of the analysis focuses on the relation between the threshold and DPOAE fine structure.

11.1 Comparison of standard and high resolution audiometry results

No severe hearing impairment is observed in any of the standard audiometry results. Neither an exceptional good hearing characterizes any of the subjects.

A comparison between the thresholds determined using the standard audiometer, based on the ascending method, and the implemented audiometer, based on the FINESS algorithm, is carried out. Figure 11.1 shows two examples of threshold obtained by the two audiometries. To facilitate the visual comparison between both results, the high resolution thresholds are vertically shifted minimizing the square difference between thresholds.

Differences can be observed between the two methods when comparing individual results. The difference in level between both audiometric measurements is evidenced. For Subject 6, the shapes of the two thresholds are similar. However, for Subject 2 there are significant differences (i.e. at 1800

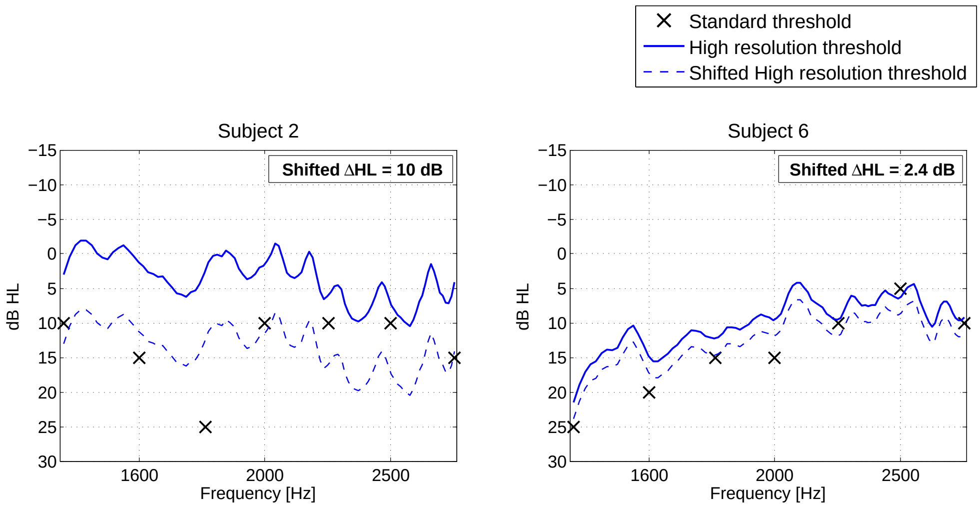

Figure 11.1: Comparison of the standard and high resolution audiometry results for subject 2 and 6.

Hz). From the individual data it can not be concluded why such differences appear.

Consequently, a Two-sample t-Test is conducted in order to check whether the thresholds determined with the standard and high frequency resolution audiometers present a similar distribution. Since the Two-sample t-Test is conducted in order to check if the mean of two groups of data differs, the shifted high resolution threshold values are used for the analysis. Seven frequency points, common for both measurements, are analyzed. For each analyzed frequency, the distribution of the two groups of 12 threshold values (from the 12 subjects) is compared. The p-value obtained for each frequency are presented in Table 11.1.

Frequency	1400	1600	1800	2000	2240	2500	2800
p-value	0.6909	0.1246	0.3896	0.6487	0.0481	0.0342	0.9814

Table 11.1: p-value obtained from the Two-sample t-Test for the analysis of the similarities in the distribution of the standard and high frequency resolution audiometry results, at 7 common frequencies.

For a level of significance of 1 % the null hypothesis can not be rejected for all the frequencies. Therefore, it can not be stated that significant differences between the distribution of the two audiometric measurements exits.

The average across the 12 subjects at each common frequency and the correspondent standard deviation between subjects are shown in Figure 11.2.

The results are compared with the average reference curve proposed in the ISO 389.

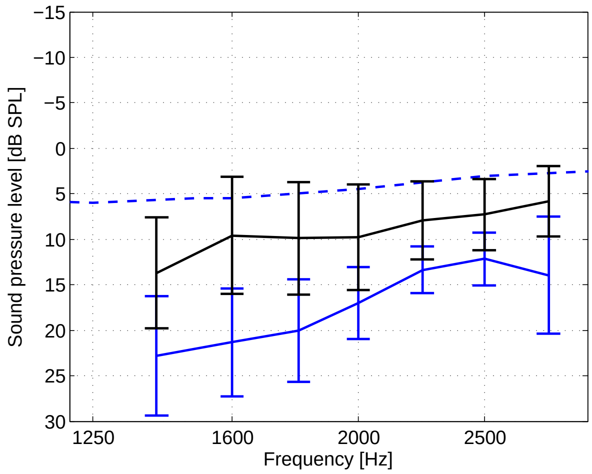

Figure 11.2: Average and standard deviation, at the common frequencies, of the thresholds determined with the standard audiometer based on the ascending method (blue) and with the high resolution audiometer (black). The results are compared with the hearing threshold reference curve proposed in ISO 389 (dashed).

The average curve obtained for the high resolution audiometer is more similar to reference curve. Information about the standard deviation from the average reference for audiometric results using the Sennheiser HDA 200 headphones is not provided in the ISO 389. However, in the reference curve for the HDA 200 headphones reported by Poulsen et al. [Han 89], the standard deviation within the studied frequency range is around 5 dB SPL. Therefore, the average data from the high resolution audiometry will fall into the range of the standard deviation from the average reference curve.

The average of the determined high resolution thresholds is still higher than the reference. This can be expected since almost non of the subjects reported an absolute threshold higher than 0 dB HL at any frequency. The differences between the population that participated in the current experiment compared to the experiments conducted to obtain the reference curve given in ISO 389, have to be considered. For instance, the number of subjects that participated in the current experiment is smaller and they are also older regarding the average age.

The average values of the threshold obtained with the standard audiometer are higher than the reference and the results provided by the implemented audiometer. According to Lydolf [Lydo 99], the ascending method produces very high threshold level when compared to the 50 % detection level definition of the threshold.

11.2 High resolution audiometer reliability

A test/retest high resolution audiometry was conducted with four of the subjects (see Chapter 10) in order to check the reliability of the implemented high resolution audiometer.

The results of the test/retest measurements are summarized in Figure 11.3. The correlation coefficient r (see Equation 10.1) gives information regarding the correlation between the output thresholds from the two experiments in terms of overall shape.

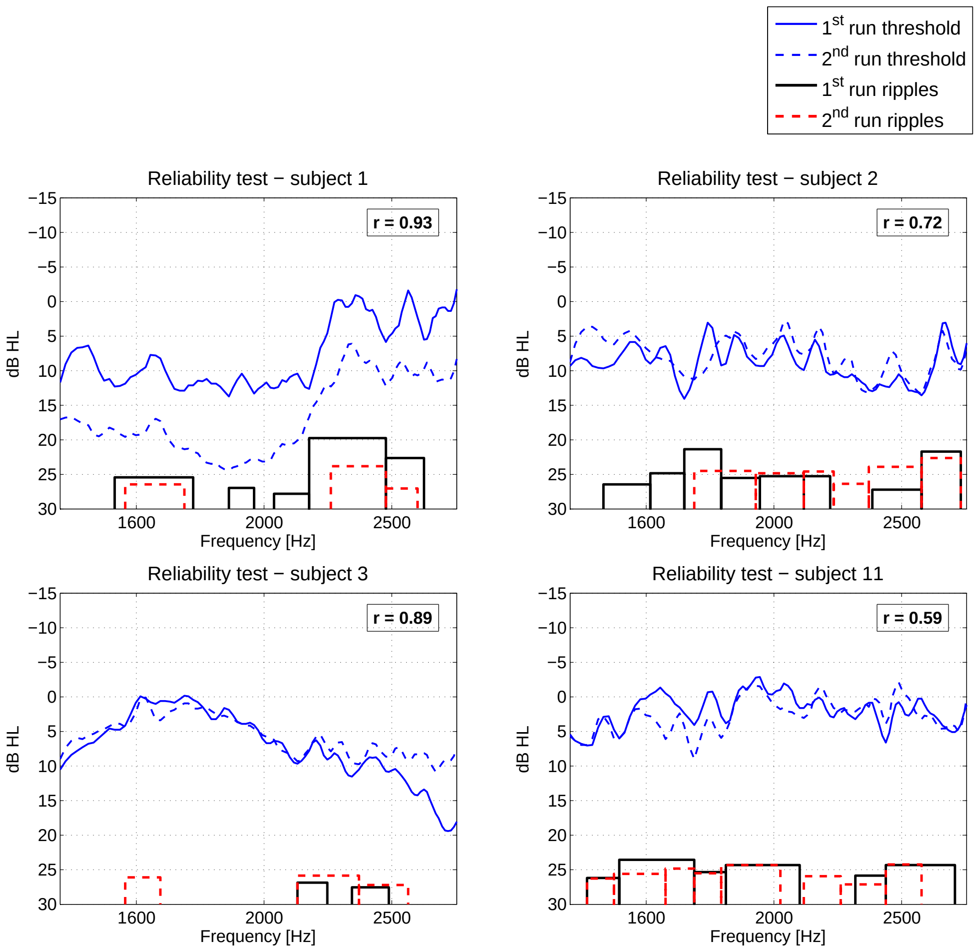

Figure 11.3: Test/retest of the high frequency resolution audiometer based on the FINESS algorithm [Heis 08] results.

Subject 1 presents the best correlation between the shape of the two thresholds, despite the level differences. On the other hand, Subject 11 shows the weakest correlation but there are no significant differences regarding the absolute level. The lack of correlation is this case appears due to differences in the shape of the thresholds mainly in the frequency range from 1.5 kHz to 1.9 kHz.

The resulting average correlation coefficient is 0.82[1]. This indicates that, in general, the audiometer provides a good reproducibility of the shape of the threshold, whereas the level is not necessarily precise.

Since the audiometer is implemented to screen fine structure in the threshold, it is important to check how precisely the distribution of peaks and valleys is reproduced. Therefore, the ripple parameters obtained by applying the fine structure detector to the two determined curves are analyzed.

The results of the analyzed prevalence of threshold fine structure in the test/retest measurements are presented in Table 11.2. The average difference between the percentage of ripple prevalence in test and retest is 13.9 %, whereas the average of equally judge frequency ranges[2] is 74.2 %, showing a good reproducibility of the audiometric system regarding ripple prevalence.

Subjects	1	2	3	11
1^{st} Test	65.7 %	79.8 %	19.2 %	77.8 %
2^{nd} Test	38.4 %	73.7 %	39.4 %	75.8 %
Equally judge ranges	72.6 %	69.7 %	79.8 %	77.8 %

Table 11.2: Percentage of threshold ripple prevalence in each measurement (first and second rows) and percentage of equally judge frequency ranges comparing the two measurements (third row).

The shifting of frequency regarding the absolute maximum of the ripples, and the spacing and height deviation of the coincident detected ripples in the test/retest thresholds, are presented in Tables 11.3, 11.4 and 11.5 respectively.

The average frequency shifting of the frequencies corresponding to the maximum ripple level individually, between the test/retest thresholds is 1/68 octaves (or 1.01 %), with a standard deviation of 1/67 octaves (or 1.03 %).

The ripple spacing deviation is 1/28 octaves for the average across subjects, with a standard deviation of 1/30 octaves between subjects. The ripple

[1] The average correlation coefficient is calculated by applying Fisher's transformation to the correlation coefficients, calculating the arithmetic mean of the transformed coefficients and transforming it back by the inverse Fisher's transformation [Heis 08].

[2] The equally judge frequency ranges are the frequency ranges which classification as fine structure or not is coincident in the test and retest measurement.

Subjects	1	2	3	11	All
Average [octaves]	1/81	1/179	1/113	1/38	1/68
Standard deviation [octaves]	1/339	1/162	1/2450	1/52	1/67

Table 11.3: Frequency shifting in octaves of the frequencies corresponding to the maxima of the threshold ripples, when comparing the coincident ripples in the test/retest results.

Subjects	1	2	3	11	All
Average [octaves]	1/25	1/69	1/18	1/20	1/28
Standard deviation [octaves]	1/57	1/50	1/41	1/26	1/30

Table 11.4: Spacing deviation in octaves of the coincident ripples in the test/retest results.

Subjects	1	2	3	11	All
Average [dB SPL]	3.2	1.0	0.6	0.5	1.2
Standard deviation [dB SPL]	1.5	1.1	0.4	0.5	1.4

Table 11.5: Height deviation in dB SPL of the coincident ripples in the test/retest results.

height variates on average 1.2 dB SPL with a standard deviation of 1.4 dB SPL.

The high correlation between the test and retest results indicates that the implemented high resolution audiometer is reliable. Therefore, it can be used to track hearing threshold and proceed to the analysis of the relationship between threshold and DPOAE fine structure.

11.3 Relationship between DPOAE and threshold fine structure

A possible relationship between the threshold and DPOAE fine structure obtained in the experimental results is analyzed here.

First, a study of the fine structure parameters ripple prevalence, ripple spacing and ripple height is made, taking into account both the pooled and the individual results.

Then, the subjects are gathered into different groups regarding their DPOAE measurement results. The threshold and DPOAE characteristics shown within each group are studied in detail.

An rough analysis of this ripple parameters is also presented in Appendix D, where the threshold measurements are compared to the DPOAE measurements as a function of the distortion product frequency $2f_1 - f_2$, the primary frequency f_2 and the geometric mean of the two primaries $\sqrt{f_1 f_2}$. DPOAE plotted as a function of f_2 and $\sqrt{f_1 f_2}$ are very similar. Further analysis will only present the comparison of the results as a function of $2f_1 - f_2$ and f_2, regarded in the literature as the two sources responsible for DPOAE generation.

However, it is of course a point for discussion whether the distortion product component is generated closer to f_2 or $\sqrt{f_1 f_2}$. Since the excitation signal used in the DPOAE measurements was chosen with a difference of primary levels higher than 20 dB ($L_1/L_2 = 65/45$ dB), it is considered that the f_2 place will be more representative of the distortion component generation site. With $L_1 > L_2$, the f_1 traveling wave is expanded towards the base and its excitation peak is also shifted in the same direction, resulting on the frequency shift of the overlap region towards f_2 according to He and Schmiedt [He 97].

11.3.1 Prevalence

The ripple prevalence is analyzed to objectively quantify the amount of fine structure present within the frequency range under study. This allows to check if the presence of fine structure in threshold involves presence of DPOAE fine structure or vice versa.

Figure 11.4 shows the average of ripple prevalence in the threshold and in the DPOAE measurements for each subject, within the frequency range from 1.4 kHz to 2.8 kHz.

It is observed that in general the threshold prevalence is lower than the DPOAE prevalence. Subjects 2 and 11 present a prevalence of the threshold ripples higher than 70 %. This corresponds in both cases to a presence of DPOAE ripples of 90 % or higher as a function of f_2. This suggests that in general more fine structure is present in the DPOAE than in the threshold curves. Just subject 7 presents a higher prevalence in threshold than DPOAE.

The average across subjects of the ripple prevalence is shown in Figure 11.5 in 1/3 octave bands. It can be seen that the prevalence of DPOAE ripples as a function of f_2 presents the highest value at the mid frequency range centered at 2.5 kHz. Similar results are reported by Reuter and Hammershøi [Reut 06]. The maximum ripple prevalence in the threshold fine structure also appears in the 2.5 kHz band. A correlation between the prevalence curves of the threshold and DPOAE as a function of f_2 can be noticed.

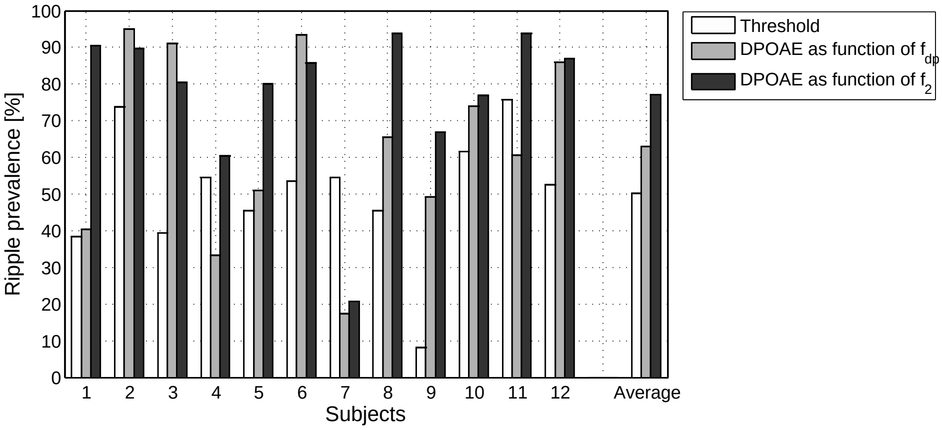

Figure 11.4: Average ripple prevalence for each subject, within the frequency range from 1.4 kHz to 2.8 kHz.

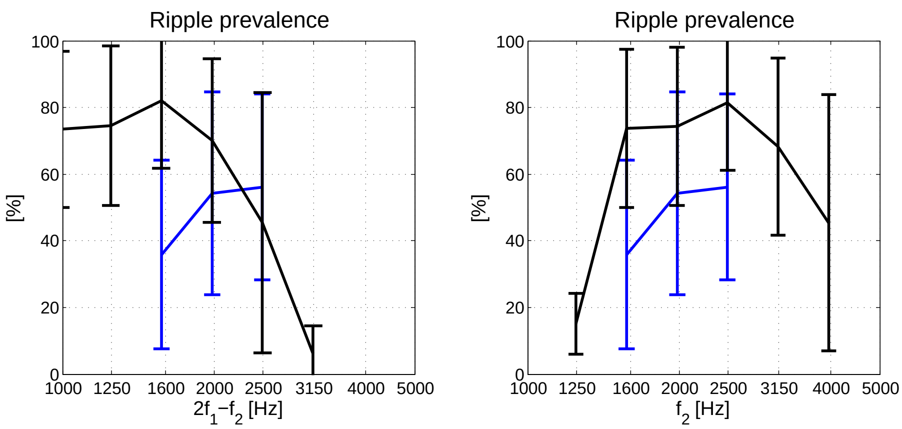

Figure 11.5: Average ripple prevalence across subjects of the threshold (blue) and DPOAE (black) fine structure, analyzed in 1/3 octave band. The errorbars represent the standard deviation between subjects.

11.3.2 Spacing

The ripple spacing is analyzed in order to establish a possible relationship between the threshold and DPOAE fine structure periodicity.

The threshold and DPOAE ripple spacing in octaves is presented in Figure 11.6 for each subject, within the frequency range from 1400 Hz to 2800 Hz. The individual results fluctuate between 1/25 and 1/6 octaves.

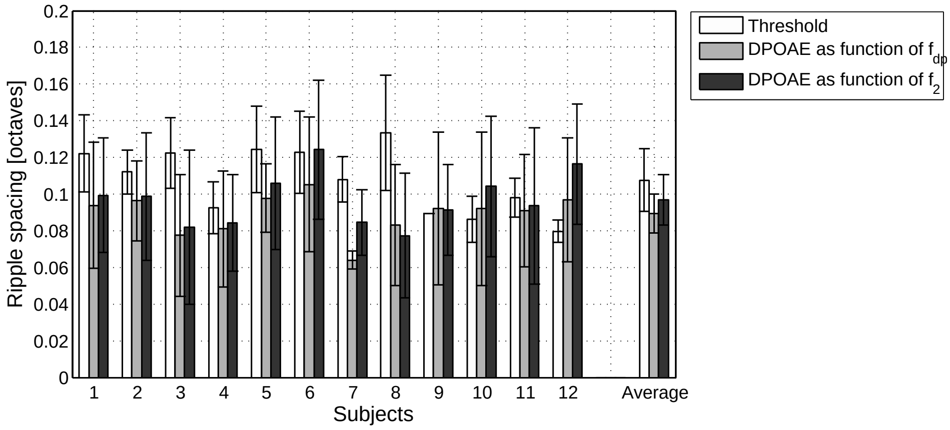

Figure 11.6: Ripple spacing in octaves for each subject.

The ripple spacing analyzed in 1/8 octave bands for each subject and averaged over all the subjects is presented in Figure 11.7, in octaves and in Hz respectively.

The threshold ripple spacing fluctuates around 1/10 octaves, with a maximum average spacing over all subjects of 1/8 octaves and a minimum of 1/15 octaves. At the lowest frequency the average spacing is 70 Hz and it increases up to 193 Hz on average at higher frequencies. In the literature there is no agreement on the exact periodicity range of the threshold fine structure. It varies from one study to another [Heis 08].

When analyzing the DPOAE ripple spacing as a function of $2f_1 - f_2$ the average spacing is 1/11 octaves with a standard deviation of 1/72 octaves. Hence, the spacing increases from 47 Hz at the lowest frequency up to 154 Hz at high frequencies. If the DPOAE ripple spacing is now analyzed as a function of f_2 the average spacing is also 1/11 octaves, with a standard deviation of 1/69 octaves. This corresponds to a spacing from 68 Hz at the lowest frequency to 255 Hz at high frequencies.

The ripple spacing is however dependent on the parameters defined by the fine structure detector (see Chapter 9). When an objective fine structure detector algorithm is designed, it is necessary to define some parameters that establish the rules to neglect or accept ripples as fine structure. Those parameters are based in general on a compromise between frequency spacing and level height of the ripples, meaning that specific values of those are already expected. This will itself influence the analysis and could therefore be a reason for disagreement among different studies.

Nevertheless, a similar growth is observed in the DPOAE ripple spacing as a

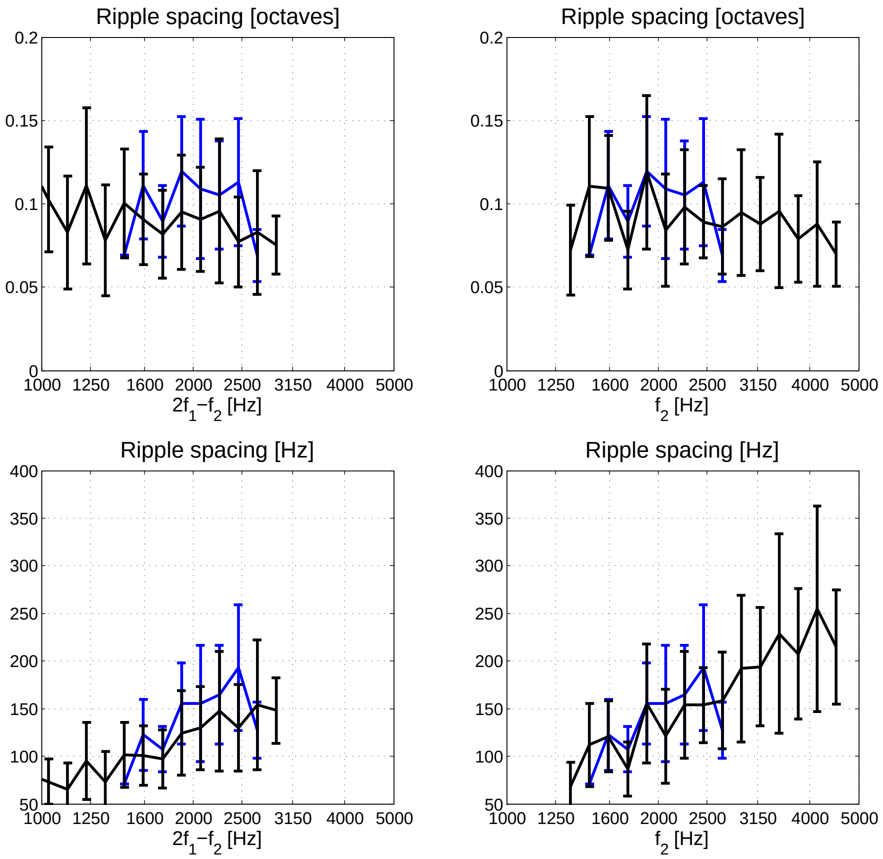

Figure 11.7: Ripple spacing averaged across subjects in octaves (up) and in Hz (bottom), of the threshold (blue) and DPOAE (black) fine structure, analyzed in 1/8 octave bands. The errorbars represent the standard deviation between subjects.

function of f_2 when compared to the results presented by Reuter and Hammershøi [Reut 06]. Moreover, this pseudo-linear growth curve appears to be in concordance with the threshold ripple spacing as a function of frequency. When looking at the results in octaves, the average spacing curves present a flat tendency, revealing a more or less constant periodicity. Therefore, the similarity on the threshold and DPOAE fine structure suggested in Chapter 5 appears to be confirmed by the experimental results.

11.3.3 Height

The average and standard deviation of the threshold and DPOAE ripple height, calculated for each subject within the frequency range from 1400 Hz to 2800 Hz, is presented in Figure 11.8. The DPOAE ripples are in general more pronounced than the threshold ripples.

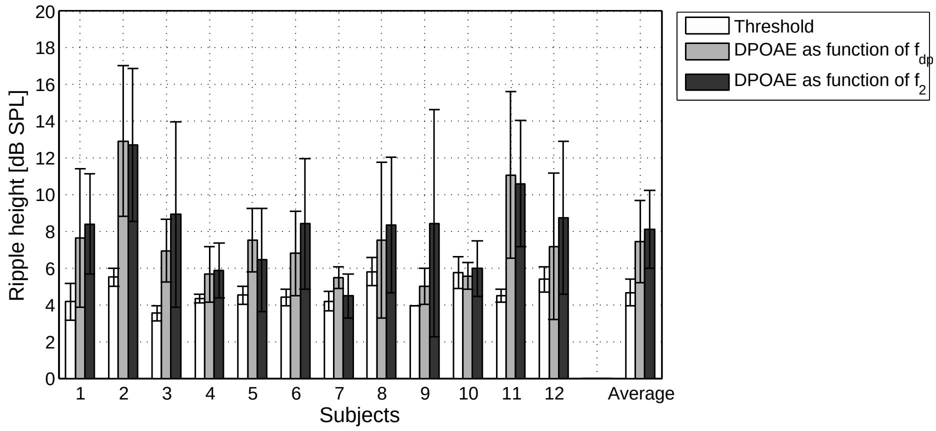

Figure 11.8: Ripple height in dB SPL from each subject.

The average threshold and DPOAE ripple height is shown in Figure 11.9 as a function of $2f_1 - f_2$ and f_2. The height of the ripples is calculated in 1/8 octave bands and averaged over the 12 subjects.

The threshold ripple height fluctuates around 4.8 dB SPL on average with a standard deviation of 1.4 dB SPL. The height of the DPOAE ripples is 8 dB SPL on average among the analyzed 1/8 octave frequency bands, with a standard deviation of 3.9 dB SPL.

A specific trend as a function of frequency can not be found for the ripple height, neither for the threshold nor for the DPOAE fine structure. However, the threshold ripple height appears to be less fluctuating than the height of the DPOAE ripples.

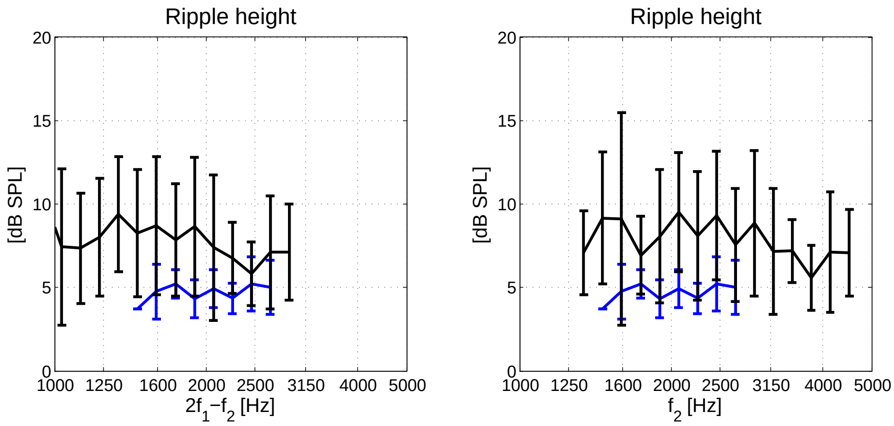

Figure 11.9: Ripple height averaged across subjects in dB SPL, for the threshold (blue) and DPOAE (black) fine structure, analyzed in 1/8 octave bands. The errorbars represent the standard deviation between subjects.

11.3.4 Analysis of individual results

From the visual inspection of the DPOAE measurement individual results, presented in Appendix C, the subjects have been gathered into three different groups. The ripple prevalence in the threshold curves (see Appendix B) within each group of subjects is also analyzed. The specific characteristics of each group are detailed next:

- **Group 1**: Constituted by subjects 2 and 11. These subjects present a very high DPOAE ripple prevalence in the measured frequency range. Furthermore, the ripples are in general significantly high (more than 10 dB SPL on average). When looking at the prevalence of the threshold ripples in Figure 11.4, it can be seen that it is higher than 70 % in both cases.

- **Group 2**: Constituted by subjects 1, 3, 5, 6, 8, 9, 10 and 12. These subjects present also significant amount of DPOAE ripples, but not as high as the prevalence shown by Group 1. The height of the ripples within the measured frequency range is in general lower than 10 dB SPL. The prevalence of the threshold ripples (see Figure 11.4) is around 40 % for subjects 1, 3, 5. Subjects 6 and 12 have a prevalence around 50 %, subject 9 has almost no threshold fine structure and subject 10 presents around 60 % of threshold ripple prevalence.

- **Group 3**: Constituted by subject 4 and 7. These subjects present almost no DPOAE fine structure, however, their results show the highest

DPOAE level and a better signal to noise ratio. The ripple prevalence in the threshold curves is around 55 % in both subjects (see Figure 11.4).

These three groups present very different characteristics. Groups 1 and 3 are constituted only by two people each, however they are of significant interest. They represent examples of opposite phenomena (presence of fine structure versus high DPOAE level). Theoretical models of the basilar membrane have been implemented in order to analyze the different results provided by each group. A description of this model and the results obtained are given in the next chapter.

12
Cochlear model simulations

The results of the high resolution audiometry and DPOAE measurements are to be analyzed with respect to the theory presented in Chapters 3 - 5. For this purpose, simplified cochlear models were implemented and applied to each subject's result with respect to the groups gathered in Chapter 11.

12.1 Analytical models

In order to analyze the individual data, simulations of the cochlear behaviour have been implemented following simplified versions of the models by Talmadge et al. [Talm 98] described in Chapter 5. Considering an ideal uniform behaviour of the cochlea (absolute values of all reflectances are independent of frequency), two major cases have been studied to evaluate the DPOAE fine structure:

- the amplitude of the reflection component is higher than the amplitude of the distortion component ($a_{refl} > a_{dist}$)
- the amplitude of the reflection component is lower than the amplitude of the distortion component ($a_{refl} < a_{dist}$).

The variations of DPOAE according to changes in the cochlear behaviour are presented in Figure 12.1. The condition of the basilar membrane is described by a simple function $E(\omega) \leq 1$ simulating an impaired region, in which $|R_a|$ and a_{dist} are reduced by up to 30 dB:

$$|R_a| = E(\omega) R_{a0} \tag{12.1}$$

$$a_{dist} = E(\omega) a_{dist,0} \tag{12.2}$$

where R_{a0} and $a_{dist,0}$ are the initial absolute values of R_a and a_{dist}.

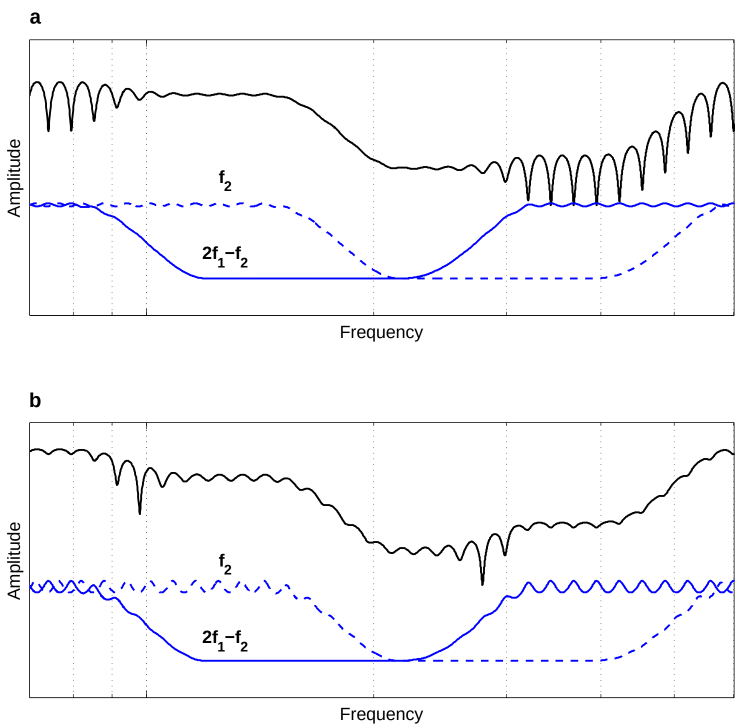

Figure 12.1: Simulated DPOAE (black) and threshold (blue) fine structure as a result of an artificial generated excitation function $E(\omega)$. The DPOAE fine structure appears to be directly dependent on $2f_1 - f_2$. The upper figure (a) presents the behaviour with $R_{a0} = 0.8$, whereas the curves for $R_{a0} = 3$ are presented in the bottom (b).

The amplitudes of the DPOAE and the threshold are calculated according to the simplified models presented in Chapter 5 as follows:

$$a_{DPOAE} = E(\omega_2)a_{dist,0} \cdot \frac{1 + \mathscr{R}_d \cdot E(\omega_{dp})R_{a0}e^{i\phi(\omega_{dp})}}{1 - R_b \cdot E(\omega_{dp})R_{a0}e^{i\phi(\omega_{dp})}} \tag{12.3}$$

$$a_{Threshold} = E(\omega) \cdot \frac{1}{1 - R_b \cdot E(\omega)R_{a0}e^{i\phi(\omega)}} \tag{12.4}$$

Figure 12.1a illustrates the case where $a_{refl} < a_{dist}$, represented by a maximum apical reflectance $R_{a0} = 0.8$ (for simplicity, $\mathscr{R}_d = 1$). The DPOAE fine structure is reduced when $2f_1 - f_2$ falls into an impaired region, whereas the average DPOAE level remains constant. The DPOAE level fluctuates around an average level of a_{dist}. Since a_{dist} is influenced by the BM condition at the tonotopic location of f_2, the overall level changes when f_2 falls into the impaired region. Experiments by e.g. Mauermann [Maue 99] show similar results.

The threshold fine structure disappears almost completely in this model since $|R_a|$ is reduced in the impaired region. Hence, the ripple height is directly related to $|R_a|$ in both DPOAE and threshold fine structure as long as $|R_a| \leq 1$.

A different behaviour occurs, when $|R_a|$ exceeds 1. In this case the overall DPOAE level is also influenced by the reflection component, as illustrated in Figure 12.1b. The maximum apical reflectance is set in this example to $R_{a0} = 3$. This results in a reduction of the DPOAE fine structure due to the unequal levels of a_{refl} and a_{dist}, since the ripples are expected to be highest when $a_{refl} \approx a_{dist}$. Once $2f_1 - f_2$ falls into an impaired region resulting in a decrease of R_a, the DPOAE level is reduced at first while the ripple height increases. When $|R_a|$ falls below 1, the DPOAE show the same behaviour as presented in Figure 12.1a.

Due to the initially high reflectance R_{a0}, the fine structure of the hearing threshold is more pronounced in the second example.

12.1.1 Comparison of the models with individual results

The individual results from the experiment were analyzed with respect to the cochlear models. In order to see similarities between the measurements and the models, an excitation function $E(\omega)$ has been developed for each subject based on the overall shape of the threshold determined with the high resolution audiometer. The Parameters R_{a0}, R_b and $\mathscr{R}_d$ were adjusted individually to find the best correlation with the experimental results. The main purpose of this analysis was to check if the appearance of ripples at specific frequencies is compatible with the models.

An example for a simulated DPOAE and threshold fine structure for Subject 1 is given in Figure 12.2. Similar to the measured results, the models show the highest DPOAE ripples in the range $1800\,\text{Hz} < f_2 < 2600\,\text{Hz}$. Furthermore, the DPOAE level increases while the fine structure decreases for $2f_1 - f_2 > 2200\,\text{Hz}$.

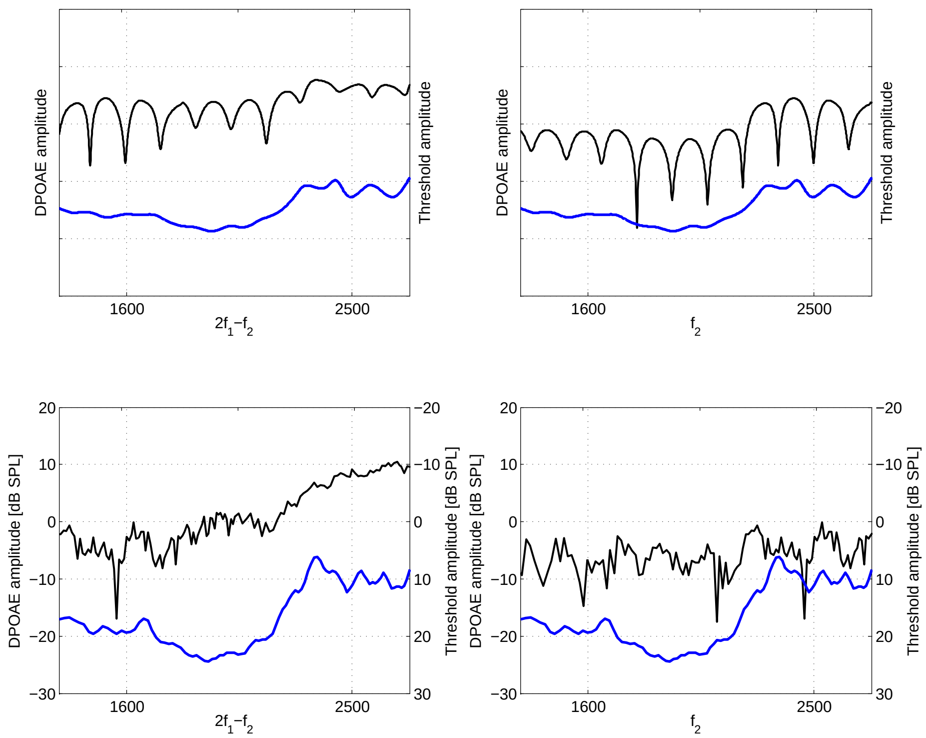

Figure 12.2: DPOAE (black) and threshold (blue) fine structure simulations as a function of $2f_1 - f_2$ and f_2 (top left and right) of Subject 1. For comparison, the results from the measurements are presented as well (bottom).

The performance of the simulations varied a lot among the subjects. Hence, it was checked if a general trend regarding the groups developed in Chapter 11 could be observed.

The two subjects of **Group 1** showed generally pronounced fine structure in DPOAE as well as in the hearing threshold. Since the notches in the DPOAE are very deep, it is expected according to the models that the distortion component and the reflection component have similar levels. The best comparable results where obtained by setting R_{a0} in the models slightly higher than 1. The pronounced ripples in the modeled threshold are supported by comparably high values of R_b. Figure 12.3 shows a representative example for the comparison of the simulations and measurements of this group.

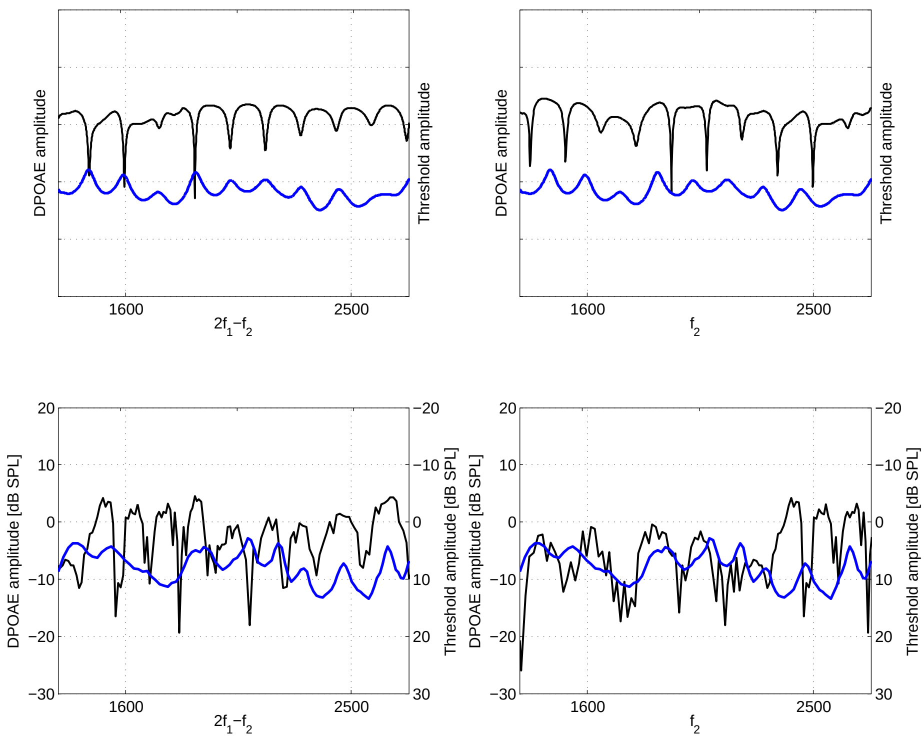

Figure 12.3: Comparison of modeled (top) and measured (bottom) fine structures of Subject 2 (Group 1). Blue lines indicate the threshold and black lines DPOAE.

A completely different picture of fine structure can be seen for the subjects in **Group 3**. Since the threshold shows a higher prevalence of fine structure than the average, high values for either $|R_a|$ or $|R_b|$ are expected. On the other hand the DPOAE measurements show just very little fine structure, but a generally high level. This may be modeled by assuming a strong imbalance between a_{dist} and a_{refl}, leading to an either very high or low value for $|R_a|$. The overall shapes of the threshold and the DPOAE are more similar when the DPOAE is plotted with respect to $2f_1 - f_2$, as shown in Figure 12.4. This assumes a direct influence of $|R_a|$ on the DPOAE level. Hence, a high value for R_{a0} returns the best results.

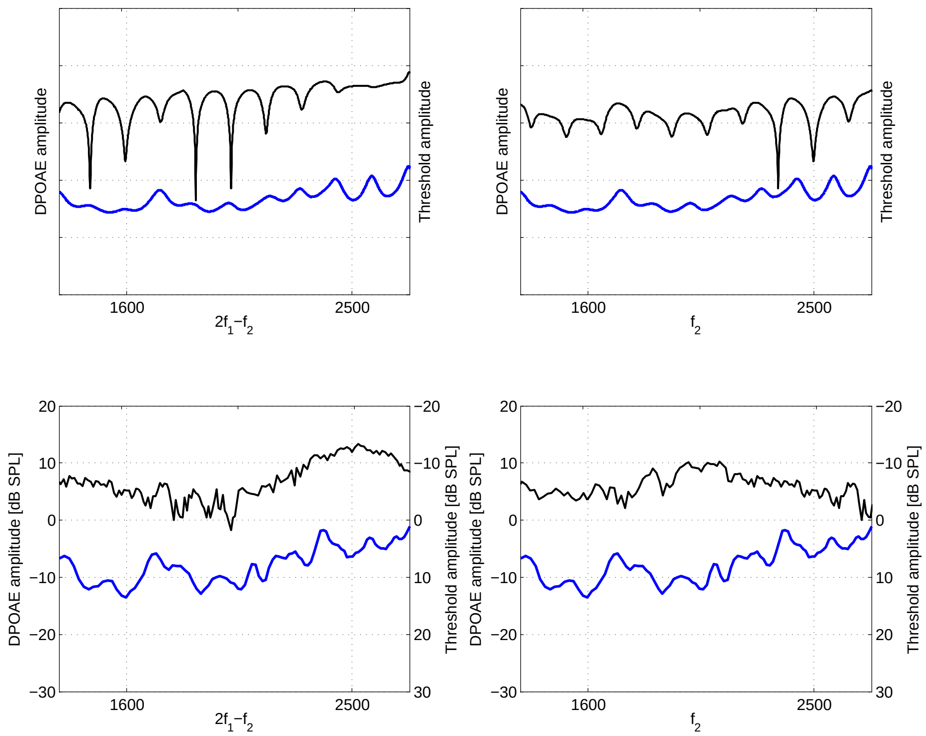

Figure 12.4: Comparison of modeled (top) and measured (bottom) DPOAE and threshold fine structure of Subject 7 (Group 3). Blue lines indicate the threshold and black lines DPOAE. The DPOAE fine structure is reduced when the excitation increases at $2f_1 - f_2$, which is a result of applying a relatively high value for $|R_a|$.

Group 2 represents the majority of the all subject with no remarkable characteristics. Variations among the fine structure, e.g. reduction of ripple height, may have different reasons, for instance $|R_a|$ can be either higher or smaller than 1. Hence, the simulations give a lot of different results and are strongly dependent on the choice of the desired characteristics. A specific trend for the cochlear reflectances of all the subjects in this group can therefore not be observed.

13 Discussion

This chapter evaluates the limitations and compromises of the conducted experiment. Furthermore the results and their validity are discussed and interesting findings are emphasized.

Measurements of fine structures in hearing threshold and otoacoustic emissions require a high frequency resolution and precision regarding small level changes. An increasing resolution usually leads to a higher measurement time, which is a drawback especially regarding psychoacoustic measurements.

Audiometries require full concentration of the subject during the whole test, hence, it is necessary to use a method which provides both a low measurement time and a high resolution. The implemented audiometer based on the FINESS algorithm provides both requirements, but also involves certain compromises.

One compromise is the absolute threshold level. Since the FINESS algorithm is a tracking method, the absolute level might be influenced by several parameters, such as the reaction time of the subject, and is therefore not reliable.

However, the purpose of this experiment was to evaluate the height and the periodicity of low level variations of the individual threshold. For this analysis, the absolute threshold level is of minor importance than the individual shape. The reliability tests showed a high correlation between the same experiment performed in different weeks. Additionally, a comparison with another audiometric method such as the ascending method showed no significant differences. This approved the method to be valid for the purpose of screening threshold fine structure.

Another compromise had to be made regarding the measured frequency range. Just one octave was screened with the high resolution audiometer which lasted approx. 20-25 minutes. For audiometries a longer time is not recommended, since a very high concentration is required. Unfortunately, the range which allows to analyze both excitation regions of the DPOAE regarding the threshold is therefore very small (approx. 1/3 octaves).

The limited time was also a reason for choosing just one set of parameters for the DPOAE measurements. A variation of L_1/L_2 or f_2/f_1 might have shown different and interesting results.

The test was performed with 12 subjects (7 male, 5 female), which were between 20 and 31 years old. None of the subjects showed either a severe hearing impairment or an exceptional high sensitivity. Since the aim was to find a general correlation representing the human average, the subjects were not screened beforehand for any special threshold patterns.

In general, the determined fine structures show a good agreement with reported fine structure data by other authors. However, due to the detection algorithm the results are biased in a certain way. Since there is no clear definition whether variations in DPOAE or threshold are considered as fine structure or not, the limits of the detector were adjusted according to previous investigations. Hence, all parameters like ripple spacing, height and prevalence are influenced by initial restrictions for the classification of a ripple.

The obtained data of DPOAE and threshold fine structure shows on average results which coincide with the theory and the models. The ripple spacing in octaves just shows very little variations among frequency, and both threshold and DPOAE fine structure indicate a common periodicity. Similarities with previous investigation of different authors can also be found regarding the ripple height. In general, the fine structure of DPOAE is more pronounced and shows a higher level difference between adjacent maxima and minima. According to the theory, more parameters are involved in the generation of DPOAE than in the threshold fine structure, hence the higher variation in the ripple height of the DPOAE is comprehensible.

Additionally, a higher prevalence of the fine structure is observed on average for DPOAE compared to the threshold curves. However, regions with a high threshold prevalence do not necessarily show a high prevalence of DPOAE fine structure. A surprisingly high similarity between the two prevalences analyzed in 1/3 octave bands can be found when presenting the DPOAE as a function of f_2. This result can not be explained with the models or previous studies, since the reflection component generated at the tonotopic site of $2f_1 - f_2$ is assumed to be responsible for the appearance of fine structure, whereas the distortion component rather seems to influence the overall DPOAE level.

In contrast, the differences in prevalences of threshold and DPOAE as a function of $2f_1 - f_2$ can be supported by the results of the model simulations. In cases for which the reflection component is stronger than the distortion component, a reduction of the DPOAE fine structure is possible, whereas the threshold fine structure remains or even increases. Subjects 1, 4 and 7 show a similar behavior. Hence, the comparison of those subject's results with the models may lead to the assumption that apical reflectances higher than 1 are possible. This suggests that the cochlear amplifier is strongly involved in the generation of the DPOAE fine structure and may even compensate for differences due to the longer propagation distance of the reflection component.

The reflectances $|R_a|$ applied in the models to achieve a maximum agreement with the measurements seem however to be too high to explain this phenomenon just by the cochlear amplification. Other processes are thus expected to be involved which are not regarded in the simplified models. There will always be numerous limitations when comparing real measurements to cochlear models. Just considering the high individual variations will already make the computation of a perfect model impossible.

14 Conclusion

The purpose of this project was to examine a possible relationship between the fine structures of distortion product otoacoustic emissions (DPOAE) and those of the hearing threshold.

For this purpose DPOAE and threshold fine structures of different subjects needed to be analyzed. An experiment was hence conducted where the hearing threshold and DPOAE were screened with a high frequency resolution.

The theory behind both fine structure phenomena and results from previous researches have been studied beforehand to design the measurement procedure and the strategy for the analysis of the results. Numerous choices had to be made regarding the execution and setup of the experiment, which also involved certain limitations.

A high resolution audiometer was implemented in order to screen the hearing threshold fine structure of each subject. It is based on the "FINESS" algorithm developed by Heise et al. The subject's threshold fine structure was determined in the frequency range between 1400 and 2800 Hz.

The DPOAE fine structure was measured with the Otodynamics ILO96 measurement system with the primary levels $L_1/L_2 = 65/45$ dB SPL and the frequency ratio $f_2/f_1 = 1.22$. The frequency range for f_2 between 1300 and 4700 Hz was chosen in order to evaluate the influences of the two sources considered to be responsible for the DPOAE fine structure.

Twelve subjects participated in the experiment which consisted of three major tests. First, a standard audiometry was carried out to check the overall status of the subject's hearing in the complete analyzed frequency range. The threshold fine structure was screened with the implemented high resolution audiometer in the second test. Finally, the fine structure of the DPOAE was measured.

A comparison of the data obtained from the standard and the high resolution audiometer revealed no significant differences in the data distribution across subjects. Additionally, the reliability of the high resolution audiometer was checked with four subjects in a test/retest experiment. The two curves obtained for each subject showed a high correlation and thus approved the precision of the implemented audiometer.

In order to examine a relationship between both fine structures, a detection algorithm was implemented to extract individual ripples and specify their characteristics. This allowed an analysis of the individual results but also an overall comparison of both fine structures regarding the average across the subjects.

Simplified models were implemented and compared with the results of the measurements in order to evaluate possible trends regarding cochlear parameters such as basal and apical reflectances.

An certain agreement of the results with previous studies and the models was observed. However, since the generation of the DPOAE fine structure involves more parameters than the fine structure of the threshold according to the models, it is hard to establish a direct relation.

Regarding the average among all subjects, the observed fine structure in DPOAE was in general more pronounced and showed a higher prevalence. On the other hand, presence of fine structure in the threshold did not necessarily coincide with an increased ripple prevalence or height in the DPOAE and vice versa. It appears, according to the models, that this is due to a high variation of the cochlear parameters involved in the fine structure generation across subjects. It is hard to predict those parameters just from either the threshold or the DPOAE curve. Hence, a direct relation regarding the ripple height and prevalence between both DPOAE and threshold fine structure could not be determined.

High similarities were found in the periodicity instead. The ripple spacing of the DPOAE and threshold fine structure can hence be considered to be of the same origin. An average ripple spacing of approx. 1/10 octaves was observed which showed just very little variations in frequency. This strongly agrees with the analyzed models, where the rapidly varying phase of the apical reflectance is assumed to be the reason for the periodicity. This phase influences the spacing between fine structure minima and maxima in both models in the same way.

Despite the observed similarities and agreements with the models, a universal tool for an estimation of the threshold from the DPOAE fine structure and level could not be provided.

15
Future work

With the purpose of studying a possible relationship between their fine structures, the threshold and DPOAE were screened. Measurements of the hearing threshold require of concentration of the subjects and therefore, the time duration of this test should be kept short. This limits the frequency range of the measurement. However, measurements in a wider frequency range will allow a more complete comparison of fine structures, since both threshold and DPOAE are very frequency dependent. Hence, the design of a test procedure that allows a longer measurements time without biasing the subject's performance could be studied.

Although the implemented high resolution audiometer is a fast and precise method for tracking threshold fine structure, it is not accurate on the estimation of absolute threshold level. Therefore, it could be interesting to analyze and implement other high resolution audiometric methods and test their performance for screening hearing thresholds.

The screening of DPOAE is highly dependent on the choices of measurement parameters. It has been reported in the literature that the choice of the primary frequency ratio and levels has a significant influence on the DPOAE level and the presence of fine structure. The choices made can even produce a shifting of the fine structure minima and maxima along the frequency axis in a DP-gram. This constitutes an obvious limitation to use DPOAE as an objective audiometry and therefore an appropriate line of research.

Similarities between the threshold and DPOAE fine structure periodicity are observed in the experimental results, thus supporting the analytical models. However, the models present certain restrictions to explain the generation mechanisms responsible of the threshold and DPOAE fine structure. Further investigation of the different parameters involved in the simulation of the cochlear behavior could lead to a more realistic relation between measurements and cochlear models.

Moreover, the effect of variability between subjects could be reduced by classifying the tested population regarding their hearing status. This would facilitate the comparison of DPOAE and threshold fine structure, since it might show common characteristics within different groups.

Finally, it could be an interesting future work to analyze the relationship between threshold and DPOAE fine structure by the use of Input/Output functions, since they appear to be a good estimator of absolute hearing threshold in the cases of subject presenting cochlear hearing loss.

Part I

Appendices

A
Standard Audiometry Tests Journal

Prior to the DPOAE measurement and the high resolution audiometry, a standard pure tone audiometry test which complies with ISO 8253-1 was performed.

Since threshold tracking methods are not expected to be precise absolute threshold estimates, the aim of this test was to obtain an estimate of the absolute hearing threshold level at a discrete number of frequencies. Furthermore, the data obtained from the standard audiometry test was used to check for possible hearing damage in the analyzed frequency range.

The audiometric test was performed using the ascending method introduced by Carhart and Jeger (1959) [Lydo 99] in the range from 1250 to 4500 Hz with a resolution of 6 points per octave.

A.1 Setup

The test was performed in the Audiometric Cabin A (room B5-102) in the Acoustics Laboratory at Aalborg University, Fredrik Bajers Vej 7, 9220 Aalborg E. Figure A.1 shows the setup of the clinical audiometer.

During the test, the equipment and the operator were in the same room as the subject. It is important to ensure that the subject is not distracted by the operator or any indications of the equipment during the test. This was simply done by turning the chair where the subject was seated towards the wall.

A.2 Equipment

The equipment used for the standard audiometry test is detailed in Table A.1.

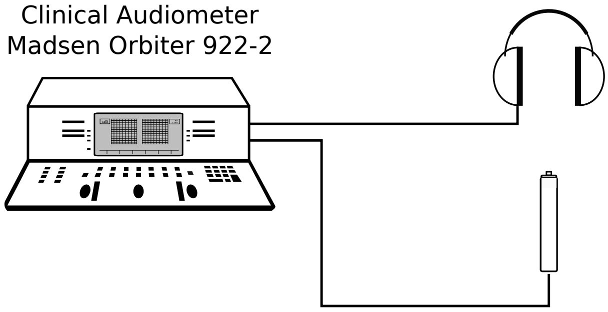

Figure A.1: Setup used for the standard audiometry.

Model	**Type**	**AAU no.**	**Room**
Madsen Orbiter 922	Clinical audiometer with push-button	33968	B5-102
Sennheiser HDA200	Audiometry headphone	52735	B5-102

Table A.1: Standard audiometer setup equipment.

The audiometer has a built-in headphone amplifier, hence, the headphones can be connected directly to the headphone output. It is important that the two channels are connected correctly. Additionally, the audiometer provides two external pushbuttons for each ear to record the subjects responses.

A.3 Test Procedure

The algorithm of the test follows a method introduced by Carhart and Jeger. It is a particular implementation of the ascending method and has been recommended by the American Speech and Hearing Association (ASHA) in 1978 [Lydo 99].

The algorithm starts at 40 dB hearing level and decreases with 10 dB steps. 5 dB steps are used for the ascents to detect the hearing threshold. A threshold level is validated after being detected two times at the same point.

The detection of the threshold runs automatically for each frequency, but when analyzing in the resolution of 6 points per octave the start level and the frequency of each point to has to be set manually.

The procedure to run the standard audiometry test in the given frequency range is as follows:

1. Select the 'Auto Threshold' (softkey 1) program in the menu for special test (softkey 'Special').
2. In the Setup, change the frequency resolution to 6 points per octave and press 'Setup' again to return to the test program.
3. Make sure that the subject feels comfortable in the cabin, has the headphones in the right position and understands the task.
4. Give the subject the correct pushbutton for their response (blue to test the left ear, red to the right ear).
5. Select the ear to be tested with the key 'L/R Shift' (left is default).
6. With the knobs for 'Frequency' and 'Level' select 1250 Hz and 40 dB HL as a starting point and run the test for this frequency by pressing 'Sing. Frq. Start' (softkey 5). When finished, the determined threshold will be marked with an 'X' (left) or 'O' (right).
7. Repeat the same procedure with the following frequencies: 1250, 1400, 1600, 1800, 2000, 2240, 2500, 2800, 3150, 3550, 4000, 4500 Hz. Start always at 40 dB HL.
8. When the test is completed, write down the threshold values of the subject.

A.4 Results

The results obtained in the standard audiometry test are shown in Figures A.2 and A.3, in a frequency range from 1250 to 4500 Hz and a resolution of 6 point per octave. The cross symbols indicate the absolute level in dB HL determined at the correspondent frequency specified in the x-axis.

The absolute threshold values vary from 0 to 30 dB HL among all the subject's results. For most of the subjects the absolute threshold fluctuates around 10 or 15 dB HL.

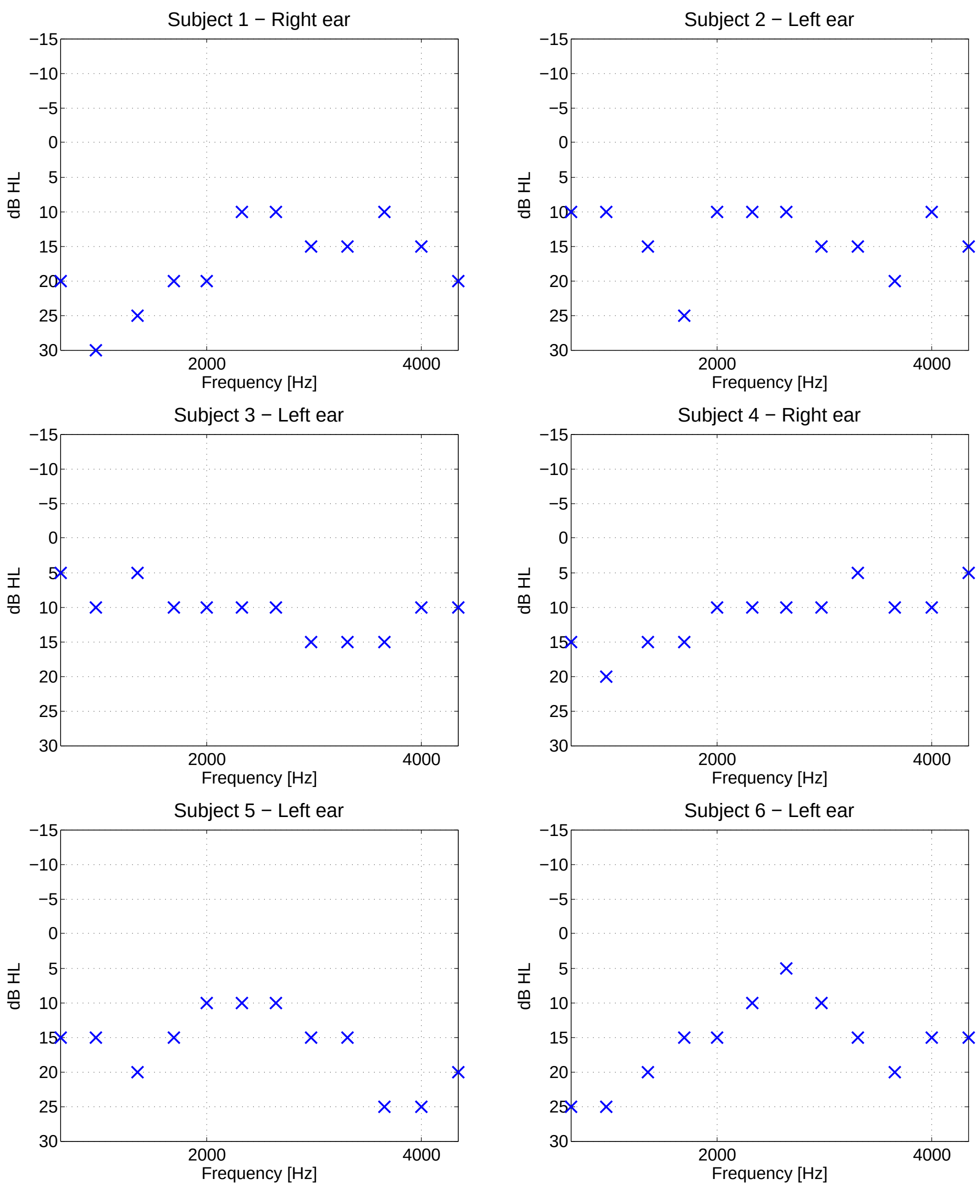

Figure A.2: Standard audiometry results from subjects 1 to 6.

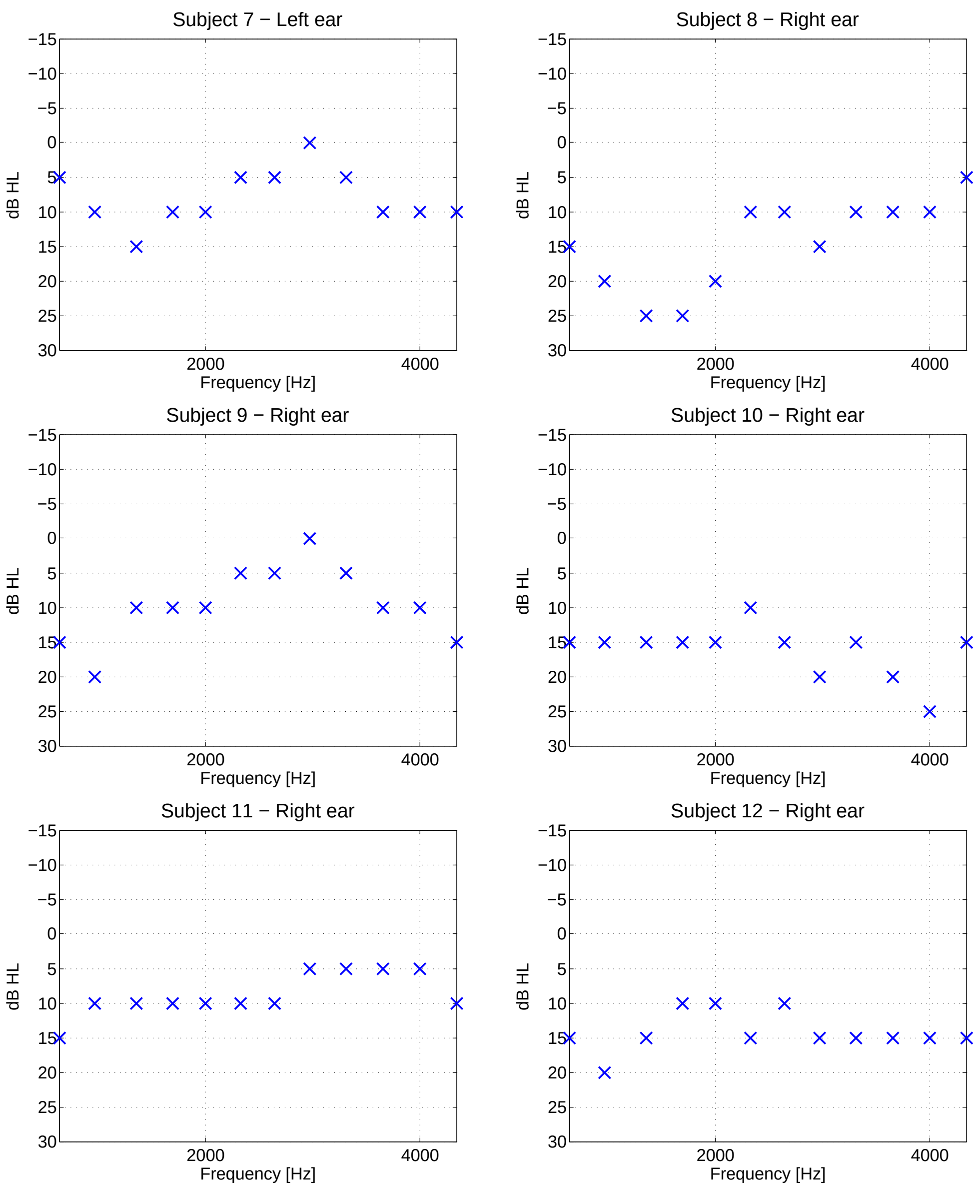

Figure A.3: Standard audiometry results from subjects 7 to 12.

B

High Resolution Audiometry Tests Journal

The high resolution audiometry test was performed in order to screen the threshold fine structure of the subjects. A high frequency resolution audiometric system was implemented for that purpose. The system is based on the FINESS algorithm described in Chapter 7. The algorithm was implemented in Matlab[1].

The calibration of the system and the noise estimation are described in Appendix E.

B.1 Setup

The high resolution audiometry test was performed in the Audiometry Room B4-103 at Aalborg University, Fredrik Bajers Vej 7, 9220 Aalborg E. Wall connections to the neighboring Control Room A B4-105 allow to place the main equipment in a separate room.

The system's setup is shown in Figure B.1. The test subjects were seated in the Audiometry Room, with the headphones put on. They were given a pushbutton and asked to press it for as long as they heard a tonal sound and to release it whenever they stopped hearing it.

The experimenter stayed in the Control Room A to control the test. Since the algorithm runs automatically, the experimenter had to make sure that the hardware connections were correct, the headphones were settled in the right position and the data was saved correctly after the test. The experimenter also had to control the necessary time breaks during the test.

[1]The Matlab files of the implemented high resolution audiometer can be found in the enclosed CD.

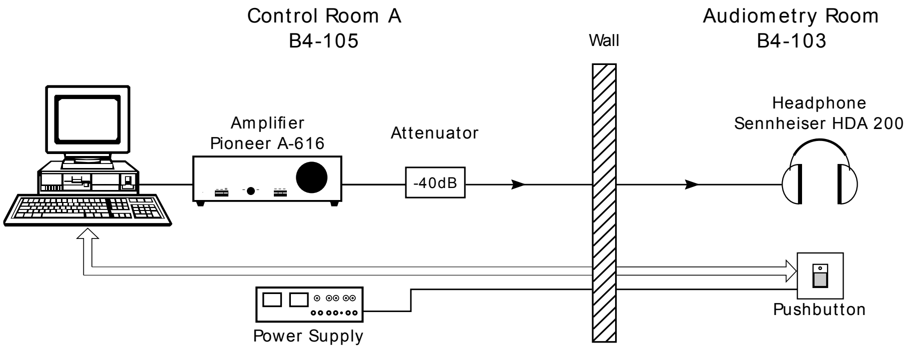

Figure B.1: Setup used for high resolution audiometry test.

B.2 Equipment

The equipment used in the high resolution audiometer setup is detailed in Table B.1.

Model	Type	AAU no.	Room
FujitsuSiemens-Computers	PC with RME DIGI96/8 PST sound card	60907	B4-105
Pioneer A-616	Stereo amplifier	08340	B4-105
	Attenuator -40 dB		B4-105
B&O SN16A	Power supply	08013	B4-105
Sennheiser HDA 200	Audiometry headphone	33378	B4-103
	Pushbutton		B4-103

Table B.1: High resolution audiometer setup equipment.

The headphones and pushbutton in the Audiometry Room were connected to the equipment in the Control Room A through the wall. This way the Audiometry Room was completely isolated from the acoustic noise produced by equipment. Figure B.2 illustrates the system connections.

The necessary connections to send a sound signal to the headphones from a Matlab program using the computer in the Control Room A are described in the following:

- The internal sound card is attached to the PCI slot of the computer.
- The line output of the sound card is connected to the power amplifier.

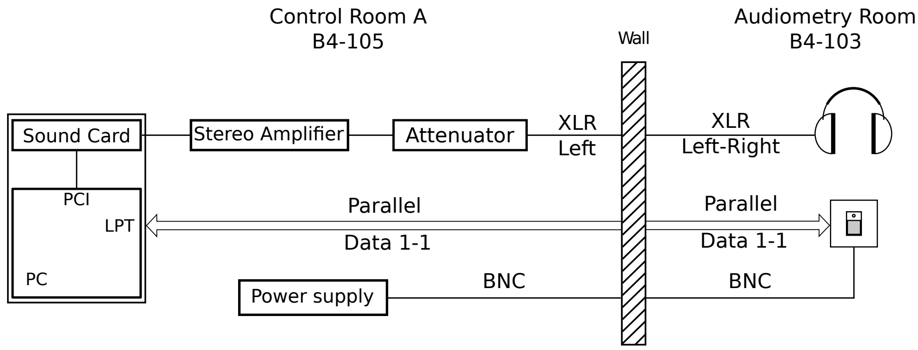

Figure B.2: High resolution audiometry equipment connections.

- The output of the power amplifier is connected to an attenuator of -40 dB to reduce the noise generated by the sound card and the amplifier and to prevent the reproduction of high level sound through the audiometry headphones.
- The attenuator output connects to the left channel of the audiometry headphones via an XLR connection through the wall.
- Both left and right input of the headphones are connected to the wall, but only the left receives signal depending on the ear tested. Since the used headphones are completely symmetric they can also be worn the other way around, hence, the right ear can be measured with the originally intended left driver of the headphones.

The connections to supply power to the pushbutton and to read the data from it are detailed next:

- The pushbutton is connected via a parallel interface (IEEE 1284) to the wall in the Audiometry Room. A parallel cable connects the wall with the LPT input of the PC.
- The power supply in the Control Room provides power (from 7 to 12 V) to the pushbutton in the Audiometry Room via a BNC 50 Ω coaxial connection in the wall.

B.3 Test Procedure

The procedure followed to carry out the high resolution audiometry test is described next:

1. Prepare the implemented Matlab program for a new subject: introduce the string inputs correspondent to the subject's ID and tested ear in the function *Audiometry_Gui("ID","ear")*[2].
2. Make an equipment and connections check according to the graphical guide:
   - Headphones power amplifier is "on".
   - Pushbutton power supply is "on".
   - Headphones and pushbutton in the Audiometry Room are connected to the wall.
3. Make sure that the subject feels comfortable, has the headphones in the right position (the left headphone is always on the ear under test) and understands the task.
4. Leave the subject alone in the Audiometry Room, close the door and press "start".
5. After each part, the currently determined curve will be displayed.
6. Control the breaks between the test parts (at least 3 minutes breaks).
7. Check that the data has been correctly saved in a *.mat* file with the subjects ID in the folder */hr_results*.

B.4 Results

Figure B.3 and B.4 show the results from the high resolution audiometry test. The blue solid line represents the threshold values determined at high frequency resolution (100 points per octave). The threshold fine structure detector (see Chapter 9) is applied to the results[3]. The detected ripples are indicated by the gray rectangles.

The criteria used to classify a ripple as fine structure are determined by a minimum level difference between two adjacent extreme values $\Delta L_{min} = 2$ dB, a minimum frequency spacing of $\Delta f_{min} = 1/25$ octaves and a maximum frequency spacing of $\Delta f_{max} = 1/5$ octaves.

[2]The implemented Matlab function *Audiometry_Gui.m* is included enclosed CD. The "ID" is necessary to identify the subjects results and the "ear" input denotes the ear under test, "L" (Left) or "R" (Right).

[3]The threshold ripples are detected by the use of the Matlab function *FINESS_detector.m* included in the enclosed CD.

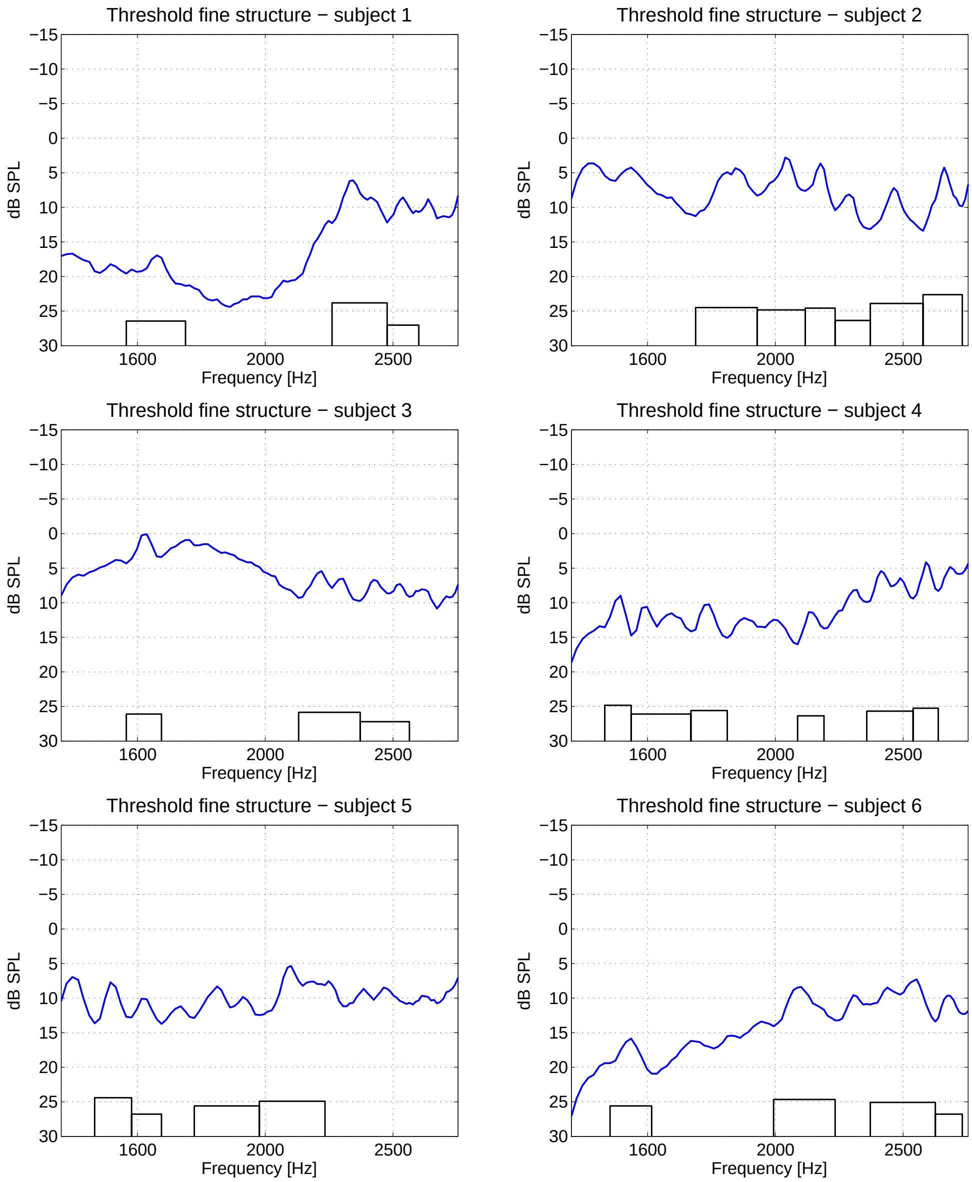

Figure B.3: High resolution audiometry results from subjects 1 to 6.

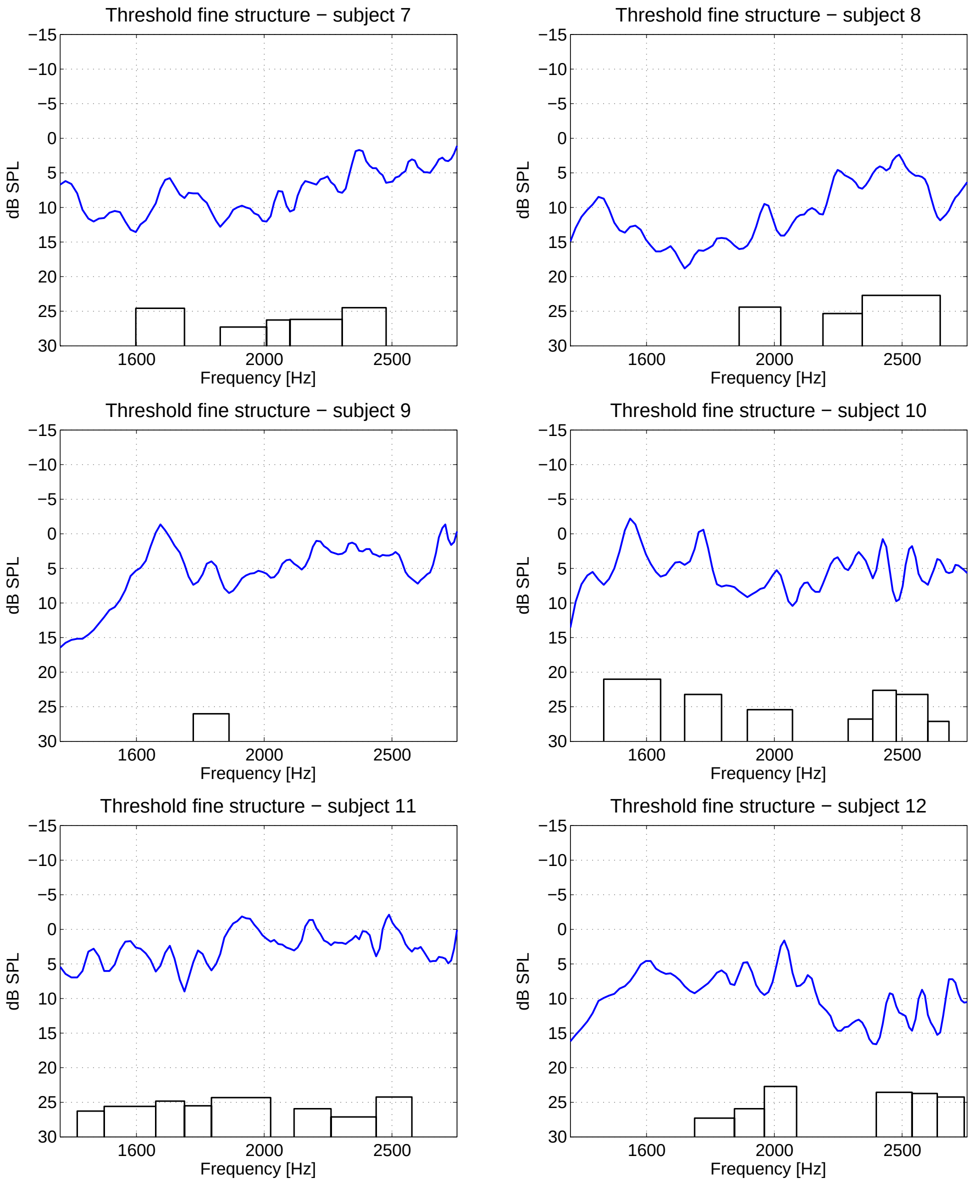

Figure B.4: High resolution results from subjects 7 to 12.

C

DPOAE fine structure measurements Tests Journal

The DPOAE measurements were performed in order to screen the DPOAE fine structure of the subjects. The ILO96 Research system from Otodynamics was used for this measurements. The DP-gram test of the ILO's DPOAE function was configured to fulfill the requirements of the system specified in Section 8.1.

C.1 Setup

The DPOAE measurements test was performed in the Audiometry Room B4-103 at Aalborg University, Fredrik Bajers Vej 7, 9220 Aalborg E.

The system's setup is shown in Figure C.1.

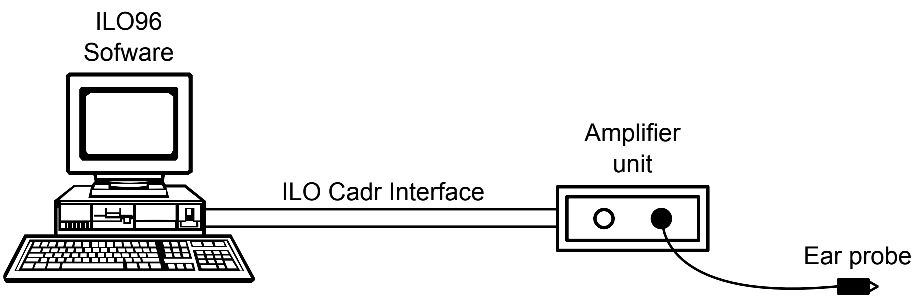

Figure C.1: Setup used for DPOAE measurements test.

The test subjects were seated in the Audiometry Room where the equipment was placed. The ear probe had to be properly fitted into their ears.

C.2 Equipment

The equipment used in the DPOAE measurements setup is detailed in Table C.1.

Model	**Type**	**AAU no.**	**Room**
Siemens	PC	43919	B4-103
Otodynamics ILO96	Otoacoustic emissions measuring system including software, amplifier unit and ear probe	52661	B4-103

Table C.1: DPOAE measurements setup equipment.

The ILO OAE software is a DOS application which runs on MS Windows 98. The software analyzes the data, extracting the DPOAE amplitude spectrum and the noise by the use of internal algorithms.

The card interface of 2x2 channels generates the stimuli signals and receives the recorded signals from the microphone. It is also responsible of controlling the internal switches and attenuations.

The amplifier unit amplifies and/or attenuates the output/input signals (generated stimuli and received signals). The probe is connected to the amplifier unit by an eight-pin DIN connector.

C.3 Test Procedure

To screen the DPOAE fine structure within the frequency range specified in Section 8.1.3 several measurements were required. The DP-gram test of the ILO96 system was set to a micro resolution. This provides measurements within a range of 200 Hz for $f_2 < 3$ kHz and of 400 Hz for $f_2 > 3$ kHz, presenting 17 pairs of primary tones. Hence, 13 concatenated measurements were required to cover the desired frequency range.

Prior to each measurements the program executes a probe checkfit. It uses a click stimulus to measure the frequency response of the ear canal, detecting anomalies in the probe fit. The data from the checkfit is used to balance and normalize the two primary stimulus levels.

The spectrum analysis is performed by the system applying Fast Fourier Transform (FFT) with a 12.2 Hz resolution. The noise is estimated taking the 10 closest to $2f_1 - f_2$ components in the FFT, excluding the distortion product itself. The system presents two noise curves. The lower curve indicates one standard deviation and the higher two standard deviations from the background noise, thus specifying the limit of the 95 % confidence interval.

The measurements procedure followed to carry out the DPOAE measurements is described next:

1. Start the program ILO OAE.
2. Select the option "D)DPOAE".
3. Click on *Menu* → *Setup* → *Load parameters* and load the file "DP_PARAM.PAR" in the current directory. This will set the primary level to $L_1/L_2 =$ 65/45 dB SPL.
4. The next steps are repeated for each of the 13 measurements of 0.1 octave to cover the desired frequency range:
   - Select the DP-gram test in *Menu* → *Test select* → *DP-gram* (or press F6).
   - Chose the "Micro structure (0.1 oct)" resolution.
   - Enter the correspondent central value of f_2 in the range of the current measurement.
   - Perform the probe checkfit. If the fitting is not successful the spectrum will present frequency regions colored in red and the test stimulation will not be optimal. When the best possible probe fit is achieved, press "OK" to continue the measurements.
   - The stimuli levels are set automatically according to the checkfit data. Press "OK" to start the DP-gram measurements.
   - The DP-gram measurement starts automatically. The measurements at the 17 points within the current range are repeated continuously. Press "Normal Stop" to finish the measurements when an acceptable S/N ratio is achieved and DPOAE amplitude points are above the noise measurements, if possible.
   - Press "Quick save" to save the measurements. Input the subjects ID and press F10 and "OK" to confirm the storage.
   - Press "Exit" to start a new measurement or to finish the test.
5. The measurements are to be saved as spreadsheets once the experiment is over. Each measurement should be loaded pressing *Menu* → *Analysis* → *Numerical analysis*. By pressing any key a pop-up menu appears on the screen. Select the option "save as spreadsheet" and save the file. The 13 measurements should be loaded and saved as spreadsheets.

6. Concatenate the 13 measurements results using the Matlab function *dpoae_fine_str.m*[1].

C.4 Results

Figures C.2 and C.3 show the DPOAE measured in 12 ears from 12 different subjects, as a function of the primary frequency f_2. The curves of the standard deviations from the background noise representing the 95 % confidence interval are also shown.

The DPOAE fine structure detector (see Chapter 9) is applied to the results[2]. The detected ripples are indicated by the gray rectangles. The criteria followed to classify the DPOAE ripples as fine structure are given by the next parameters:

- minimum level difference between two adjacent extreme values $\Delta L_{min} =$ 3 dB
- minimum frequency spacing $\Delta f_{min} = 1/25$ octaves
- maximum frequency spacing $\Delta f_{max} = 1/5$ octaves

[1] The Matlab function *dpoae_fine_str.m* is included in the enclosed CD.

[2] The DPOAE ripples are detected by the use of the Matlab function *OAE_fs_detector.m* included in the enclosed CD.

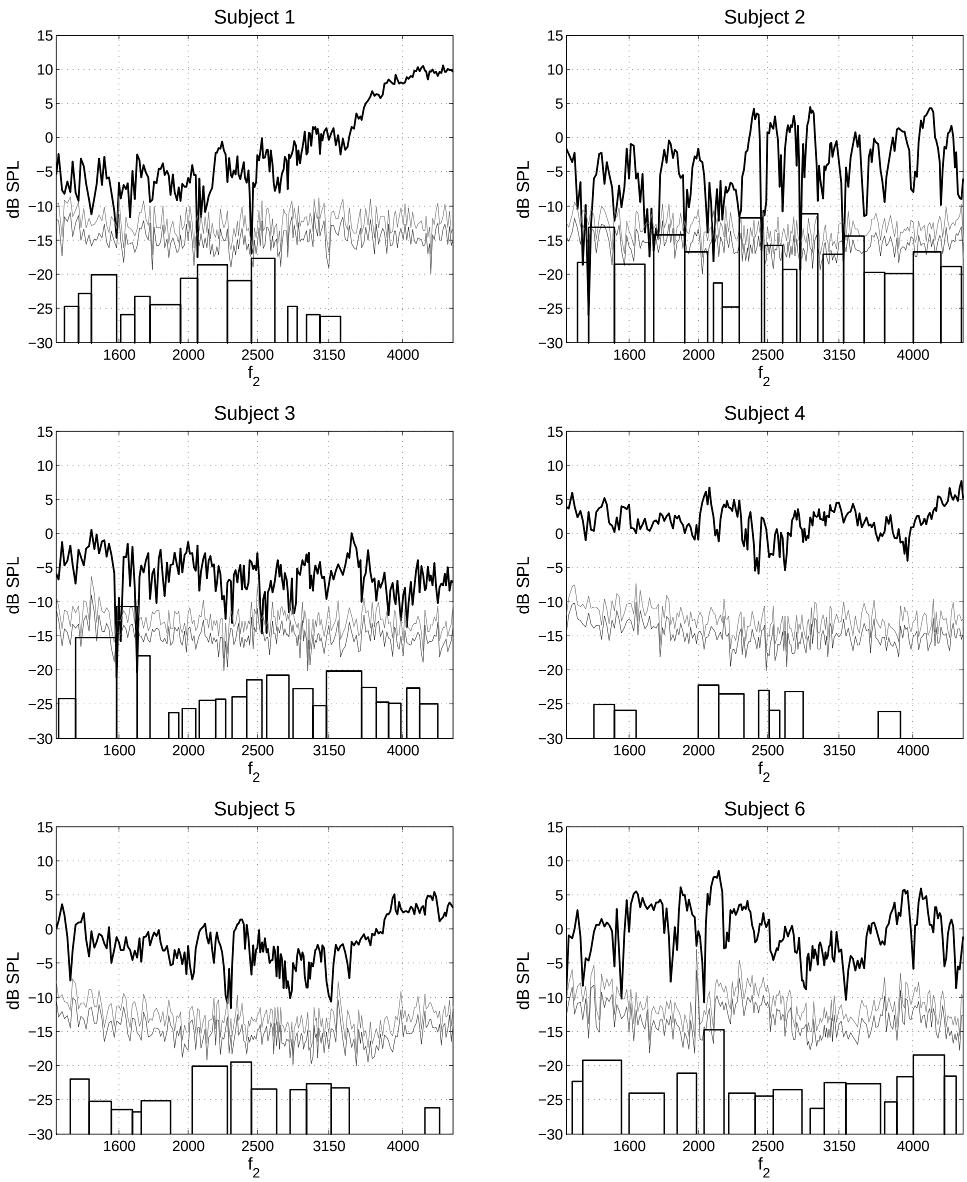

Figure C.2: Distortion product otoacoustic emissions and background noise measured, and DPOAE ripples detected in subjects number 1 to number 6, as a function of f_2.

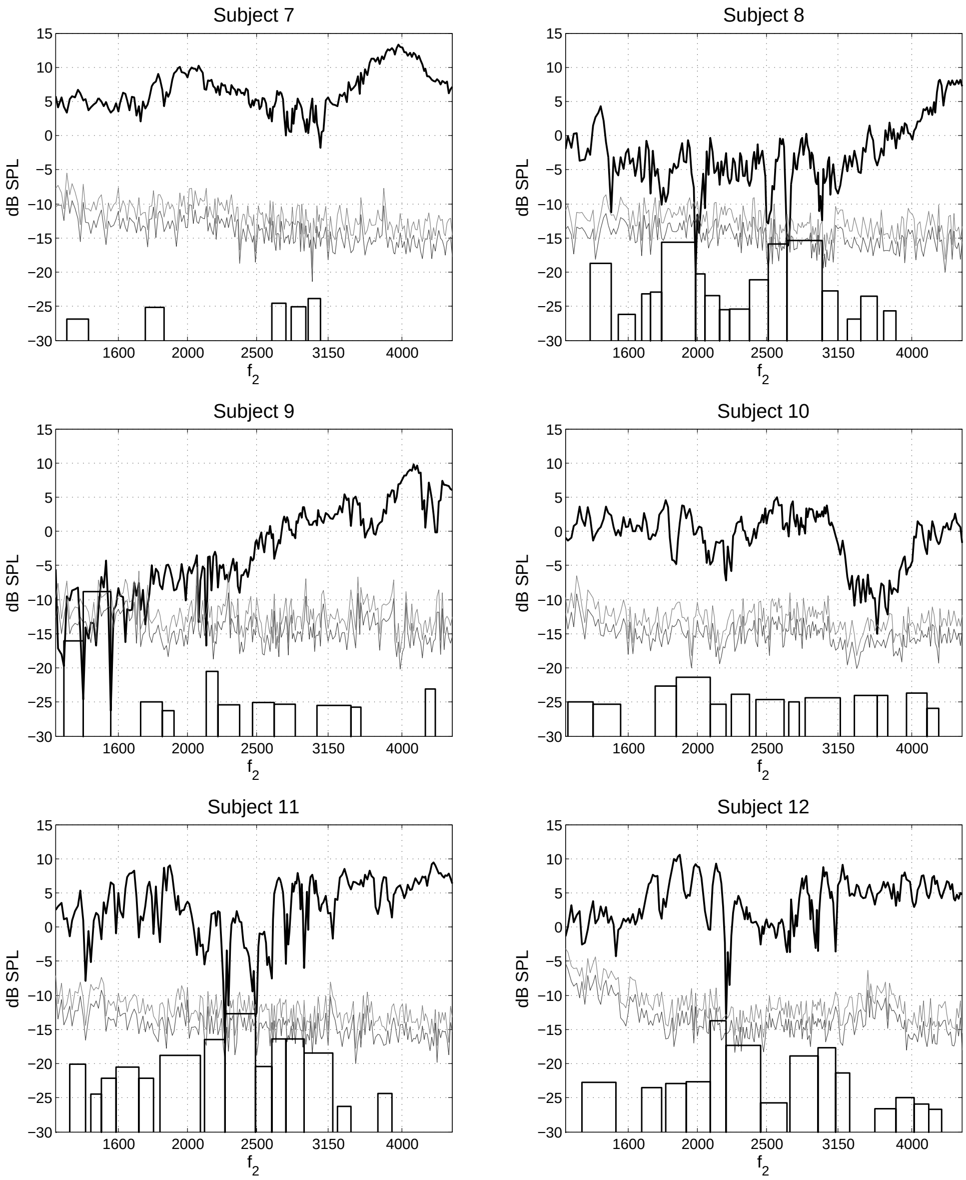

Figure C.3: Distortion product otoacoustic emissions and background noise measured, and DPOAE ripples detected in subjects number 7 to number 12, as a function of f_2.

D

Threshold and DPOAE fine structure comparison of results

A comparison of the results obtained from the threshold screening and the DPOAE measurements is roughly presented in this appendix.

The figures presented in the following provide a visual comparison between the threshold and DPOAE fine structure detected for each subject's results as a function of the distortion product frequency $2f_1 - f_2$, the second primary frequency f_2 and the geometric mean $\sqrt{f_1 f_2}$.

The ripple prevalence is calculated in 1/3 octave bands for each subject. Thus, the percentage of ripples present in each band for each subject are represented in the two gray scale bars. The upper bar corresponds to the threshold fine structure prevalence and the lower bar indicates the percentage of DPOAE ripples detected.

However, since the generation of both threshold and DPOAE fine structure are the result of complicated phenomena occurring in the cochlea (see Chapters 3, 4 and 5) it is nearly impossible to establish a relationship by simple visual inspection.

Therefore, in the following sections the different fine structure parameters (ripple prevalence, spacing and height) obtained from the experimental results are presented as a function of $2f_1 - f_2$, f_2 and $\sqrt{f_1 f_2}$.

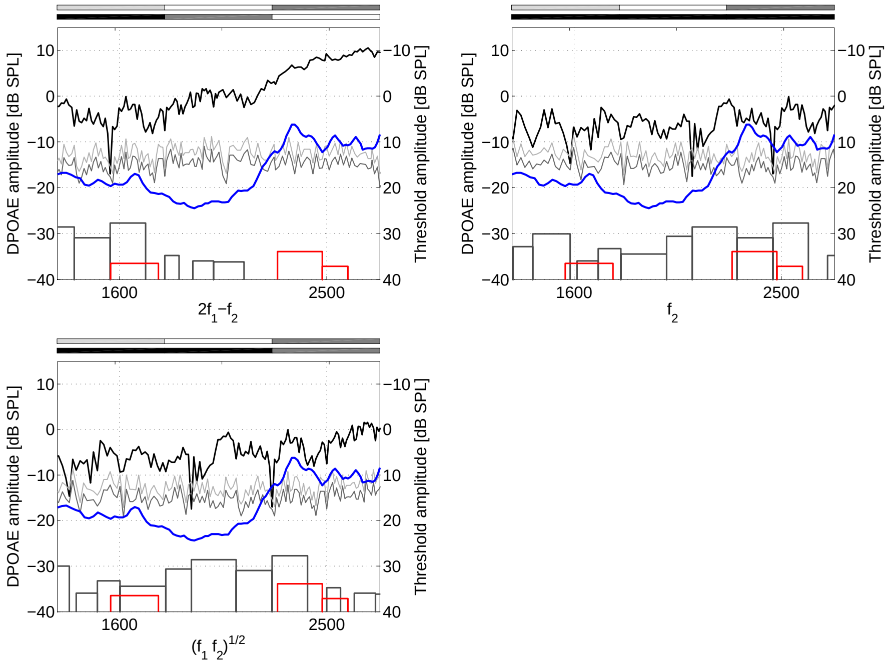

Figure D.1: Threshold and DPOAE fine structure of subject 1.

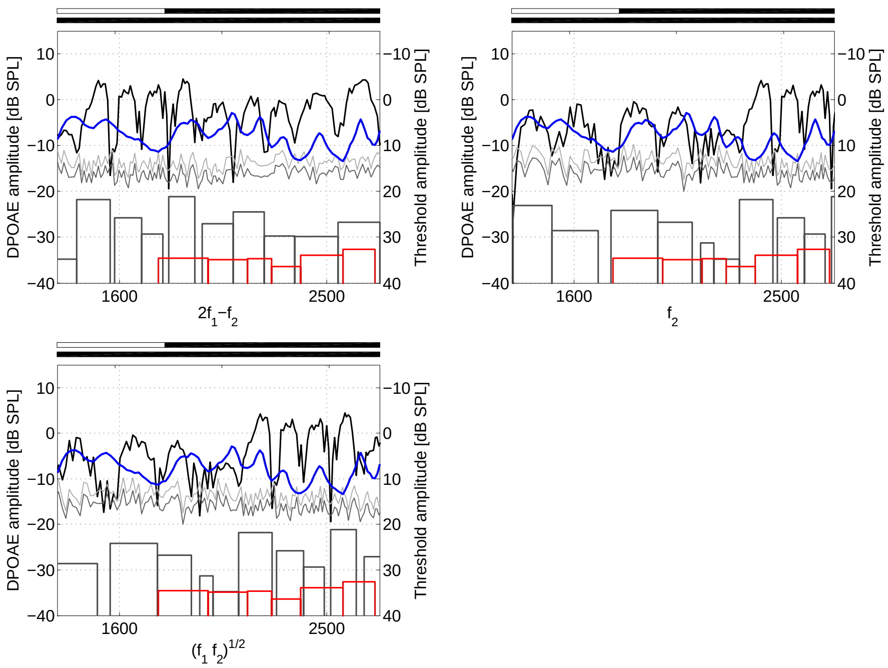

Figure D.2: Threshold and DPOAE fine structure of subject 2.

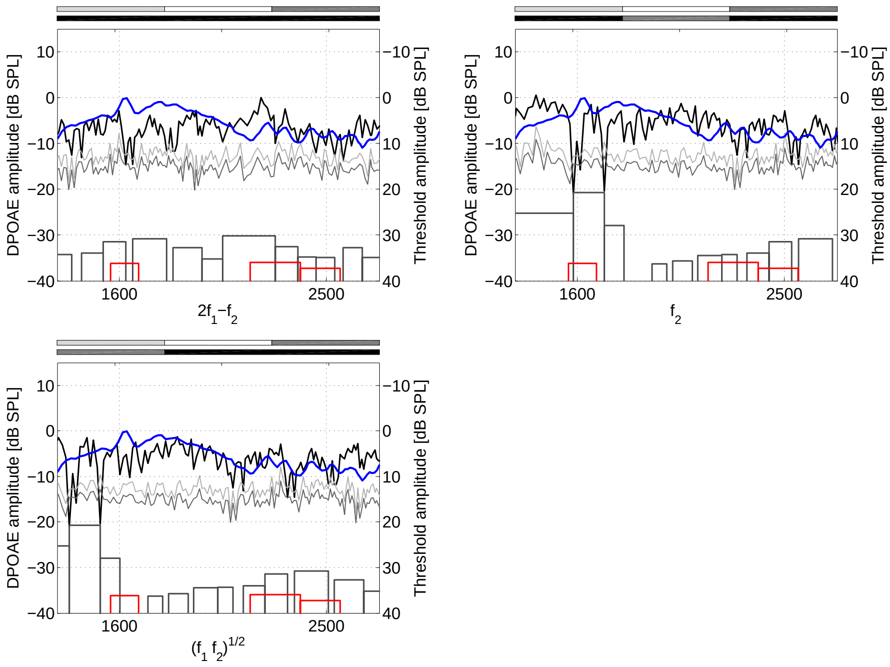

Figure D.3: Threshold and DPOAE fine structure of subject 3.

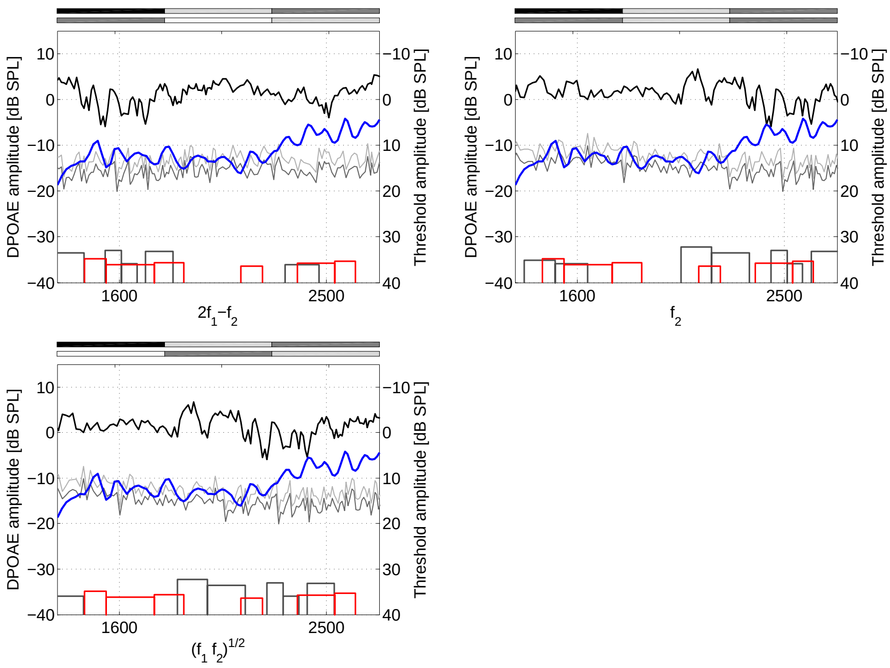

Figure D.4: Threshold and DPOAE fine structure of subject 4.

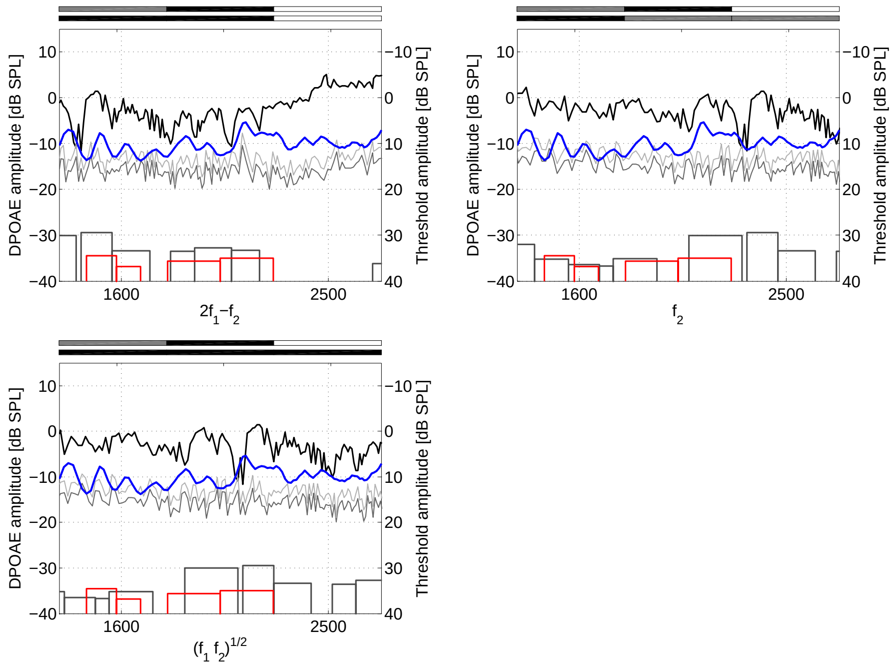

Figure D.5: Threshold and DPOAE fine structure of subject 5.

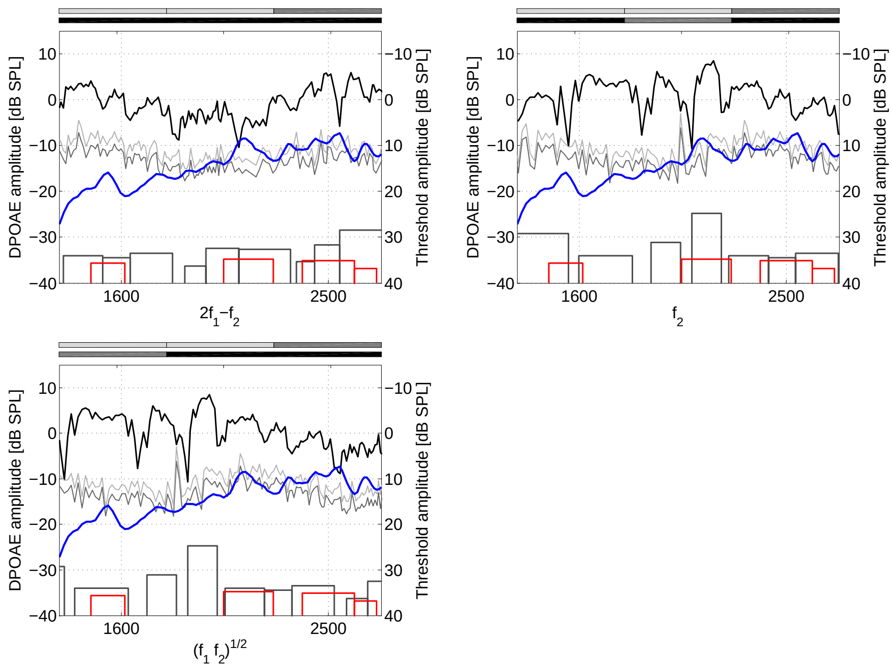

Figure D.6: Threshold and DPOAE fine structure of subject 6.

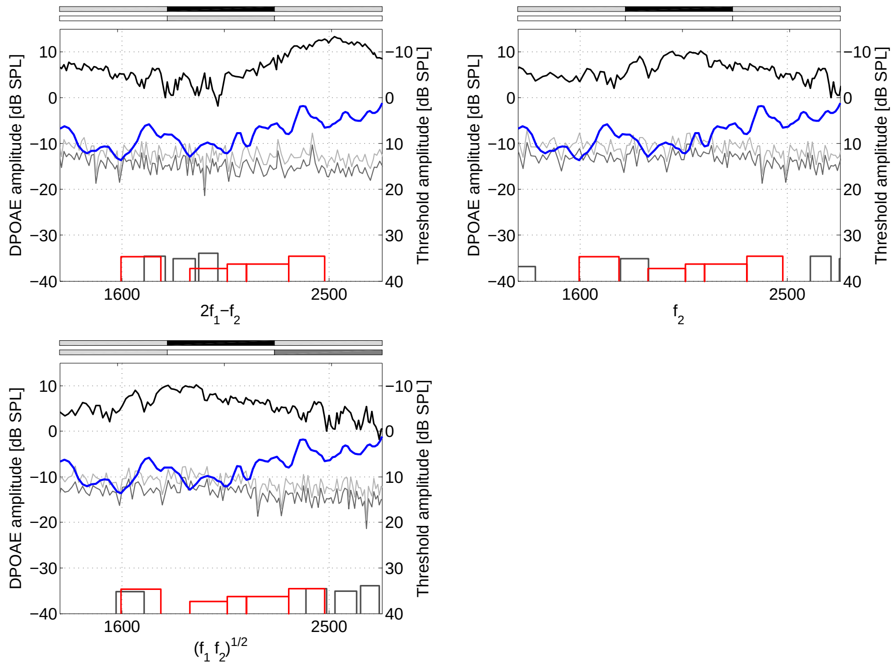

Figure D.7: Threshold and DPOAE fine structure of subject 7.

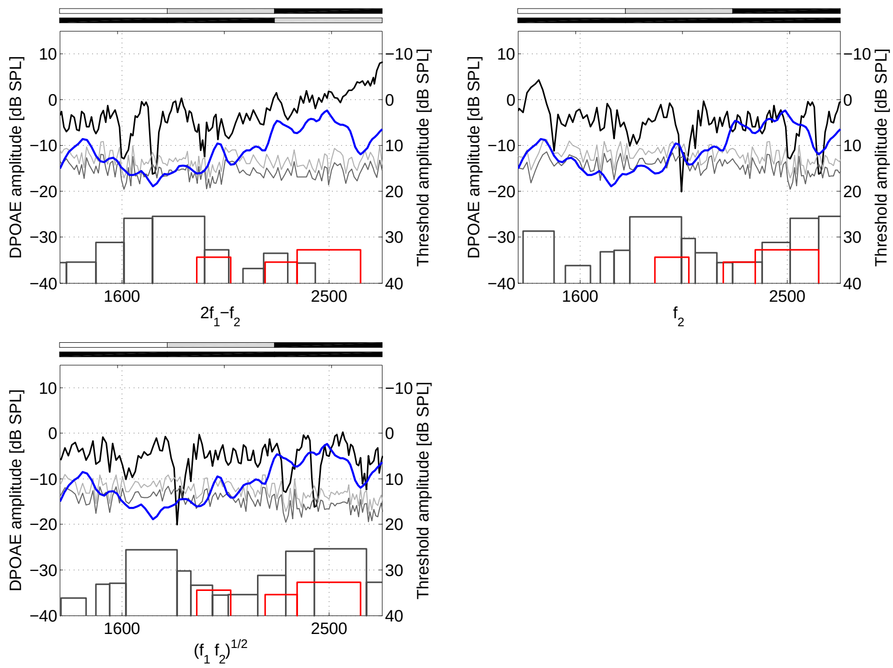

Figure D.8: Threshold and DPOAE fine structure of subject 8.

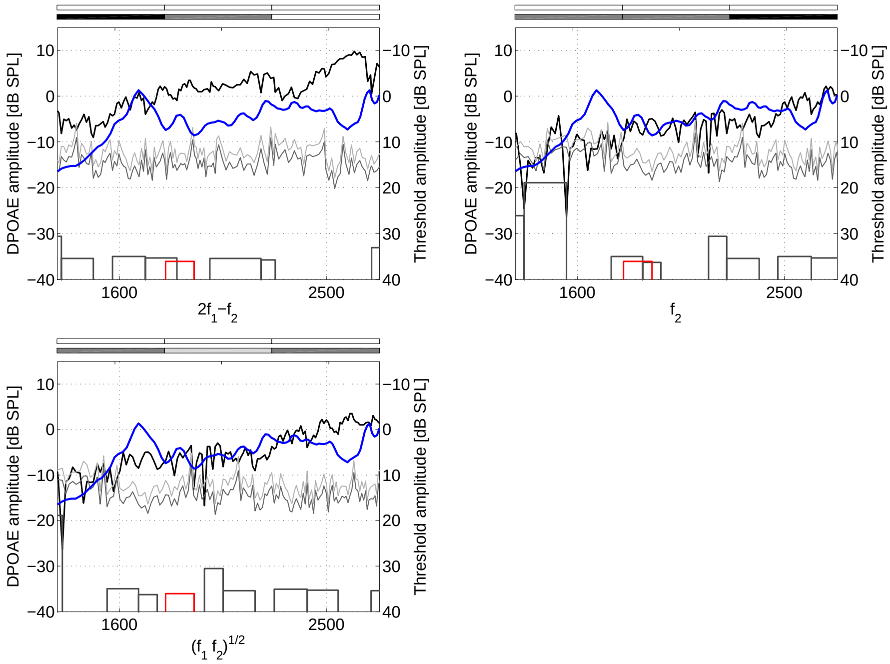

Figure D.9: Threshold and DPOAE fine structure of subject 9.

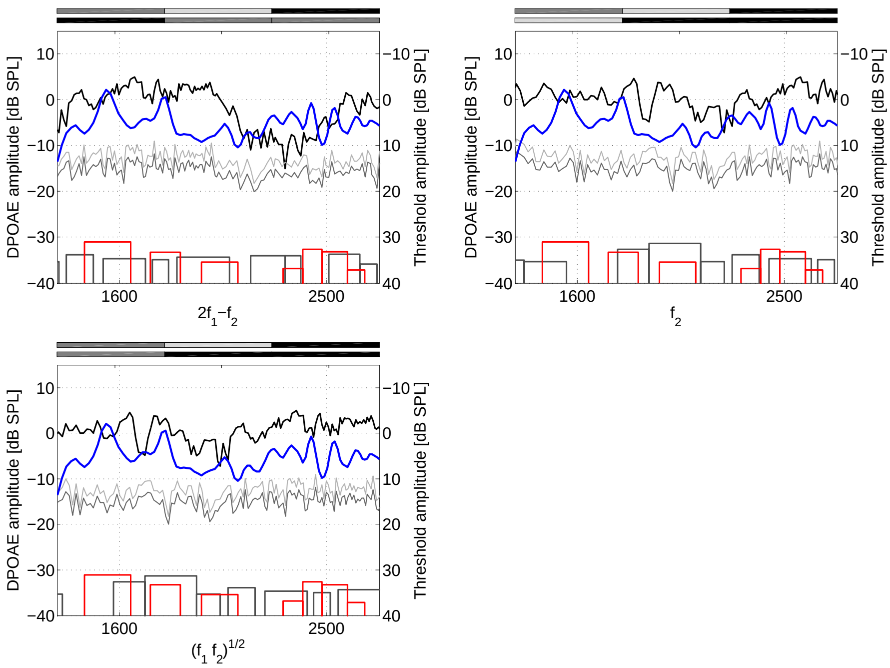

Figure D.10: Threshold and DPOAE fine structure of subject 10.

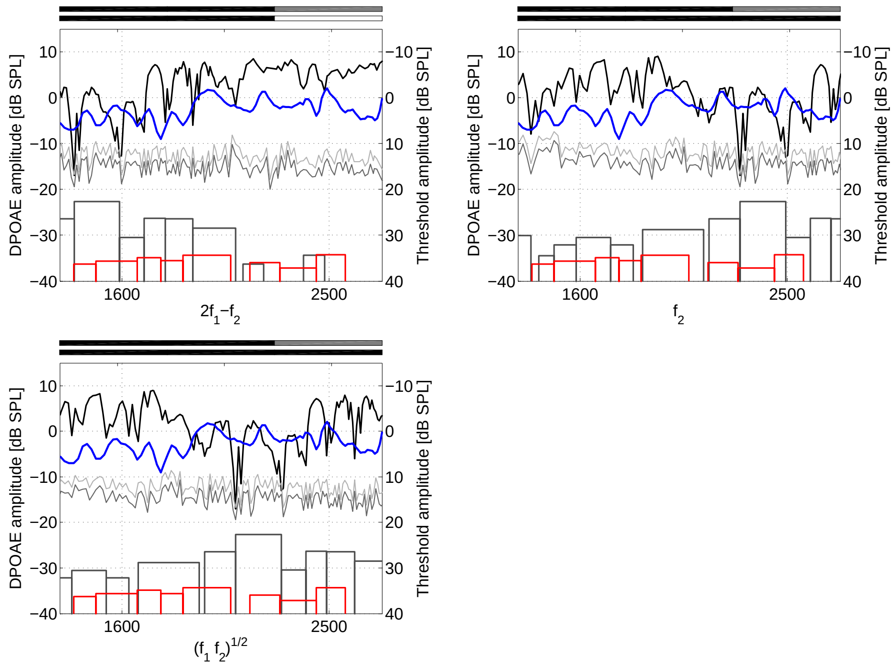

Figure D.11: Threshold and DPOAE fine structure of subject 11.

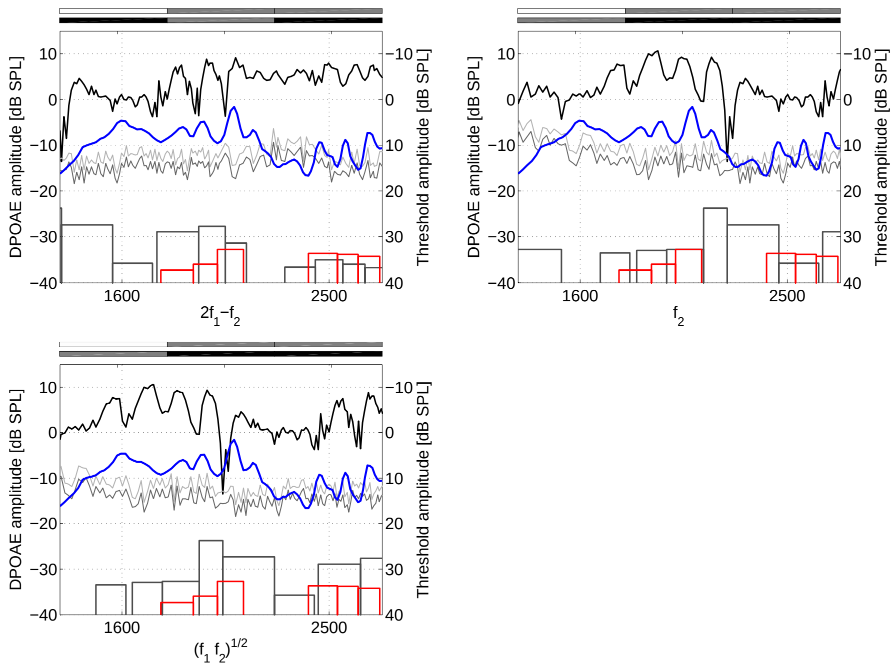

Figure D.12: Threshold and DPOAE fine structure of subject 12.

D.1 Ripple prevalence

The average and standard deviation of the threshold and DPOAE ripple prevalence, calculated for each subject within the frequency range from 1400 Hz to 2800 Hz, is presented in Figure D.13.

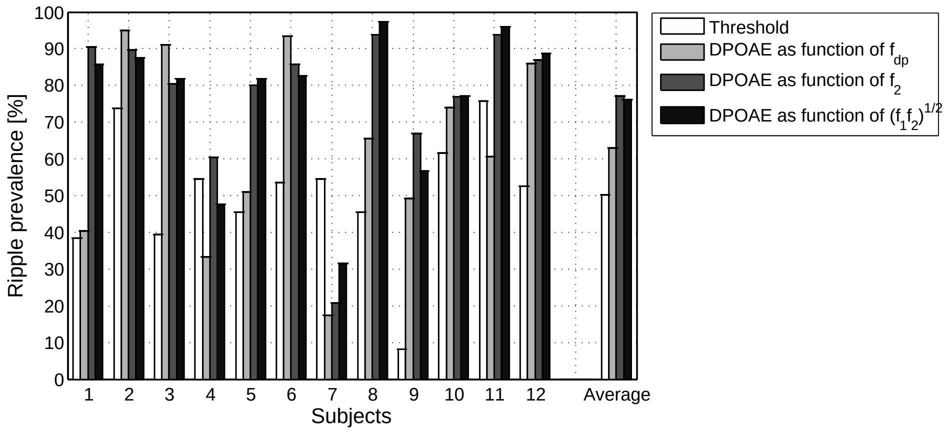

Figure D.13: Average ripple prevalence for each subject.

The threshold and DPOAE ripple prevalence is calculated in 1/3 octave bands for each subject and averaged over all the subjects, as illustrated in Figure D.14.

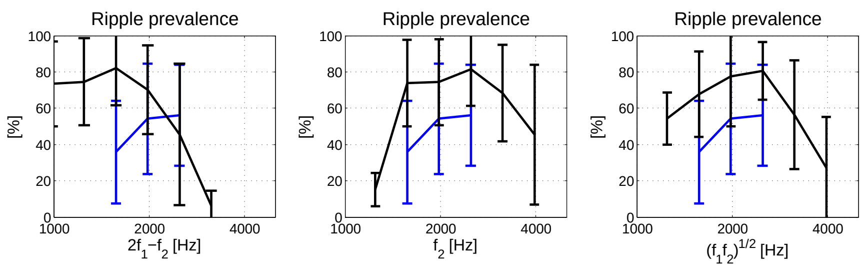

Figure D.14: Average of the ripple prevalence across the subjects, in 1/3 octave bands, for the threshold (blue) and DPOAE (black) fine structure as a function of $2f_1 - f_2$ (left), f_2 (middle) and $\sqrt{f_1 f_2}$ (right). The errorbars represent the standard deviation between subjects.

D.2 Ripple spacing

The average and standard deviation of the threshold and DPOAE ripple spacing, calculated for each subject within the frequency range from 1400 Hz to 2800 Hz, is presented in Figure D.15.

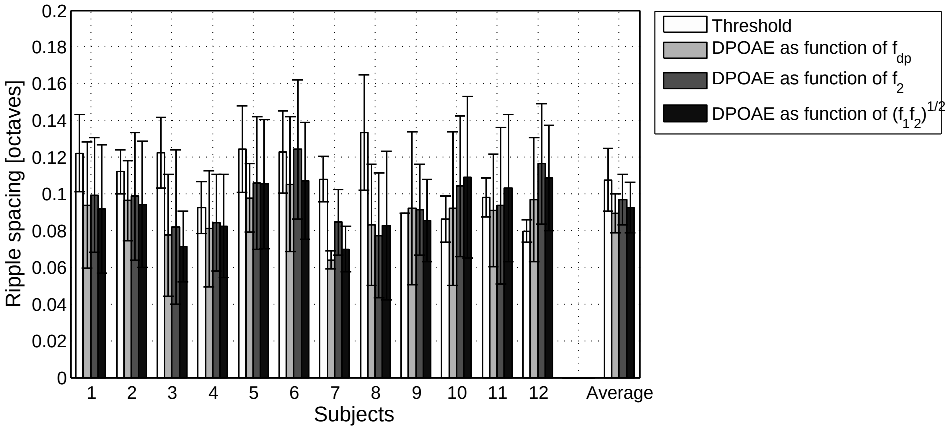

Figure D.15: Average ripple spacing in octaves for each subject.

The threshold and DPOAE ripple spacing is also calculated in 1/8 octave bands for each subject and averaged over all the subjects. The results are shown in Figures D.16 and D.17, where the spacing is given in octaves and Hz respectively.

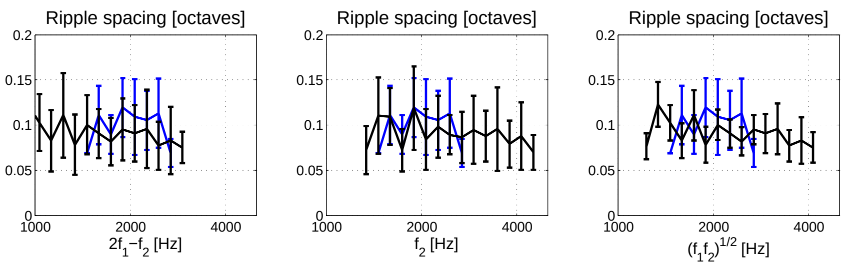

Figure D.16: Average of the ripple spacing across the subjects in octaves, in 1/8 octave bands, for the threshold (blue) and DPOAE (black) fine structure as a function of $2f_1 - f_2$ (left), f_2 (middle) and $\sqrt{f_1 f_2}$ (right). The errorbars represent the standard deviation between subjects.

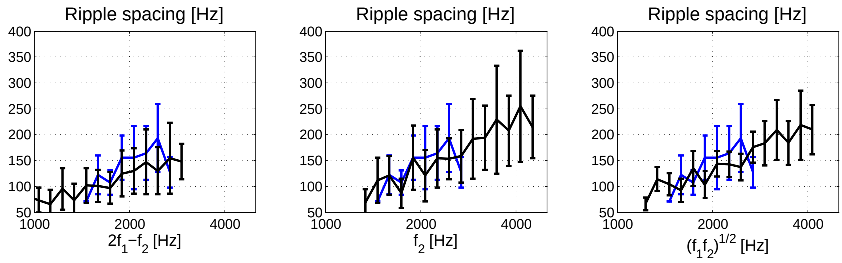

Figure D.17: Average of the ripple spacing across the subjects in Hz, in 1/8 octave bands, for the threshold (blue) and DPOAE (black) fine structure as a function of $2f_1 - f_2$ (left), f_2 (middle) and $\sqrt{f_1 f_2}$ (right). The errorbars represent the standard deviation between subjects.

D.3 Ripple height

The average and standard deviation of the threshold and DPOAE ripple height, calculated for each subject within the frequency range from 1400 Hz to 2800 Hz, is presented in Figure D.18.

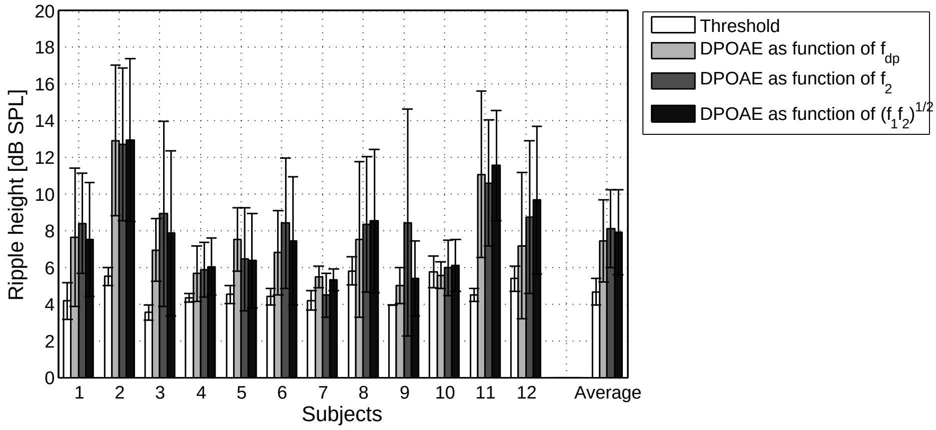

Figure D.18: Ripple height in dB SPL from each subject.

The threshold and DPOAE ripple height is calculated in 1/8 octave bands for each subject and averaged over all the subjects, as shown in Figure D.19.

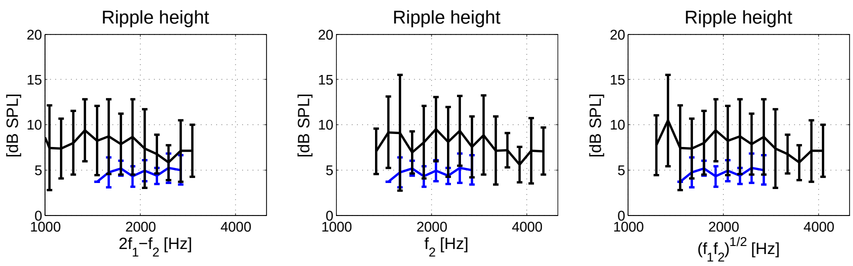

Figure D.19: Average of the ripple height across the subjects in dB SPL, in 1/8 octave bands, for the threshold (blue) and DPOAE (black) fine structure as a function of $2f_1 - f_2$ (left), f_2 (middle) and $\sqrt{f_1 f_2}$ (right). The errorbars represent the standard deviation between subjects.

E

High Resolution Audiometry Calibration and Noise Estimation

E.1 Setup and Procedure

The complete high resolution audiometer setup needed to be calibrated according to ISO 389. After developing the basic algorithm and setting up all the required equipment, the calibration was performed in the audiometric cabin (B4-103) and the Control Room A (B4-105).

The equipment listed in Table E.1 was used in addition to the setup specified in Appendix B according to ISO 389.

Model	**Type**	**AAU no.**	**Room**
Brüel & Kjær 4153	Artificial ear (IEC 60318) with adapter DB 0348	07631	B4-103
Brüel & Kjær 4134	$0,5$" measurement microphone mounted in B&K 4153	08129	B4-103
Brüel & Kjær 2669	Microphone preamplifier	56509	B4-103
Brüel & Kjær 2636	Measuring amplifier	08451	B4-105
Brüel & Kjær 2807	Microphone power supply	07305	B4-105
Brüel & Kjær 4230	Sound level calibrator	08373	B4-103
Toshiba T3200SX with MLSSA	Notebook with installed Acoustical measurement system	26855 25827	B4-105
Brüel & Kjær 2133	Real-time frequency analyzer	08596	B4-105

Table E.1: Equipment used for high resolution audiometer calibration.

The Sennheiser HDA 200 audiometric headphone was mounted on the B&K 4153 artificial ear, which complies with IEC 60318, with a force of approx.

10 N according to ISO 389-8. The force was obtained using a 0,5 l plastic bottle filled with water as a weight.

E.1.1 Headphone Transfer Function

The transfer function of the audiometric headphone was measured with the MLSSA Acoustical Measurement System. The output of the computer was connected directly to the Pioneer amplifier. To provide the required power for the B&K 4134 measurement microphone in the artificial ear, the B&K 2807 power supply was connected between the microphone and the input of the computer.

The MLS signal was recorded with the default setup and a 10-times average. It was saved in time and in frequency domain for further analysis.

E.1.2 Equipment Calibration

The equipment was calibrated with a sinusoidal signal at 1 kHz and different gain factors in Matlab. The signal s was created using the following equation:

$$s = g \cdot \sin 2\pi f_0 t \tag{E.1}$$

where $f_0 = 1\,\text{kHz}$ and g is the gain factor set in Matlab. With the B&K 2636 measuring amplifier, the output voltage of the microphone was measured. The apparent sound pressure in the artificial ear can be calculated with the sensitivity of the B&K 4134. A detailed sketch of the calibration setup is given in Figure E.1

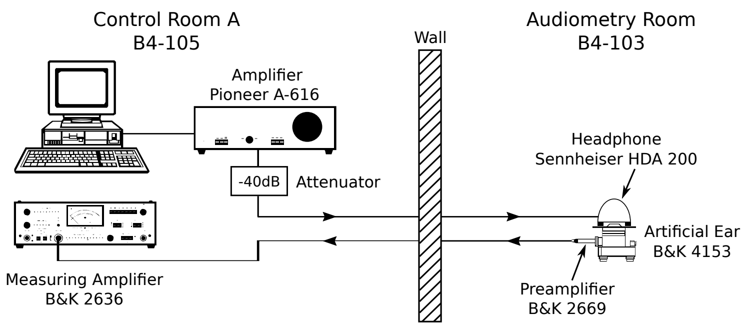

Figure E.1: The equipment, its connections and position used for the calibration of the high resolution audiometer.

E.1.3 Noise Estimation

The noise floor of the equipment was estimated by measuring the voltage at the terminals of the headphone while no signal was played with the setup. It was analyzed in third-octave bands with the B&K 2231. In order to obtain a reference to compute the sound pressure level, a 1 kHz signal with a gain $g = 0.1$ was played while measuring the voltage at the terminal with the same setup in a third-octave band centered at 1 kHz. The measured voltage of this signal was 2.21 mV, which can be referred to a sound pressure level of approx. 63 dB SPL.

With the data from the calibration and the headphone frequency response, the apparent sound pressure level of the noise at the ear could be estimated. A detailed sketch of the noise estimation setup is given in Figure E.2

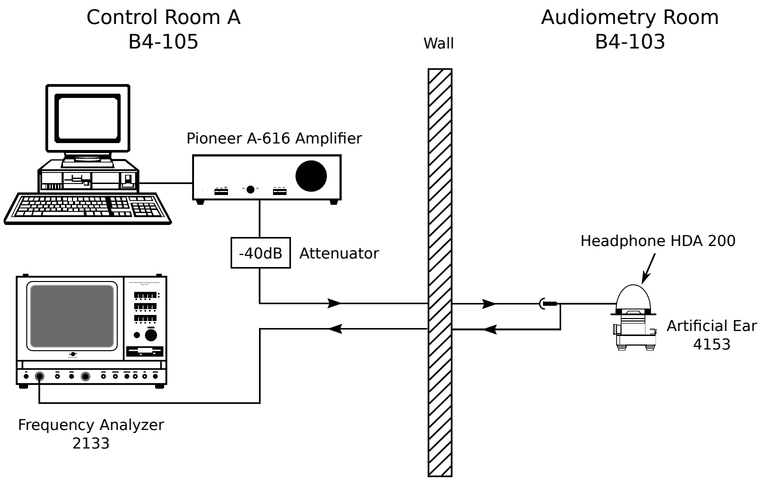

Figure E.2: The equipment, its connections and position used for the noise estimation.

E.2 Calibration Data

Date of Calibration: 31 March 2010

Location: Aalborg University, Fredrik Bejers Vej 7

- Control Room A(B4-105)
- Audiometry Room (B4-103)

Sensitivity of Microphone in Setup: $12.5\,\frac{\mathrm{mV}}{\mathrm{Pa}}$

E.2.1 Gain Factors and Associated SPL

Gain Factor g	Measured Voltage	associated SPL
0.4	1.3 mV	74.3 dB SPL
0.2	0.66 mV	68.4 dB SPL
0.1	0.33 mV	62.4 dB SPL
0.05	0.17 mV	56.6 dB SPL
0.025	0.09 mV	51.1 dB SPL

The noise measured with the given setup was fluctuating at approximately 46 dB SPL. Since these fluctuations were already visible for gain factors of 0.05 and 0.025, those measured values were neglected for further calculations.

E.2.2 Headphone Transfer Function

The normalized transfer function $\frac{H(f)}{H(1000\,\mathrm{Hz})}$ of the Sennheiser HDA 200 headphone used for the audiometric tests is given in Figure E.3

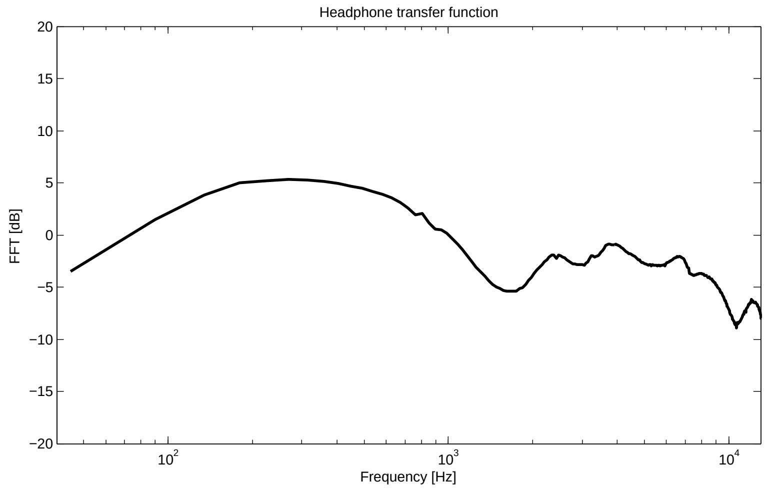

Figure E.3: The headphone transfer function of Sennheiser HDA 200 normalized at 1 kHz.

E.2.3 Noise Measurements

Figure E.4 shows the electric noise measured in third-octave bands at the terminals of the headphone. According to the data obtained from the calibration, this would result in a sound pressure level of maximum -8.8 dB. The sound pressure level and the hearing level according to ISO 389 is presented in Figure E.5.

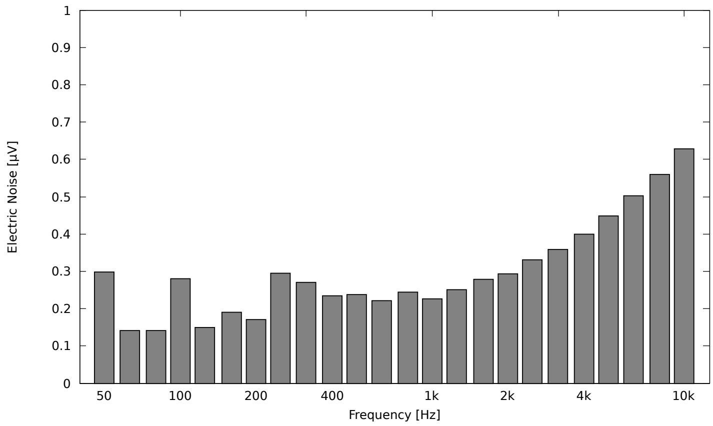

Figure E.4: The electric noise measured at the terminals of the headphones.

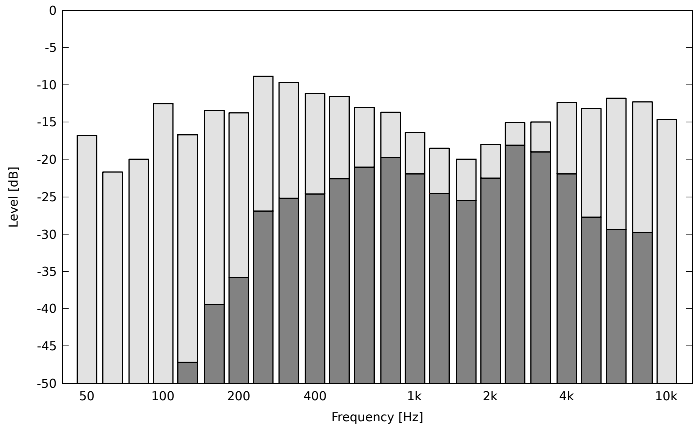

Figure E.5: The sound pressure level (light gray) and the hearing level (dark gray) produced in the headphone as a result of the electric noise.

E.3 Application of the Calibration Data

The data from the calibrations measurements is used to ensure an exact presentation of the desired hearing level with the audiometric equipment specified in Appendix B.

The reference equivalent threshold sound pressure levels for Sennheiser HDA 200 circumaural headphones are given in ISO 389-8:2004(E). These values are used to calculate the corresponding sound pressure level to a given hearing level. Due to the low resolution of the given values, interpolations are necessary.

From Section E.2.1, following relation between the gain g and the sound pressure p at the headphones at 1 kHz can be obtained:

$$g(1\,\mathrm{kHz}) = 3.8 \cdot \frac{p}{\mathrm{Pa}} \tag{E.2}$$

In order to obtain the gain factor at a specific frequency f different than 1 kHz, the normalized transfer function of the headphone (see Section E.2.2) is inverted and multiplied in linear scale:

$$g(f) = g(1\,\mathrm{kHz}) \cdot \frac{H(1000\,\mathrm{Hz})}{H(f)} \tag{E.3}$$

For security reasons this correction is limited to a maximum amplification of 12 dB, which might happen for frequencies higher than 12 kHz. Audiometric measurements in this frequency range are not recommended with the given setup.

The gain factor calculated in Equation (E.3) is used to generate the pure-tone stimulus s of the desired hearing level in Matlab[1] according to following equation (compare to Equation (E.1)):

$$s = g(f) \cdot \sin 2\pi f t \tag{E.4}$$

[1] The implemented Matlab function *get_gain.m* to obtain the gain g for a given hearing level and frequency is included in the enclosed CD.

F

Listening experiment instructions

The listening experiment you are participating in consists of three single tests for hearing assessment. Only one ear will be tested and it will be the same in the three tests. The tests will take place in the Audiometry Room B4-103. There will be short time breaks (5 minutes) between tests. During the breaks you can relax and enjoy the coffee/tea and cookies we offer you.

Test 1 Pure tone audiometry

This test will take approximately 10 minutes.

You will be wearing headphones during the test. Make sure they fit your ears correctly. The red earphone should be placed on the right ear and the blue one on the left ear. You also will be given a pushbutton.

Your task: You will hear different tones at different frequencies and levels. Since tones around your threshold of hearing will be presented you will need to be very concentrated to detect the lowest tones you are able to hear. Relax, try to control your breath and **press the pushbutton every time you hear a tone**. Do not try to guess.

Test 2 High-resolution audiometry

The test will last approx. 20-25 minutes.

The test consists of two parts of approx. 6 minutes each. In each part the test is running continuously without any break, so you should try to stay focused during the whole period. It is important that you are aware that there are no wrong responses, just try to perform in the best way you can. Depending on the previous results, a third part will be required, which will be of equal duration or shorter than the two previous.

You will be wearing headphones during the test. Make sure they fit your ears correctly and the headphone's wire corresponds to the ear under test.

You will find a LED on indicating the button that you have to press. Press the button whenever you feel ready to start and the LED will turn off indicating that the experiment begins.

Your task: You will hear short duration tonal sounds of a certain level. You must **press the button as soon as you hear the sound and keep it pressed for as long as you can hear it**. You must **release the button when you stop hearing any sound**. You will be presented to very weak sounds so it is very important that you stay relaxed and concentrated, and that you react as fast as you can.

At the end of each test part the left or right LED of the pushbutton (depending on the tested ear) will be turned on. Since your task requires a high concentration, you should take a break of at least 3 minutes to relax. You may leave the room during that time.

Test 3 DPOAE measurements

A prove will be inserted in your ear canal, in a similar way as inserting an ear plug. It does not hurt. The measurements will be carried out only in the same ear as in the previous test.

You will hear a two tones sound that will increase in frequency. You don't have to do anything. Just try to relax, not to move and do not swallow.

The test lasts approximately 20-30 minutes.

You are very welcome to ask any questions you need.

Please, inform to the experimenter if think you might be under conditions that can affect to your performance during the test (i.e.: if you have a cold, hangover, etc.).

The results of the experiment will be used in a 10^{th} semester project and they will remain anonymous.

Thank you very much for your collaboration.

G

Questionnaire

Full name: ____

Age: ____________ Gender: ☐ Male ☐ Female

Please, fill in the following questionnaire. Feel free to ask any questions whenever you consider it necessary.

1. Do you have any known hearing disorder?
   ☐ Yes ☐ No If yes, please specify which kind:
   ____
2. Have you ever had any serious injuries or illness that might have affected your hearing?
   ☐ Yes ☐ No If yes, please specify which kind:
   ____
3. Have you ever worked under loud noise conditions?
   ☐ Yes ☐ No If yes, please specify when and for how long:
   ____
4. Have you ever been exposed to very high sound levels that might have caused a hearing trauma?
   ☐ Yes ☐ No
5. Have you been exposed to high noise levels within the last 48 hours?
   ☐ Yes ☐ No If yes, could you describe the situation, please?
   ____
6. Are you taking any medicine at the moment?
   ☐ Yes ☐ No If yes, could you specify which kind, please?
   ____

7. How often do you listen to music via headphones?
☐ (almost) never ☐ sometimes ☐ (almost) daily

8. Have you ever performed a hearing test before?
☐ Yes ☐ No If yes, please specify when and where?
____

The information gathered here will be treated as strictly confidential.

I agree with the storage of my data and their use in this 10^{th} semester master project:

Date: ________________ Signature: ________________

Bibliography

[Clev 79] W. S. Cleveland. "Robust Locally Weighted Regression and Smoothing Scatterplots". *Journal of the American Statistical Association*, Vol. 74, No. 369, December 1979.

[Cran 08] J. L. Cranford. *Basics of Audiology. From Vibrations to Sounds.* Plural Publishing, 2008.

[Elli 58] E. Elliott. "A Ripple Effect in the Audiogram". *Nature*, April 1958.

[Fast 07] H. Fastl and E. Zwicker. *Psychoacoustics. Facts and Models.* Springer, 3rd Ed., 2007.

[Fitz 04] M. J. Fitzpatrick. "Real-Time implementation of a hearing testing technique". *Master of science, Department of Electrical and Computer Engineering, Clarkson University*, 2004.

[Han 89] L. A. Han and T. Poulsen. "Equivalent Threshold Sound Pressure Level for Sennheiser HDA 200 Earphone and Etymotic Research ER-2 Insert Earphone in the Frequency Range 125 Hz to 16 kHz". *Scandinavian Audiology*, Vol. 105, No. 12, 1989.

[Harr 89] F. Harris, B. Lonsbury-Martin, B. Stagner, A. Coats, and G. Martin. "Acoustic distortion products in humans: Systematic changes in amplitude as a function of f2/fl ratio". *Journal of the Acoustical Society of America*, Vol. 85, No. 1, January 1989.

[He 97] N. ji He and R. A. Schmiedt. "Fine structure of the 2 f1-f2 acoustic distortion product: Effects of primary level and frequency ratios". *Journal of the Acoustical Society of America*, Vol. 101, No. 6, June 1997.

[Heis 08] S. Heise, J. Verhey, and M. Mauermann. "Automatic screening and detection of threshold fine structure". *International Journal of Audiology*, 2008.

[Howa 96] D. M. Howard and J. Angus. *Acoustics and Psychoacoustics.* Focal Press, 1st Ed., 1996.

[ILO 97] *ILO OAE Instrument. User Manual.* Otodynamics Ltd, October 1997.

[Kemp 07] D. T. Kemp. "Otoacoustic Emissions: Concepts and Origins". *Active Processes and Otoacoustic Emissions in Hearing*, Vol. 30, No. Chapter 1, December 2007.

[Kemp 79] D. Kemp. "The evoked cochlear mechanical response and the auditory microstructure - evidence for a new element in cochlear mechanics". *Scandinavian Audiology Supplementum*, Vol. 9, 1979.

[Knig 98] R. Knight and D. Kemp. "Relationships between DPOAE and TEOAE amplitude and phase characteristics". *Auditory Biophysics Group, ILO, University College London, RNTNE Hospital, 330-332 Gray's Inn Road, London WC1X 8EE, United Kingdom*, December 1998.

[Laro 97] C. Laroche and R. Hétu. "A study of the reliability of Automatic Audiometry by the Frequency Scanning Method (AUDIOSCAN)". *Audiology*, Vol. 36, No. 1-18, 1997.

[Lydo 99] M. Lydolf. *The threshold of hearing and contours of equal loudness - a study on measuring methods and normal hearing.* Department of Acoustics, Aalborg university, Denmark, ph.d. dissertation Ed., 1999.

[Maue 04a] M. Mauermann, G. Long, and B. Kollmeier. "Fine structure of hearing threshold and loudness perception". *Journal of the Acoustical Society of America*, Vol. 116, No. 2, August 2004.

[Maue 04b] M. Mauermann. "Fine structure distorsion product otoacoustic emissions and auditory perception". *Ph.D. Thesis, Institut für Physik an der Fakultät für Mathematik und Naturwissenschaften der Carl von Ossietzky Universität Oldenburg*, 2004.

[Maue 99] M. Mauermann, S. Uppenkamp, P. W. J. van Hengel, and B. Kollmeier. "Evidence for the distortion product frequency place as a source of distortion product otoacoustic emission (DPOAE) fine structure in humans. II. Fine structure for different shapes of cochlear hearing loss". *Journal of the Acoustical Society of America*, Vol. 106, No. 6, December 1999.

[Moor 03] B. C. J. Moore. *An introduction to the psychology of hearing.* Academic Press, 5th Ed., 2003.

[Moor 07] B. C. J. Moore. *Cochlea Hearing Loss. Physiological, Psychological and technical Issues.* John Wiley & Sons, ltd, 2nd Ed., 2007.

[Reut 05] K. Reuter and D. Hammershøi. "Characterization of DPOAE fine structure". *Forum Acusticum, Budapest*, 2005.

[Reut 06] K. Reuter and D. Hammershøi. "Distorsion product otoacoustic emissions fine structure analysis of 50 normal-hearing humans". *Journal of the Acoustical Society of America*, Vol. 1, No. 120, July 2006.

[Reut 07] K. Reuter and D. Hammershøi. "Distortion product otoacoustic emission of symphony orchestra musicians before and after rehearsal". *Journal of the Acoustical Society of America*, Vol. 1, No. 121, January 2007.

[Ross 04] S. M. Ross. *Introduction to Probability and statistics for Engineers and Scientists.* Elsevier Academic Press, 3rd Ed., 2004.

[Shaf 03] L. A. Shaffer, R. H. Withnell, S. Dhar, D. J. Lilly, S. S. Goodman, and K. M. Harmon. "Sources and Mechanisms of DPOAE Generation: Implications for the Prediction of Auditory Sensitivity". *EAR & HEARING*, October 2003.

[Soun 07] *Sound & Hearing.* Widex, 3rd Ed., 2007.

[Talm 98] C. Talmadge, A. Tubis, G. Long, and P. Piskorski. "Modeling otoacoustic emission and hearing threshold fine structures". *Journal of the Acoustical Society of America*, Vol. 104, No. 3, September 1998.

[Talm 99] C. Talmadge, G. Long, A. Tubis, and S. Dhar. "Experimental confirmation of two-sources interference model for the fine structure distortion product otoacoustic emissions". *Journal of the Acoustical Society of America*, Vol. 105, No. 1, January 1999.

[Whit 95a] M. L. Whitehead, M. J. McCoy, B. L. Lonsbury-Martin, and G. K. Martin. "Dependence of distortion-product otoacoustic emissions on primary levels in normal and impaired ears. I. Effects of decreasing L2 below L1". *Journal of the Acoustical Society of America*, Vol. 97, No. 4, April 1995.

[Whit 95b] M. Whitehead, M. McCoy, B. Lonsbury-Martin, and G. Martin. "Dependence of distortion-product otoacoustic emissions on primary levels in normal and impaired ears. II. Asymerty in L1,L2 space". *Journal of the Acoustical Society of America*, Vol. 97, No. 4, April 1995.

[Zhao 02] F. Zhao, D. Stephens, and C. Meyer-Bisch. "The Audioscan: a high frequency resolution audiometric technique and its clinical applications". *Clin. Otolaryngol.*, Vol. 27, No. 4-10, October 2002.

[Zwei 95] G. Zweig and C. A. Shera. "The origin of periodicity in the spectrum of evoked otoacoustic emissions". *Journal of the Acoustical Society of America*, Vol. 98, No. 4, October 1995.

[Zwic 90] E. Zwicker and H. Fastl. *Psychoacoustics. Facts and Models.* Springer, 1st Ed., 1990.